Univerzita Karlova v Praze

Přírodovědecká fakulta

Studijní program: Fyzikální chemie

Mgr. Martin Beneš

Studium komplexačních rovnováh kapilární zónovou elektroforézou

Study of complexation equilibria by capillary zone electrophoresis

Dizertační práce

Vedoucí dizertační práce: Doc. RNDr. Iva Zusková, CSc.

Praha 2014

Předkládaná dizertační práce shrnuje výsledky získané během mého doktorského studia ve Skupině elektroforetických a chromatografických separačních metod (ECHMET) na Katedře fyzikální a makromolekulární chemie Přírodovědecké fakulty Univerzity Karlovy v Praze.

Práce byla financována v souvislosti s řešením projektů GA UK, č. grantu 323611, KONTAKT LH11018 a CEEPUS CIII-RO-0010-08-1314-M-69316. Děkujeme firmě Cyclolab, Budapešť, Maďarsko, za darování cyklodextrinu PABCD.

Prohlášení:

Prohlašuji, že jsem dizertační práci zpracoval samostatně a že jsem uvedl všechny použité informační zdroje a literaturu. Tato práce ani její podstatná část nebyla předložena k získání jiného nebo stejného akademického titulu.

V Praze ....

podpis

Poděkování

Na tomto místě musím poděkovat především dvěma osobám. Ivě, která se mě zeptala, jestli bych nechtěl vypracovat bakalářku na Fyzikální chemii. Děkuji jí za to, že se neurazila, když jsem se jí na to zdvořile vysmál a odešel. A že nabídka po půl roce pořád ještě platila. Díky tomu jsem mohl zažít několik let v pestrém světě fyzikálních chemiků. A Janině, v podstatě za všechno – protože bez ní by žádná dizertační práce nebyla. Jani, díky moc. Ty víš za co, já vím za co, tak to tady nemusím přede všema rozmazávat…

Jsem moc rád, že jsem potkal skupinu ECHMET a mohl s ní prožít několik let. Byla to vzácná zkušenost, potkal jsem spoustu úžasných lidí a zažil spoustu radosti. Ze všech bych vypíchnul ty nejzásadnější:

Děkuji:

Lále, že mě naučila dodržovat pitný režim

Květušce, že je taková, jaká je

Velké Malé Evě za spoustu podezřelé chvály a dodávání sebevědomí

katedře, že mi našla Štolu, a že mi umožnila tam ve volném čase docházet

Štole, že mi umožnila ve volném čase docházet na katedru

v neposlední řadě svojí rodině a všem svým kamarádům za to, že mi pomáhali překonávat složitější období a sem tam mě pořádně vyprudit, když to bylo potřeba…

Díky moc!!!

Klíčová slova

kapilární zónová elektroforéza, komplexační rovnováhy, simulace, separace enantiomerů, Simul 5 Complex, PeakMaster 5.3 Complex, elektromigrační disperze, konstanta stability

Keywords

capillary zone electrophoresis, complexation equilibria, simulations, enantiomer separation, Simul 5 Complex, PeakMaster 5.3 Complex, electromigration dispersion, complexation constant

Anotace

Kapilární zónová elektroforéza patří mezi hojně používané analytické metody vhodné k separaci chirálních analytů. Enantioselektivní prostředí je zajištěno přídavkem komplexačního činidla přímo do základního elektrolytu, což zajišťuje vysokou flexibilitu separačního systému – komplexační činidlo či jeho koncentrace mohou být snadno měněny. Interakce mezi analyty a komplexačním činidlem je charakterizována komplexačními rovnováhami, jejichž studium je předmětem této dizertační práce.

Jednou z hlavních výhod kapilární elektroforézy je existence jejího kompletního matematického modelu a simulačních programů umožňujících předpovídat výsledky elektroforetických separací. Žádný z dosavadních modelů však není použitelný pro komplexující systémy. V rámci této práce byl představen matematický model elektroforézy rozšířený o komplexační rovnováhy. Model byl implementován do dynamického simulátoru elektroforézy Simul 5 a jeho platnost byla experimentálně ověřena. Nová verze programu Simul 5 Complex je schopna předpovědět mobilitu, amplitudu i tvar píku analytu v prostředí obsahujícím komplexační činidlo. V dalším kroku byly komplexační rovnováhy začleněny také do linearizovaného modelu elektromigrace simulátoru PeakMaster 5.3 Complex. Ten je schopen během několika vteřin předpovědět tvar píku v závislosti na separačním prostředí. Může tedy pomoci vybrat vhodné experimentální podmínky vedoucí k úzkým a symetrickým píkům (potlačení elektromigrační disperze) a optimalizaci separačních podmínek za výrazné úspory experimentálního času a chemikálií. Současně byl PeakMaster 5.3 Complex využit k vysvětlení vlivu komplexace analytu s komplexačním činidlem na tvar píku analytu.

Komplexační činidlo přidané do základního elektrolytu může interagovat nejen s analyty, ale také se složkami pufru. Tato interakce může významně změnit vlastnosti základního elektrolytu jako pH, iontovou sílu či vodivost. Bylo prokázáno, že interakce komplexačního činidla se složkami pufru může také významně ovlivnit stanovení komplexačních parametrů. Komplexační parametry určené v takových systémech mohou být zcela nesprávné a tak poskytovat mylnou informaci o síle komplexace. Proto by měla být možnost interakce komplexačního činidla se složkami pufru prověřena před samotnými experimenty např. kontrolou pH po přídavku komplexačního činidla do základního elektrolytu.

Abstract

Capillary zone electrophoresis (CZE) is one of the most widely used analytical methods for separation of chiral analytes. In contrast to the other common chiral separation methods, chiral complexation agent is usually added directly to the background electrolyte to create enantioselective separation environment. Thus, the type and the concentration of chiral selector can be easily varied, which results in high flexibility of separation system. The detail understanding of electrophoretic separation systems with complexation involved is the main goal of this thesis.

One of the most important advantages of capillary electrophoresis is existence of its complete mathematical model, which was implemented in several simulation programs. They can provide detail insight into the separation process or predict the separation results. However, none of the available simulators is suitable for complexing separation systems, which limits its applicability for chiral separation systems. For this reason, in the scope of this thesis we introduce the complete mathematical model of electromigration for separation systems with complexation agents. The model was implemented in our dynamic simulator Simul 5 and was verified experimentally. The new version of Simul 5 Complex provides the overall picture about the electrophoretic separation with complexation agents and allowed us to demonstrate the development of unforeseen electromigration dispersion connected with complexation. This phenomena was further elucidated using our second simulator PeakMaster 5.3 Complex, whose linearized model of electromigration was extended by complexation equilibria. The new version of PeakMaster 5.3 predicts the extent of electromigration dispersion of analyte peaks depending on concentration of complexation agent. Thus, it can be used for optimization of separation conditions to obtain symmetrical and sharp analyte peaks. Complexation agent added to the background electrolyte can interact not only with analytes but also with buffer constituents. This interaction can significantly influence the buffer properties, such as pH, ionic strength or conductivity. We showed that the value of complexation constant determined in the interacting buffers environment can be totally wrong and may provide misleading information about the strength of complexation. Therefore, the interaction of buffer constituents with the complexation agent should always be considered and tested before the very experiments, e.g. by pH measurement after adding of complexation agent to the separation buffer.

Obsah

Seznam použitých zkratek a symbolů

A	analyt
AC	komplex analytu a komplexačního činidla
ACE	afinitní kapilární elektroforéza
β-CD	β-cyklodextrin
BGE	základní elektrolyt
C	komplexační činidlo
CZE	kapilární zónová elektroforéza
EMD	elektromigrační disperze
EOF	elektroosmotický tok
HVL	Haarhoffova-van der Lindeho funkce
HVLR	Houghtonem upravená HVL funkce
CHES	N-cyklohexyl-2-aminoethan sulfonová kyselina
Mal-β-CD	6-O-α-maltosyl-β-cyklodextrin
MES	2-(N-morfolin)ethansulfonová kyselina
MOPS	3-morfolinpropan-1-sulfonová kyselina
NMR	nukleární magnetická rezonance
PremCE	tlakem zprostředkovaná kapilární elektroforéza
R-flurbiprofen	(R)-(-)-2-fluoro-α-ethyl-4-biphenyloctová kyselina
SDS	dodecylsíran sodný
tricin	N-(2-hydroxy-1,1-bis(hydroxymethyl)ethyl)glycin

[ ]	rovnovážná molární koncentrace
α	stupeň komplexace analytu
a_i	aktivita i-té složky systému
c_H	koncentrace hydroxoniových iontů
c_i	celková koncentrace i-tého analytu
$c_{i,z}$	koncentrace i-tého analytu v iontové formě s nábojovým číslem *z*
c_L	celková koncentrace komplexačního činidla
$c_{L,l}$	koncentrace komplexačního činidla v iontové formě s nábojovým číslem *l*
c_{OH}	koncentrace hydroxidových iontů
$c_{x,i,z,l}$	koncentrace komplexu i-tého analytu v iontové formě s nábojovým číslem *z* a komplexačního činidla v iontové formě s nábojovým číslem *l*
$J_{k,f}$	látkový tok k-té složky systému ve své formě f
κ	specifická vodivost základního elektrolytu
K	termodynamická konstanta stability
$K´$	zdánlivá konstanta stability
$K_{x,i,z,l}$	konstanta stability i-tého analytu v iontové formě s nábojovým číslem *z* a komplexačního činidla v iontové formě s nábojovým číslem *l*
μ_A	mobilita volného analytu
$\mu_{A,eff}$	efektivní mobilita analytu
μ_{AC}	mobilita komplexu analyt - komplexační činidlo
$\mu_{MAX,A}$	mobilita analytu určená z maxima píku
pK_A	záporný dekadický logaritmus disociační konstanty
$S_{EMD,A}$	*nonlinear elektromigration mobility slope of the analyte zone*
S_X	*relative velocity slope*
u_{EMD}	nelineární elektroforetická mobilita
v	elektroforetická rychlost analytu
v_{EOF}	rychlost elektroosmotického toku

Úvod

Kapilární zónová elektroforéza (CZE) je analytická separační metoda založená na rozdílné rychlosti iontů v elektrickém poli. Mezi hlavní přednosti CZE patří nízká spotřeba použitých chemikálií (separačních pufrů i vzorků) a vysoká rychlost a účinnost separace. CZE je možno použít pro separaci široké řady látek od malých iontů až po makromolekuly. Významné uplatnění nachází také v případě chirálních separací. Pro separaci chirálních látek (např. enantiomerů) je třeba vytvořit enantioselektivní separační prostředí, například přídavkem vhodného komplexačního činidla do separačního pufru, které vytváří s jednotlivými chirálními analyty komplexy. Ty již elektroforeticky rozdělit lze. Jako chirální komplexační činidla (chirální selektory) se používají např. cyklodextriny, makrocyklická antibiotika, crown ethery, cyklofruktany, či chirální micely. Výhodou kapilární elektroforézy je možnost jednotlivé selektory lehce měnit, upravovat jejich koncentraci nebo pracovat s jejich kombinacemi.

Nejčastěji využívanými komplexačními činidly jsou cyklodextriny. Jedná se o cyklické oligosacharidy, složené nejčastěji z 6 až 9 jednotek glukosy. Molekula cyklodextrinu má charakteristický tvar komolého kužele, jehož vnější plášť tvoří hydrofilní skupiny, kdežto dutina (kavita) je hydrofobní. V kavitě se nacházejí asymetrické uhlíky, proto cyklodextriny mohou sloužit jako chirální selektory. V analytické praxi se používají jak cyklodextriny nativní, tak derivatizované. Chemickou modifikací se připravují derivatizované cyklodextriny neutrální, aniontové i kationtové. Touto modifikací lze velmi významně ovlivnit vlastnosti cyklodextrinů včetně schopnosti tvořit inkluzní komplexy.

Vazebné interakce mezi analytem a komplexačním činidlem charakterizuje konstanta stability (komplexační, asociační konstanta). Kapilární elektroforéza je nejen účinnou separační technikou, ale používá se též ke stanovování různých fyzikálně-chemických charakteristik látek včetně konstant stability. V rámci kapilární elektroforézy bylo vyvinuto několik metod na určení konstanty stability. Mezi nejčastěji využívané patří afinitní kapilární elektroforéza (ACE).

Významnou výhodou kapilární elektroforézy je její kompletní matematický popis, který umožňuje predikci experimentálních výsledků. V naší skupině byly vyvinuty dva simulační programy Simul a PeakMaster, které umožňují optimalizovat separační podmínky, čímž šetří často drahé chemikálie a experimentální čas. Žádný běžně

dostupný simulátor elektroforézy neumožňuje v plné míře předvídat výsledky v prostředí obsahujícím komplexační činidlo. V rámci této doktorské práce byl stávající matematický model elektroforézy rozšířen o komplexační rovnováhy. Tento model byl implementován do nové verze programu Simul 5, Simul 5 Complex. Teoretický model a simulační program byly následně ověřeny na několika experimentálních systémech (Publikace I a II).

V rámci ověřování platnosti nového modelu byl odhalen dříve nepopsaný trend v elektromigrační disperzi píku analytu v prostředí s komplexačním činidlem. Toto chování nelze vysvětlit změnami vodivosti či pH prostředí, je tedy nutně spojeno se samotnou komplexací. Abychom tento jev dokázali pochopit a vysvětlit, odvodili jsme částečný linearizovaný model elektroforézy s neutrálním komplexačním činidlem, který dokáže předvídat elektromigrační disperzi píku analytu. Tento model byl začleněn do simulačního programu PeakMaster 5.3 Complex. Model byl následně také ověřen – a to jak experimentálně, tak pomocí simulačního programu Simul 5 Complex. Současně nám tento model umožnil vysvětlit vliv komplexace na elektromigrační disperzi a vybrat separační podmínky vedoucí k minimální deformaci píků (Publikace III a IV).

Nezbytnými vstupními daty k jakýmkoliv simulacím systémů s komplexačními činidly jsou parametry popisující interakci analytu s komplexačním činidlem – konstanta stability a mobilita komplexu. Ve třetí části této práce jsme se proto věnovali určování konstant stability. Bylo prokázáno, že cyklodextriny mohou interagovat nejen s analyty, ale také se složkami základního elektrolytu (BGE). Těmito interakcemi se mohou zásadně změnit vlastnosti separačního prostředí a tak ovlivnit stanovení komplexačních parametrů (Publikace V a VI).

Dizertační práce shrnuje nejdůležitější výsledky dosažené prací na výše zmíněných tématech.

Cíle práce

Cíle této dizertační práce lze shrnout do následujících bodů:

1. Rozšířit dynamický simulační program Simul 5 o komplexační rovnováhy a experimentálně ověřit platnost navrženého modelu (Publikace I a II).

2. Potvrdit funkčnost a platnost částečného linearizovaného modelu elektroforézy uvažujícího komplexaci analytu s neutrálním komplexačním činidlem implementovaného do programu PeakMaster 5.3 Complex. Využít tento model k vysvětlení vlivu komplexace na tvar píku analytu (Publikace III a IV).

3. Vyšetřit a popsat vliv interakce složek BGE s komplexačním činidlem na stanovení konstant stability (Publikace V a VI).

1. Dynamická simulace elektroforetických systémů s komplexačními rovnováhami: Publikace I, II

1.1 Dynamická simulace elektroforézy

Nespornou výhodou kapilární elektroforézy je existence jejího uceleného matematického modelu. Vývoj těchto modelů a jejich implementace do počítačových simulačních programů probíhá již více než 30 let. V dnešní době, kdy je každá laboratoř zcela samozřejmě vybavena výkonnými počítači, přechází počítačová simulace do běžné laboratorní praxe. Hlavními výhodami simulací je i) detailní náhled do separačního procesu, který jej umožňuje pochopit a vysvětlit ii) možnost optimalizovat separační podmínky ještě před prováděním samotných experimentů a iii) využití k vzdělávacím účelům.

První matematické modely elektroforézy byly omezeny výhradně na silné elektrolyty [1] – [5]. Později byly rozšířeny také pro slabé elektrolyty [6] – [10]. Jednotlivá omezení byla postupně odstraňována tak, aby bylo možné simulovat běžné elektroforetické techniky, mimo jiné kapilární zónovou elektroforézu [11], [12], izotachoforézu [13], [14], izoelektrickou fokusaci [15], [16], či izoelektrické zakoncentrování [17]. Historický přehled včetně možných aplikací běžně dostupných simulačních programů lze najít v přehledových článcích Thormanna a kol. [18], [19].

Matematické modely kapilární elektroforézy jsou založeny na rovnicích popisujících acidobazické/komplexační rovnováhy, na podmínce elektroneutrality a rovnicích kontinuity. Rovnice kontinuity jsou nelineární parciální diferenciální rovnice vycházející ze zákona zachování hmoty a popisující distribuci koncentrací jednotlivých složek v čase a prostoru [20]. Soustava těchto rovnic nemá analytické řešení. Je však možné ji řešit numericky pomocí dynamických simulací.

V dnešní době jsou k dispozici především tři dynamické simulátory elektroforézy: GENTRANS [21] – [23], SIMUL 5 [24] a SPRESSO [25], [26]. Mosher a kol. [27] tyto simulátory na základě několika nasimulovaných systémů porovnal. Program SPRESSO je založen na jednotném obecném modelu. Obsahuje tzv. adaptivní mřížku, která slouží k zahuštění simulačních bodů v místech, kde se sledovaná veličina výrazně mění. To v některých případech může významně snížit simulační čas. Program GENTRANS obsahuje oddělené modely pro jednomocné a vícemocné složky a pro proteiny. Toto oddělení umožňuje zkrácení simulačního času pro jednodušší systémy. GENTRANS

k dalšímu zrychlení simulací nabízí možnost tzv. „vyhlazení“ dat, díky kterému se předchází numerickým oscilacím. Další výhodou programu GENTRANS je možnost odhadu elektroosmotického toku. Na rozdíl od programu SPRESSO však neobsahuje žádnou korekci vlivu iontové síly prostředí na mobilitu a také nenabízí uživatelsky přívětivé grafické rozhraní, které by umožňovalo sledovat simulaci v jejím průběhu. Program SPRESSO byl napsán v prostředí programu Matlab, GENTRANS běží v prostředí Windows.

1.2 Simulační program SIMUL 5

Dynamický simulátor kapilární elektroforézy SIMUL 5 [24] byl vyvinut v naší laboratoři. Je volně dostupný ke stažení na našich webových stránkách (echmet.natur.cuni.cz). SIMUL 5 obsahuje kompletní matematický model kapilární elektroforézy (rozšiřující model zabudovaný v předchozí verzi programu [13], [28]). Je použitelný pro jakékoliv množství konstituentů – ať už slabých či silných elektrolytů, jedno- či vícevalentních iontů a také amfolytů. Jedná se o užitečný nástroj schopný simulovat různé elektroforetické techniky: kapilární zónovou elektroforézu, izotachoforézu, izoelektrickou fokusaci či izoelektrické zakoncentrování.

SIMUL 5 je určen pro operační systém Windows a nabízí uživatelsky přívětivé a přehledné grafické rozhraní. Výhodou je snadné a přehledné zadávání vstupních parametrů. V programu je k dispozici databáze vstupních dat (limitní mobility, disociační konstanty) pro širokou škálu látek převzatá z Hirokawových tabulek [29] – [33].Tuto databázi uživatel může upravovat a rozšiřovat. Po spuštění simulace je možné celý proces krok po kroku sledovat, což poskytuje detailní náhled na proces separace, který umožňuje jeho hlubší pochopení.

Samotný model nezahrnuje efekt iontové síly. SIMUL 5 však obsahuje zabudovanou korekci mobilit na iontovou sílu podle Onsagerovy-Fuossovy teorie [34] a přepočet koncentrací jednotlivých konstituentů na aktivity užitím Debyeovy-Hückelovy teorie podle Jaroše a kol. [35]. Po aktivaci této korekce dochází k přepočtu mobilit a koncentrací v každém časovém kroku v každém bodě simulace. Taková simulace více odpovídá realitě ovšem za cenu výrazného prodloužení simulačního času.

SIMUL 5 umožňuje pevné nastavení hranic pohybující se oblasti, ve které probíhá výpočet. Vymezení úseku kapiláry, na kterém se očekávají změny v koncentracích, vede k výraznému zrychlení simulace.

1.3 Matematické modely elektroforézy zahrnující komplexační rovnováhy

Matematických modelů elektroforézy zahrnujících komplexační rovnováhy nebylo publikováno mnoho a všechny prozatím publikované jsou založeny na více či méně významných zjednodušení.

V roce 1992 Dubrovčáková a kol. [36] publikovali zjednodušený model zahrnující komplexační rovnováhy pro silný elektrolyt jako analyt a neutrální komplexační činidlo. Busch a kol. [37] představili zjednodušený model elektromigrace s komplexačními činidly, aby mohli ukázat principy a případná omezení jednotlivých metod používaných k určování konstant stability. V roce 2004 představili Dubský a kol. [38] SimulChir, který obsahoval zjednodušený model elektromigrace spolu s modelem interkonverze enantiomerů, který umožňoval výpočet rychlostních konstant interkonverze. Tento model byl později rozšířen také pro směsi komplexačních činidel [39], [40]. V naší pracovní skupině byl také vyvinut program SimulMic [41], který obsahoval model popisující chování neutrálních analytů v prostředí neutrálních cyklodextrinů a nabitých surfaktantů (SDS). Programy simulující experimenty afinitní kapilární elektroforézy dále představili Fang a kol. [42], [43] a Righetti a kol. [44]. V roce 2009 Breadmore a kol. [45] implementovali model obsahující komplexační rovnováhy do programu GENTRANS. Ovšem i v tomto případě se to neobešlo bez zjednodušení – disociační stupeň analytů a komplexačních činidel byl omezen a mobilita volného komplexačního činidla a komplexu analyt-komplexační činidlo byla automaticky stejná. Poslední verze programu GENTRANS [46], publikovaná současně s naším modelem, již umožňuje nastavit rozdílné mobility komplexu a volného komplexačního činidla. Program byl použit k simulacím izotachoforézy a kapilární zónové elektroforézy v prostředí s neutrálním cyklodextrinem.

1.4 Matematický model programu Simul 5 Complex

Jak již bylo zmíněno výše, do této doby nebyl publikován kompletní matematický model elektroforézy s komplexačními rovnováhami. Z toho důvodu byl rozšířen náš

stávající model zabudovaný v programu SIMUL 5 [24] o komplexační rovnováhy. Popis tohoto modelu je hlavním obsahem Publikace I.

Náš model je platný pro systémy, které obsahují jedno komplexační činidlo (ligand, nábojové číslo n_L,...p_L) a jakékoliv množství (i=1,...N_x) vícevalentních složek (kyselin, zásad, amfolytů) s nábojovými čísly n_i,...p_i. Předpokládáme, že komplexační činidlo může interagovat se všemi složkami prostředí, ovšem pouze v nejjednodušší, ale také nejčastější stechiometrii analyt:komplexační činidlo 1:1. Proto všechny složky prostředí budeme považovat za potenciální analyty. Interakce i-tého analytu ve své iontové formě s nábojovým číslem z (o koncentraci $c_{i,z}$) a komplexačního činidla v iontové formě s nábojovým číslem l (o koncentraci $c_{L,l}$) je charakterizována rovnovážnou konstantou stability $K_{x,i,z,l}$:

$$K_{x,i,z,l} = \frac{c_{x,i,z,l}}{c_{i,z} c_{L,l}}, \tag{1}$$

kde $c_{x,i,z,l}$ je koncentrace příslušného vznikajícího komplexu. Celkové (analytické) koncentrace jednotlivých analytů/složek (c_i) a komplexačního činidla (c_L) můžeme vyjádřit jako součet všech neutrálních, nabitých, volných a komplexovaných forem:

$$c_i = \sum_{z=n_i}^{p_i} c_{i,z} + \sum_{z=n_i}^{p_i} \sum_{l=n_L}^{p_L} c_{x,i,z,l} \tag{2}$$

$$c_L = \sum_{l=n_L}^{p_L} c_{L,l} + \sum_{i=1}^{N_x} \sum_{z=n_i}^{p_i} \sum_{l=n_L}^{p_L} c_{x,i,z,l}. \tag{3}$$

Neznámou koncentraci hydroxoniových iontů (c_H) lze určit pomocí podmínky elektroneutrality:

$$c_H - \frac{K_w}{c_H} + \sum_{z=n_i}^{p_i} z c_{i,z} + \sum_{l=n_L}^{p_L} l c_{L,l} + \sum_{i=1}^{N_x} \sum_{z=n_i}^{p_i} \sum_{l=n_L}^{p_L} (z+l) c_{x,i,z,l} = 0, \tag{4}$$

do které bylo za koncentraci hydroxidových aniontů c_{OH} dosazeno z rovnice popisující autoprotolýzu vody (iontový součin vody). Koncentrace všech forem analytů a komplexačního činidla přítomných v systému můžeme určit kombinací rovnic (1), (2), (3), (4) a příslušných acidobazických rovnováh.

Matematický model elektromigrace je založen na jednorozměrných parciálních diferenciálních rovnicích kontinuity, které vyjadřují vývoj celkové koncentrace

jednotlivých složek v čase a v prostoru. Rovnice kontinuity pro všechny analyty i komplexační činidlo (označení indexem k = L, 1,..., N_x) lze zapsat v následujícím tvaru:

$$\frac{\partial c_k}{\partial t} = -\sum_f \left(\frac{\partial J_{k,f}}{\partial x} \right). \tag{5}$$

Index f reprezentuje všechny volné i komplexované formy k-té složky systému. Veličina $J_{k,f}$ je potom její látkový tok, který se v našem případě skládá ze tří složek – difúze, elektromigrace a elektroosmotického toku (EOF) s rychlostí v_{EOF}.

Pomocí rovnic (1) – (5) je vystavěn celý model. Program Simul 5 Complex potom používá stejný algoritmus k nalezení numerického řešení nelineárních diferenciálních rovnic kontinuity jako jeho předchozí verze. Tento model nebere v úvahu žádné další efekty jako je vliv iontové síly na mobilitu a rovnovážné konstanty, teplotu či viskozitu BGE. Jako vstupní data pro simulaci jsou proto nezbytné komplexační parametry odpovídající aktuálním experimentálním podmínkám. Program však poskytuje možnost všechna ostatní vstupní data (jako iontové limitní mobility a disociační konstanty) před začátkem simulace na aktuální iontovou sílu zkorigovat.

1.5 Experimentální ověření programu Simul 5 Complex

V prvním kroku jsme ukázali, že Simul 5 Complex je vhodným nástrojem pro simulaci všech běžných elektroforetických metod, které se používají k určování konstant stability. V následujícím kroku jsme platnost modelu ověřili na třech různých experimentálních systémech, které se lišily typem analytu, komplexačního činidla a silou interakce mezi analytem a komplexačním činidlem. Simulace jsme provedli při různých koncentracích komplexačního činidla, abychom mohli posoudit vliv komplexace na separaci. Vstupní parametry (konstanty stability a mobility komplexu) byly určeny metodou ACE [47]. Simulace byly provedeny za stejných podmínek jako příslušné experimenty.

Jak je zřejmé z Obr. 1, 2 a 3, bylo dosaženo výborné shody mezi experimentálními a simulovanými daty co se týče pozice, amplitudy i tvaru píků analytu. V prvním systému byl použit jako komplexační činidlo neutrální 6-*O*-α-maltosyl-β-cyklodextrin (Mal-β-CD) a jako analyt (R)-(-)-2-fluoro-α-ethyl-4-biphenyloctová kyselina (R-flurbiprofen), který byl za daných experimentálních podmínek plně nabitý (K = 3600 ± 100

(mol.dm^{-3})$^{-1}$)[†]. Jak je vidět na Obr. 1, s koncentrací komplexačního činidla v pufru se výrazně mění také tvar píku analytu. V systému bez Mal-β-CD má pík takřka gaussovský tvar, ovšem po minimálním přídavku Mal-β-CD (0,1 mM) je pík analytu silně ovlivněn elektromigrační disperzí a má typický trojúhelníkový tvar. Tento efekt se se zvyšující koncentrací cyklodextrinu v BGE postupně tlumí, při koncentraci cyklodextrinu v BGE 2 mM je pík analytu opět takřka gaussovský.

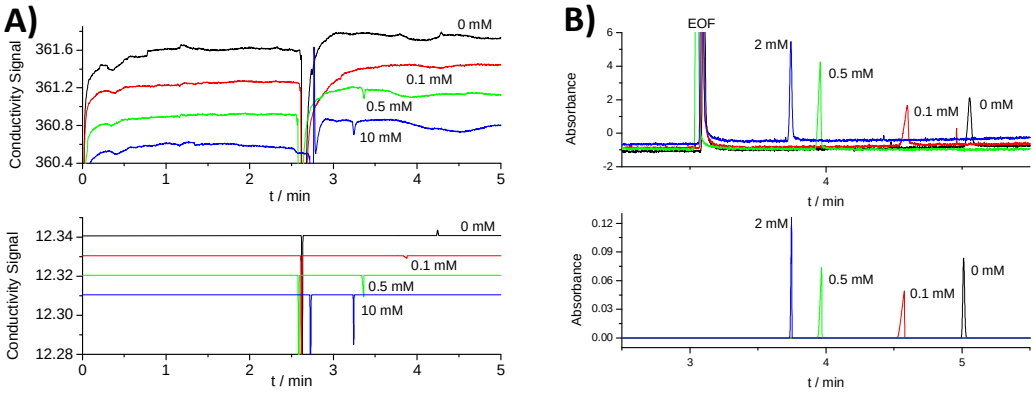

Obr. 1 Srovnání experimentálních (nahoře) a simulovaných (dole) elektroferogramů v prvním systému – analyt R-flurbiprofen (koncentrace ve vzorku 0,3 mM), komplexační činidlo Mal-β-CD. A: vodivostní signál [48], B: UV-detekce. Jednotlivé křivky (píky) jsou označeny koncentrací komplexačního činidla v BGE. Pro lepší přehlednost byly experimentální a simulované křivky z vodivostního detektoru posunuty podél osy y.

Elektromigrační disperze se projevuje, pokud rychlost analytu závisí na jeho koncentraci v zóně – obecně se předpokládá, že vzniká v důsledku změn vodivosti a pH v zóně analytu. Ovšem přídavek 0,1 mM neutrálního cyklodextrinu nemůže způsobit žádné výrazné změny vodivosti či pH. Pík analytu by měl tedy mít stejný tvar jako v prostředí bez přídavku cyklodextrinu. Výrazná elektromigrační disperze pozorovaná v tomto systému proto musí být způsobena komplexací analytu s cyklodextrinem.

Efektivní mobilita analytu, $\mu_{A,eff}$, který se vyskytuje ve volné a komplexované formě, může být vyjádřena jako vážený průměr mobility volného analytu, μ_A, a komplexu μ_{AC}:

$$\mu_{A,eff} = \alpha\mu_{AC} + (1-\alpha)\mu_A \,, \qquad (6)$$

[†]Konstanty stability použité v tomto oddílu práce nejsou korigovány na iontovou sílu a viskozitu prostředí. Odpovídají tedy aktuálním podmínkám experimentů.

kde příslušnou váhou je stupeň komplexace analytu α. Stupeň komplexace závisí na koncentraci analytu, c_A, a koncentraci komplexačního činidla, c_L, podle následujícího vztahu:

$$\alpha = \frac{2Kc_L}{K(c_A + c_L) + 1 + \sqrt{[K(c_A + c_L) + 1]^2 - 4K^2 c_A c_L}}. \quad (7)$$

V případě silné interakce analyt – komplexační činidlo stupeň komplexace analytu silně závisí na koncentraci analytu v zóně, díky čemuž se s koncentrací v zóně mění také jeho rychlost. Proto v tomto systému pozorujeme výraznou elektromigrační disperzi.

V druhém systému byl použit stejný analyt a jiné komplexační činidlo – heptakis(2,3,6-tri-*O*-methyl)-β-cyklodextrin. Konstanta stability vznikajícího komplexu je zhruba šestkrát nižší než v předchozím případě (K = 610 ±40 (mol.dm^{-3})$^{-1}$). Jak je zřejmé z Obr. 2, pík analytu má takřka gaussovský tvar nezávisle na koncentraci komplexačního činidla v BGE. To lze vysvětlit slabší komplexací, stupeň komplexace analytu nezávisí tak výrazně na jeho koncentraci v zóně a vliv elektromigrační disperze se neprojeví.

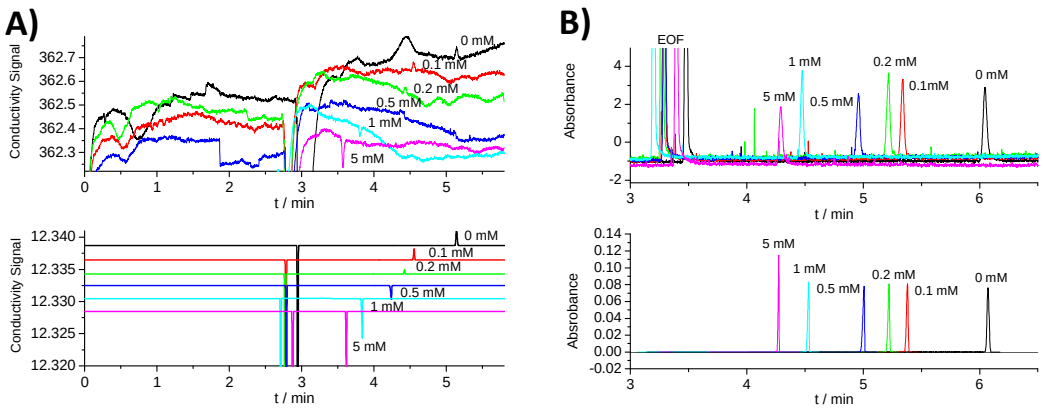

Obr. 2 Srovnání experimentálních (nahoře) a simulovaných (dole) elektroferogramů v druhém systému – analyt R-flurbiprofen (koncentrace ve vzorku 0,3 mM), komplexační činidlo heptakis(2,3,6-tri-*O*-methyl)-β-cyklodextrin. A: vodivostní signál, B: UV-detekce. Jednotlivé křivky (píky) jsou označeny koncentrací komplexačního činidla v BGE. Pro lepší přehlednost byly experimentální a simulované křivky z vodivostního detektoru posunuty podél osy y.

Ve třetím případě byl použit nabitý kationtový cyklodextrin (6-monodeoxy-6-mono(3-hydroxypropylamino)-β-cyklodextrin) a neutrální analyt (S-3-bromo-2-methylpropan-1-ol). Interakce mezi nimi byla velmi slabá (K= 114 ± 7 (mol.dm^{-3})$^{-1}$). Experimenty byly

prováděny za konstantní iontové síly – koncentrace jednotlivých složek BGE se měnily tak, aby byl kompenzován příspěvek nabitého cyklodextrinu k iontové síle. Kvůli nižším mobilitám vznikajícího komplexu byly experimenty provedeny metodou PreMCE [49], [50]. Experimentální elektroferogramy jsou složitější na vyhodnocení, proto byly experimentální i simulované výsledky převedeny z časové do mobilitní škály. Jak je vidět, i v tomto systému se uplatňuje elektromigrační disperze, ovšem její vysvětlení je výrazně složitější než v předchozích případech. Vliv bude mít nejen měnící se koncentrace cyklodextrinu, ale také měnící se složení BGE.

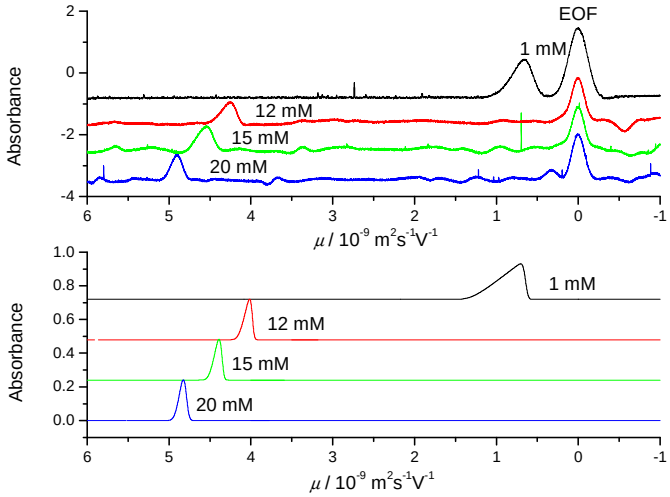

Obr. 3 Srovnání experimentálních (nahoře) a simulovaných (dole) elektroferogramů z UV-detektoru ve třetím systému – analyt S-3-bromo-2-methylpropan-1-ol (koncentrace ve vzorku 0,5 mM), komplexační činidlo 6-monodeoxy-6-mono(3-hydroxypropylamino)-β-cyklodextrin. Jednotlivé křivky (píky) jsou označeny koncentrací komplexačního činidla v BGE. Pro lepší přehlednost byly experimentální a simulované křivky posunuty podél osy y.

Simul 5 Complex byl v naší laboratoři ověřen i pro slabé elektrolyty. Byla nasimulována publikovaná experimentální data separace enantiomerů v závislosti na koncentraci komplexačního činidla a pH prostředí [51].

2. PeakMaster 5.3 Complex: Elektromigrační disperze v systémech s neutrálním komplexačním činidlem a plně nabitým analytem: Publikace III, IV

2.1 Elektromigrační disperze

Kvalita elektroforetické separace může být významně ovlivněna disperzními jevy. Disperze způsobuje rozšiřování a deformaci píků, což snižuje citlivost a účinnost separace. K celkové disperzi píků přispívá podélná difúze, vznik Joulova tepla (teplotní efekty v kapiláře), adsorpce na stěnu kapiláry, elektromigrační disperze, laminární tok,… Tyto jevy jsou detailně popsány v několika přehledových článcích [52]-[54]. Mezi nejdůležitější z těchto faktorů patří elektromigrační disperze (EMD), která způsobuje deformaci ideálního gaussovského píku na typický trojúhelníkový tvar. U takto deformovaných píků nelze použít čas maxima pro výpočet mobility. Erny a kol [55], [56] ukázali, že k nalezení správné hodnoty migračního času je třeba trojúhelníkový pík proložit Haarhoffovou-van der Lindeho (HVL) funkcí [57]. Jeden z parametrů této funkce představuje střed odpovídajícího gaussovského píku, tedy maximum píku při nekonečném zředění.

EMD je známa a zkoumána již dlouhou dobu. Vliv EMD na tvar píku analytu se projeví, pokud rychlost migrace analytu závisí na jeho koncentraci v zóně. Xu a kol. [58] zavedli pro popis EMD konstantu charakterizující analyt v daném BGE, která určuje, jak se projeví vliv EMD na tvar píku analytu (síla a směr EMD). Také jako první upozornili na to, že EMD je ovlivněna jak vodivostí, tak pH základního elektrolytu. Gebauer a kol. [59], [60] představili základní popis EMD, který charakterizuje míru EMD pomocí jednoduchých diagramů. Později [61], [62] byla zavedena veličina *velocity slope*, která je kvantitativní charakteristikou tendence daného analytu v daném BGE podléhat EMD. Na tuto práci navázali Horká a kol. [63], kteří zavedli *relative velocity slope*, S_X:

$$S_X = \lim_{c_X \to 0} \frac{\kappa}{v_X} \frac{\mathrm{d}v_X}{\mathrm{d}c_X}, \tag{8}$$

kde κ je specifická vodivost BGE, v_X je rychlost analytu a c_X jeho koncentrace. Pokud je tato veličina kladná, pík má ve směru migrace ostrou náběžnou hranu a rozmytou sestupnou hranu – chvostující pík (*tailing*). V opačném případě pozorujeme pík frontující (*fronting*). Na základě diagramů ilustrujících vývoj EMD v závislosti na pH a vodivosti BGE autoři předpověděli existenci systémů, kde se hodnoty S_X pro vybrané

analyty mohou blížit k ±∞. V takovém případě je vliv disperze velmi silný a může dojít až ke kompletnímu rozmytí píku analytu. Nezávisle na sobě Gebauer a kol. [64], [65] a Gaš a kol. [66] zkoumali často využívaný fosfátový pufr při různých hodnotách pH a vymezili oblasti disociačních konstant a limitních mobilit analytů, které v těchto pufrech budou podléhat extrémní EMD.

2.2 Linearizovaný model elektroforézy – simulační software PeakMaster

Dynamické simulace poskytují kompletní náhled do procesu elektromigrace, ale vyžadují delší simulační čas, vyšší výpočetní kapacitu a zkušeného uživatele. Uspořádání kapilární zónové elektroforézy však umožňuje rovnice popisující elektromigraci linearizovat. Linearizovaný model vychází z předpokladu, že se dávkuje tak malé množství analytu, že se složení BGE takřka nemění. Pokud jsou výchozí změny BGE malé, budou také změny v průběhu elektromigrace malé a přímo úměrné. Tento předpoklad vede k výraznému zjednodušení rovnic kontinuity a nalezení jejich analytického řešení. Avšak nesmíme zapomenout, že při nadávkování „většího“ množství analytu se projeví faktory, které linearizovaný model nezahrnuje.

Poppe a kol. [67], [68] jako první zlinearizovali rovnice popisující elektromigraci a ukázali, že jejich řešení vede k problematice matic a jejich vlastních čísel. Na tuto práci navázali Štědrý a kol. [69], kteří sestavili tyto matice tak, že jejich vlastní čísla měla rozměr elektroforetických mobilit (*eigenmobilit*), přičemž některé z nich nepříslušejí žádnému dávkovanému analytu – tzv. systémové eigenmobility. To znamená, že v kapiláře existují zóny – systémové zóny – které se pohybují rychlostí odpovídající těmto mobilitám. Počet těchto systémových zón odpovídá počtu konstituentů daného BGE, přičemž konstituentem se rozumí kyselina, báze i amfolyt bez ohledu na hodnotu pK_A či valenci. V zásadě žádná ze systémových mobilit nenabývá nulové hodnoty, ale obvykle se některé z nich pohybují s mobilitou natolik blízkou nule, že mohou sloužit jako markery elektroosmotického toku.

Štědrý a kol. odvodili linearizovaný model elektromigrace nejprve pro silné elektrolyty [69], pro uni-univalentní slabé elektrolyty [70], a nakonec obecně, bez jakýchkoliv omezení týkajících se složení či valence jednotlivých složek [71]. Tento model byl zabudován do simulačního programu PeakMaster verze 5.2 [72]. Vstupními daty pro simulace jsou fyzikálně-chemické parametry složek BGE a analytu (koncentrace,

limitní mobility, disociační konstanty). Program obsahuje databázi těchto charakteristik pro širokou škálu látek, založenou na Hirokawových tabulkách [29] – [33]. Tuto databázi může uživatel upravovat a rozšiřovat. V rámci programu je možné použít korekci na iontovou sílu, která koriguje limitní mobility na základě Onsagerovy-Fuossovy teorie a koncentrace jednotlivých konstituentů na aktivity užitím Debyeovy-Hückelovy teorie [34], [35]. Uživatel dále může volit instrumentální parametry separace – délku kapiláry k detektoru a její celkovou délku, velikost a polaritu aplikovaného napětí, mobilitu elektroosmotického toku a typ detekce (přímá či nepřímá UV-detekce, vodivostní detekce). Program je schopen vypočítat pH, vodivost, iontovou sílu a pufrační kapacitu BGE. Dále určí efektivní mobilitu analytu, charakteristiky nepřímé a vodivostní detekce analytu [73], včetně hodnoty S_X charakterizující elektromigrační disperzi. Systémové zóny jsou charakterizovány svou mobilitou a amplitudou [74]. Tyto výsledky program poskytuje jak v podobě číselných hodnot příslušných veličin, tak formou simulovaného elektroferogramu. Pro vykreslení tvaru simulovaných píků je použita HVL funkce [57].

V roce 2012 byl tento linearizovaný model rozšířen o nelineární člen migrace [75], [76]. Nová verze programu PeakMaster dokáže předpovědět tvary systémových píků. Elektromigrační disperze je charakterizována nelineární elektroforetickou mobilitou, μ_{EMD}, která odpovídá rozdílu mobility určené z maxima (vrcholu) píku a ze středu odpovídajícího gaussovského píku (neovlivněného EMD). K vykreslení tvarů píků je použita HVLR funkce, kterou jako první odvodil pro chromatografii Houghton [77]. Tato funkce více odpovídá reálným podmínkám při dávkování a dokáže vhodně modelovat i velmi široké zóny (plata). Rozšířený model byl zabudován do programu PeakMaster verze 5.3 a jeho platnost byla ověřena jak pomocí experimentů, tak simulací programem Simul 5 [24].

Zatímco dynamická simulace CZE experimentu programem Simul 5 může zabrat hodiny až dny výpočetního času, PeakMaster 5.3 poskytuje výsledky během několika vteřin. Program Peakmaster 5.3 je volně ke stažení na webových stránkách naší pracovní skupiny (echmet.natur.cuni.cz).

2.3 PeakMaster 5.3 Complex – ověření matematického modelu

V rámci Publikace III jsme představili matematický model zabudovaný do nové verze programu PeakMaster 5.3 Complex. Tento model popisuje systémy, které obsahují pouze dvě složky BGE, neutrální komplexační činidlo a plně nabitý analyt. Komplexaci předpokládáme pouze mezi komplexačním činidlem a analytem ve stechiometrii 1:1. Po zadání komplexačních charakteristik (konstanta stability, mobilita komplexu) program poskytuje dvě charakteristiky EMD: *nonlinear electromigration mobility slope of the analyte zone*, $S_{\mathrm{EMD,A}}$, a *relative velocity slope*, S_{X}. $S_{\mathrm{EMD,A}}$ lze snadno vypočítat z experimentálních či simulovaných elektroferogramů podle následujícího vztahu

$$S_{\mathrm{EMD,A}} = \frac{\mu_{\mathrm{MAX,A}} - \mu_{\mathrm{A,eff}}}{c_{\mathrm{A}}}, \tag{9}$$

kde $\mu_{\mathrm{MAX,A}}$ je mobilita analytu určená z maxima píku, $\mu_{\mathrm{A.eff}}$ je efektivní mobilita analytu určená pomocí HVL funkce a c_{A} je aktuální koncentrace analytu v zóně analytu. S_{X} potom můžeme získat jednoduchým přepočtem:

$$S_{\mathrm{X}} = \frac{1}{2}\frac{S_{\mathrm{EMD,A}}\kappa}{\mu_{\mathrm{A,eff}}}, \tag{10}$$

kde κ je vodivost BGE. Kromě těchto hodnot PeakMaster 5.3 Complex vykresluje také závislost daných veličin na koncentraci komplexačního činidla v BGE.

Platnost představeného modelu jsme ověřovali jak pomocí experimentů, tak pomocí simulací programem Simul 5 Complex. Tři testované systémy se lišily v použitém neutrálním komplexačním činidle (tedy v síle komplexace). Jak je zjevné z Obr. 4, experimenty a simulace se perfektně shodují, co se týče pozice i tvaru píků. Z experimentálních i simulovaných elektroferogramů jsme poté vypočítali hodnoty $S_{\mathrm{EMD,A}}$ a S_{X}. Hodnoty předpovězené programem PeakMaster 5.3 Complex jsou ve výborné shodě s hodnotami simulovanými. Experimentální hodnoty se mírně odchylují, avšak dodržují stejný trend.

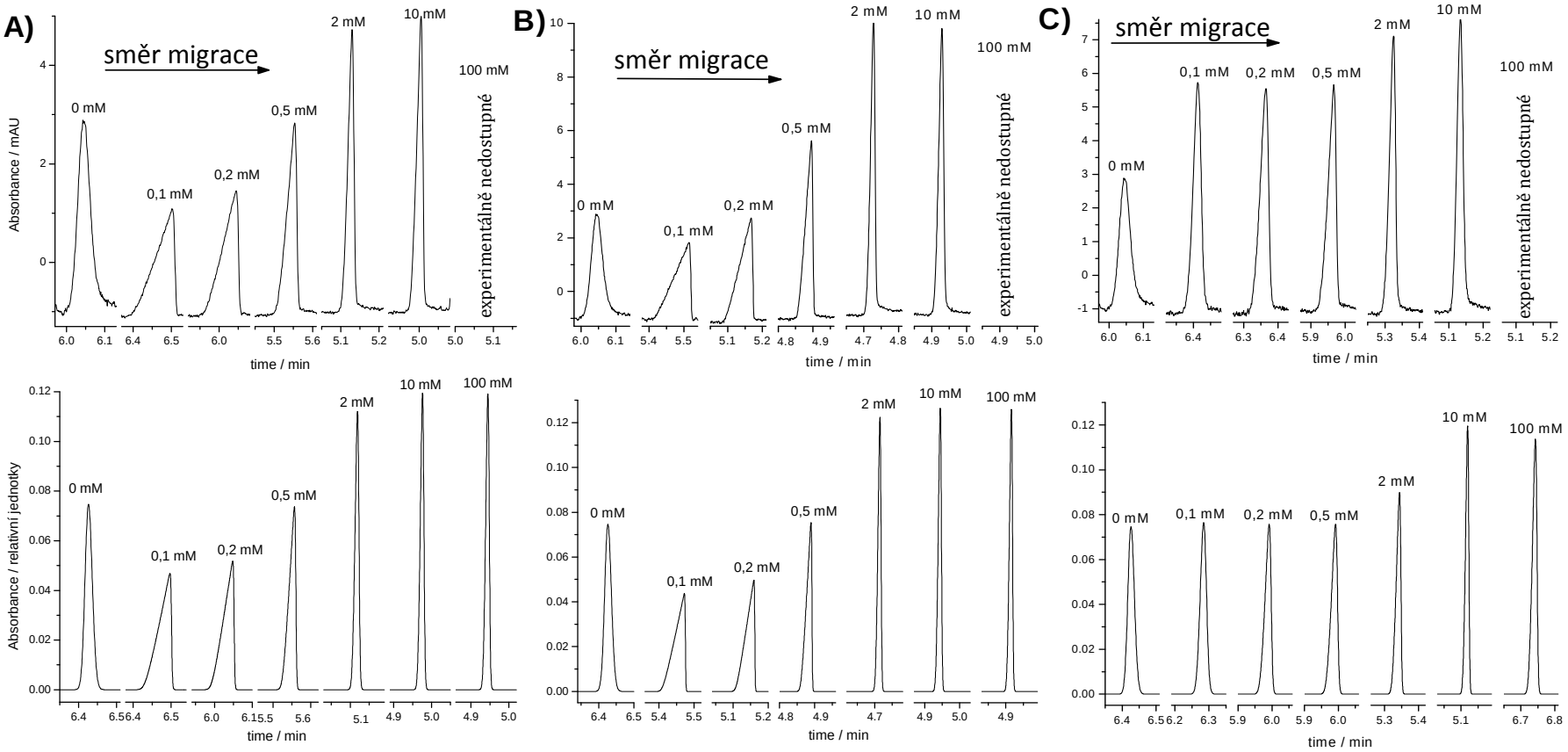

Obr. 4 Srovnání experimentálních (horní řada) a simulovaných (dolní řada) elektroferogramů pro analyt R-flurbiprofen a komplexační činidlo A) β-cyklodextrin, B) heptakis(2,6-di-*O*-methyl)-β-cyklodextrin a C) heptakis(2,3,6-tri-*O*-methyl)-β-cyklodextrin pro různé koncentrace komplexačního činidla v BGE. Jednotlivé píky jsou označeny koncentrací komplexačního činidla v BGE.

2.4 Vliv komplexace na elektromigrační disperzi

Na Obr. 5A je znázorněna závislost $S_{EMD,A}$ na koncentraci komplexačního činidla předpovězená programem PeakMaster 5.3 Complex pro dva ukázkové systémy. V prvním systému (analyt R-flurbiprofen, komplexační činidlo β-cyklodextrin, K = 4 037 (mol dm^{-3})$^{-1}$, μ_{AC} = 8,82×10^{-9} m^{2}V^{-1}s^{-1})‡ pozorujeme po přídavku nepatrného množství komplexačního činidla výraznou EMD píku analytu, která se významně redukuje při koncentraci komplexačního činidla 2 mM. Tomuto průběhu odpovídá výrazné minimum na křivce závislosti $S_{EMD,A}$ na koncentraci komplexačního činidla.

Celková elektromigrační disperze v systémech s neutrálním komplexačním činidlem a plně nabitým analytem se skládá ze tří hlavních příspěvků: (1) vliv analytu na vodivost BGE, (2) vliv komplexace a (3) vliv komplexu analyt-komplexační činidlo na vodivost BGE. V prvním bodě závislosti (c_L = 0 mM) je tvar píku ovlivněn pouze prvním příspěvkem (hodnota $S_{EMD,A}$ je takřka nulová). Naopak při vysoké koncentraci komplexačního činidla v BGE, kdy je takřka všechen analyt přítomen ve formě komplexu, ovlivňuje tvar píku pouze třetí příspěvek (hodnota $S_{EMD,A}$ je také blízká nule). Mezi těmito extrémními hodnotami koncentrace komplexačního činidla v BGE je celková EMD dána kombinací všech tří příspěvků. Vzhledem k takřka zanedbatelným hodnotám $S_{EMD,A}$ pro první a třetí příspěvek, musí hlavní roli v této oblasti koncentrací hrát příspěvek druhý, komplexace.

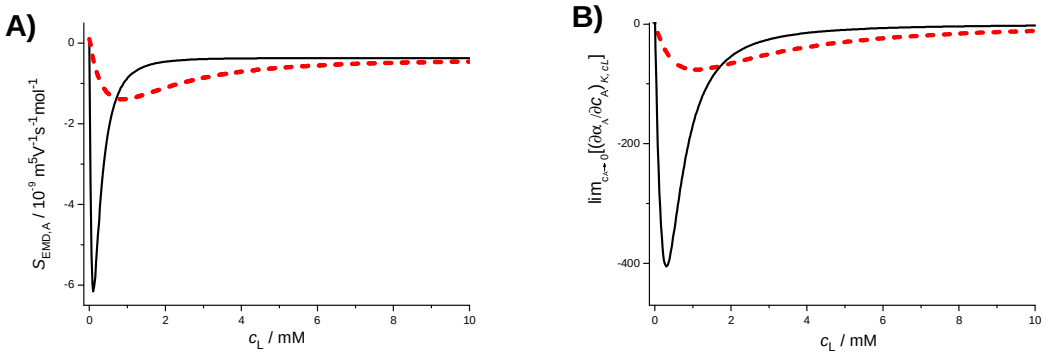

Obr. 5 Závislost $S_{EMD,A}$ předpovězená programem PeakMaster 5.3 Complex (A) a $\lim_{c_A \to 0}\left(\partial\alpha / \partial c_A\right)_{c_L,K}$ (B) na koncentraci komplexačního činidla v BGE. Komplexační činidlo: β-cyklodextrin (černá plná čára), heptakis(2,3,6-tri-*O*-methyl)-β-cyklodextrin (červená přerušovaná čára).

‡Komplexační parametry použité v tomto oddílu práce nejsou korigovány na iontovou sílu a viskozitu prostředí. Odpovídají tedy aktuálním podmínkám experimentů.

Efektivní mobilita analytu závisí na stupni komplexace analytu, α, podle rovnice (6). Vliv EMD se projeví, pokud rychlost migrace závisí na koncentraci analytu v zóně, tedy pokud se α bude výrazně měnit s koncentrací analytu. Změnu stupně komplexace s koncentrací analytu v zóně lze vyjádřit jako parciální derivaci rovnice (7) podle koncentrace analytu v limitní formě, kdy se koncentrace analytu blíží nule:

$$\lim_{c_A \to 0} \left(\frac{\partial \alpha}{\partial c_A} \right)_{c_L, K} = \frac{-2Kc_L}{(Kc_L + 1)^3}. \tag{11}$$

Závislost tohoto parametru na koncentraci komplexačního činidla pro ukázkové systémy je znázorněna na Obr. 5B. Podobnost se závislostí $S_{EMD,A}$ na koncentraci komplexačního činidla (Obr. 5A) je zřejmá. Při nízké koncentraci komplexačního činidla stupeň komplexace analytu závisí velmi výrazně na koncentraci analytu v zóně a pík analytu je silně deformován EMD. Při vyšší koncentraci komplexačního činidla (okolo 2 mM) je již takřka všechen analyt vázán v komplexu, limitní forma parciální derivace se blíží k nule, stupeň komplexace již na koncentraci analytu v zóně takřka nezávisí a EMD se neprojevuje. Což plně souhlasí s předpokladem, že v této oblasti koncentrací komplexačního činidla má největší vliv na EMD právě komplexace analytu s komplexačním činidlem.

Druhý sledovaný systém (analyt R-flurbiprofen, komplexační činidlo heptakis(2,3,6-tri-*O*-methyl)-β-cyklodextrin, K = 552 (mol dm^{-3})$^{-1}$, μ_{AC} = 6,50 × 10^{-9} m^{2}V^{-1}s^{-1}) byl zvolen tak, aby komplexační činidlo a analyt interagovali výrazně slaběji, aby bylo možné určit vliv síly interakce na EMD. V tomto systému píky analytu vykazují takřka gaussovský tvar nezávisle na koncentraci komplexačního činidla v BGE. Také odpovídající závislost $S_{EMD,A}$ na koncentraci komplexačního činidla v BGE vykazuje výrazně mělčí minimum (viz Obr. 5). Vzhledem k nízké konstantě stability (zhruba sedmkrát nižší než v prvním systému) stupeň komplexace analytu nezávisí výrazně na koncentraci analytu v zóně. Úplná komplexace analytu nastává až při vyšší koncentraci komplexačního činidla. Příspěvek komplexace k EMD je tedy nižší, ale přetrvává i do vyšší koncentrace komplexačního činidla v BGE.

V dalším kroku byl pomocí programu PeakMaster 5.3 Complex vysvětlen vliv síly komplexace a mobility vznikajícího komplexu na vývoj EMD. Na Obr. 6A je znázorněna závislost $S_{EMD,A}$ na koncentraci komplexačního činidla v BGE pro teoretické systémy se stejnou mobilitou volného analytu a konstantou stability jako

v prvním ukázkovém systému (μ_A= 19,81 × 10^{-9} $m^2V^{-1}s^{-1}$, K= 4 037 (mol dm^{-3})$^{-1}$), ale pro pět různých mobilit komplexu analyt-komplexační činidlo. Tyto závislosti procházejí výrazným minimem. Se zvyšujícím se rozdílem mobility volného analytu a komplexu je toto minimum výraznější a vede k výraznější EMD a deformovanějším píkům. Toto minimum však nastává při stejné koncentraci komplexačního činidla bez ohledu na rozdíl mobilit. Na Obr. 6B je znázorněna závislost $S_{EMD,A}$ na koncentraci komplexačního činidla v BGE pro teoretické systémy se stejnou mobilitou volného analytu a mobilitou komplexu analyt-komplexační činidlo jako v prvním ukázkovém systému (μ_A = 19,81 × 10^{-9} $m^2V^{-1}s^{-1}$, μ_{AC}= 8,82 × 10^{-9} $m^2V^{-1}s^{-1}$), ale pro pět různých konstant stability. Jak je vidět, se zvyšující se konstantou stability je minimum v závislosti hlubší, ostřejší, nastává při nižší koncentraci komplexačního činidla BGE a při nižší koncentraci komplexačního činidla také dosahuje $S_{EMD,A}$ limitní hodnoty. To znamená, že se zvyšující se konstantou stability je pozorovaná EMD výraznější, ale vliv komplexace na EMD přetrvává na užším intervalu koncentrací komplexačního činidla.

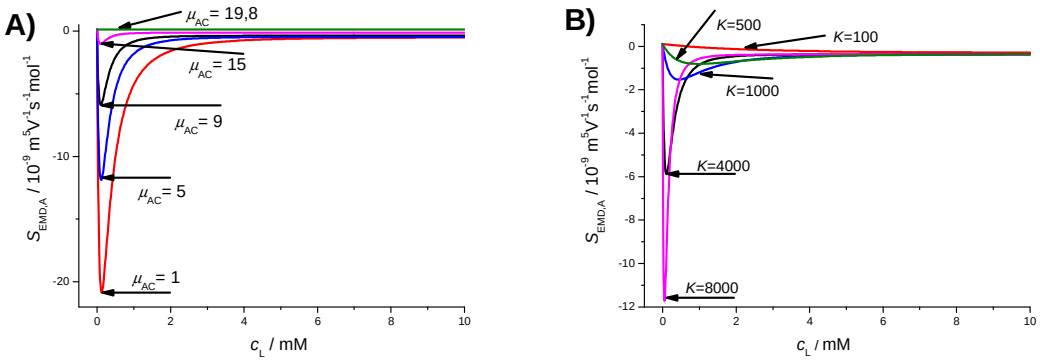

Obr. 6 Závislost $S_{EMD,A}$ na koncentraci komplexačního činidla v BGE pro analyt R-flurbiprofen a různá teoretická komplexační činidla. (A) μ_{AC} = 1, 5, 9, 15 a 19,8 × 10^{-9} $m^2V^{-1}s^{-1}$, K = 4 000 (mol dm^{-3})$^{-1}$. Jednotlivé křivky jsou označeny hodnotou mobility komplexu analyt–komplexační činidlo. (B) μ_{AC} = 9 × 10^{-9} $m^2V^{-1}s^{-1}$, K = 100, 500, 1 000, 4 000 a 8 000 (mol dm^{-3})$^{-1}$. Jednotlivé křivky jsou označeny hodnotou komplexační konstanty.

Nová verze programu PeakMaster 5.3 Complex je schopna během několika vteřin předpovědět tvar píku analytu v systémech obsahující plně nabitý analyt a neutrální komplexační činidlo. Může tedy pomoci vybrat vhodné experimentální podmínky vedoucí k potlačení EMD a optimalizaci separačních podmínek.

3. Komplexace složek pufru s neutrálním komplexačním činidlem: Vliv na určování konstant stability: Publikace V, VI

3.1 Určování konstant stability

Sílu interakce mezi analytem (A) a komplexačním činidlem (C) popisuje konstanta stability. Pro nejjednodušší a zároveň nejčastější stechiometrii interakce 1:1 chemickou rovnováhu vystihuje rovnice:

$$A+C \rightleftharpoons AC \tag{12}$$

a termodynamickou konstantu stability můžeme vyjádřit jako

$$K = \frac{a_{AC}}{a_A a_C}, \tag{13}$$

kde symbol a_i představuje aktivity jednotlivých složek. V praxi se ovšem často používá takzvaná zdánlivá konstanta stability, K':

$$K' = \frac{[AC]}{[A][C]}, \tag{14}$$

kde [ ] přestavuje rovnovážnou molární koncentraci jednotlivých složek. Takto vyjádřená konstanta ale závisí na iontové síle prostředí a platí pouze pro dané experimentální podmínky. V rámci kapilární elektroforézy bylo vyvinuto několik metod vhodných k určení konstant stability: afinitní kapilární elektroforéza (ACE), Hummel-Dreyerova metoda, vakantní afinitní kapilární elektroforéza, metoda vakantních píků, frontální analýza či kontinuální frontální analýza v kapilární elektroforéze. Podrobný popis jednotlivých metod lze najít v několika přehledových článcích [78] – [80].

Nejčastěji používanou metodou k určení konstanty stability v případě rychlého ustavení rovnováhy (zjednodušeně řečeno, pokud je ustavení komplexační rovnováhy rychlejší než separace) je metoda ACE. Ta je založena na určení závislosti efektivní mobility analytu, který je dávkován o konstantní koncentraci, na zvyšující se koncentraci komplexačního činidla v BGE. Efektivní mobilita analytu, $\mu_{A,eff}$, potom závisí na koncentraci komplexačního činidla v BGE podle vztahu

$$\mu_{A,eff} = \frac{\mu_A + \mu_{AC} K'[C]}{1 + K'[C]}, \tag{15}$$

kde μ_A je mobilita volného analytu, μ_{AC} mobilita komplexu a [*C*] je rovnovážná koncentrace komplexačního činidla. Rovnovážnou koncentraci komplexačního činidla je možno nahradit za analytickou při dostatečném nadbytku komplexačního činidla. Tato podmínka může být v CZE zajištěna proložením píku analytu HVL funkcí [57], kdy získáme migrační čas analytu při nekonečném zředění. Rovnici (15) lze převést na jeden z linearizovaných tvarů, které jsou známy v literatuře pod různými názvy [81] – [83]. Konstanty se určují ze směrnic a průsečíků linearizovaných závislostí se souřadnicovými osami. Bowser a kol. [82], [83] však ukázali pomocí simulací Monte Carlo, že nelineární regrese experimentálních dat s rovnicí (15) poskytuje přesnější a správnější výsledky než regrese lineární.

Rovnici (15) lze ovšem k vyhodnocení experimentálních dat použít pouze tehdy, pokud se efektivní mobilita analytu mění jenom v důsledku komplexace. V praxi bývá efektivní mobilita analytu ovlivněna dalšími faktory, jako je měnící se iontová síla, viskozita a teplota BGE. V takovém případě je třeba experimentální data před vyhodnocením vhodně korigovat nebo příslušné korekce zabudovat do regresní funkce [84]. Mnoho autorů tyto faktory vůbec nebere v úvahu. Takto určené konstanty stability jsou ale platné pouze v daných systémech a mohou sloužit jenom jako hrubý odhad síly interakce.

V literatuře lze nalézt více přístupů, jak sledovat a korigovat změny teploty v kapiláře způsobené vznikem Joulova tepla, například pomocí vodivostních měření [85] – [88]. Vliv měnící se viskozity BGE v důsledku zvyšující se koncentrace komplexačního činidla na mobilitu analytu bývá nejčastěji korigována pomocí viskozitního poměru (relativní viskozita) [89] – [92]. Při použití nabitých komplexačních činidel měnící se iontová síla prostředí ovlivňuje jak konstantu stability, tak jednotlivé mobility. V takovém případě je třeba pracovat buď za konstantní iontové síly, nebo data korigovat např. pomocí Onsagerovy-Fuossovy teorie [34], jak ukázali Ehala a kol. [93], [94]. V rámci naší předchozí práce jsme demonstrovali vliv těchto faktorů na určování konstant stability a představili jsme postup, jak stanovit termodynamické konstanty stability neutrálních analytů s nabitým komplexačním činidlem [95]. Navržený postup zohledňuje všechny výše zmíněné faktory ovlivňující stanovení konstant stability.

3.2 Vliv komplexace složek BGE s komplexačním činidlem na určování konstant stability

Interakce analytu s komplexačními činidly je důkladně popsána. Ovšem komplexační činidlo může současně interagovat také se složkami separačního pufru. Tento typ interakce však ještě nebyl v literatuře detailně studován [96] – [99].

V Publikaci V jsme se zaměřili na popis interakce neutrálního komplexačního činidla se složkami separačního pufru a její důsledky na základní vlastnosti použitého pufru jako pH, iontovou sílu či vodivost. Praktickým důsledkům těchto interakcí se věnujeme v Publikaci VI. Prokázali jsme, že interakce komplexačního činidla se složkou pufru může mít za důsledek vznik nežádoucích systémových píků či výrazné zhoršení separace. Další z významných důsledků těchto interakcí je vliv na určování konstant stability – a to jak plně nabitých analytů (silných elektrolytů), tak analytů pouze částečně disociovaných (slabých elektrolytů).

V případě interakce složek pufru s komplexačním pufrem se část komplexačního činidla spotřebuje a rovnovážná koncentrace volného komplexačního činidla se může zásadně lišit od koncentrace analytické. Situace je o to složitější, že nabitá a nenabitá forma složek pufru může interagovat s komplexačním činidlem jinak silně. Pro demonstraci tohoto jevu jsme určili konstantu stability R-flurbiprofenu (plně nabitý za aktuálních experimentálních podmínek) s neutrálním β-cyklodextrinem (β-CD)v několika různých pufrech. Jak je vidět na Obr. 7, komplexační konstanty určené v pufrech obsahujících ethanolamin, kyselinu fosforečnou, amoniak, kyselinu maleinovou nebo tricin (N-(2-hydroxy-1,1-bis(hydroxymethyl)ethyl)glycin) jsou takřka stejné (v rámci experimentální chyby). To znamená, že tyto složky pufrů s β-CD neinteragují takřka vůbec (případně interagují stejně silně). Avšak komplexační konstanty určené v běžně používaných pufrech obsahujících 2-(N-morfolin)ethansulfonovou kyselinu (MES), 3-morfolinpropan-1-sulfonovou kyselinu (MOPS) a N-cyklohexyl-2-aminoethan sulfonovou kyselinu (CHES) jsou významně nižší. Následně jsme stanovili komplexační konstanty ve stejných pufrech, pouze pětkrát zředěných (D). Jak je zřejmé z Obr. 7, v pufrech MES, MOPS a CHES se hodnota komplexační konstanty významně změnila. V případě interagujících pufrů určená komplexační konstanta tedy nezáleží pouze na použitém analytu a komplexačním činidle, ale také na typu a koncentraci pufru. Takto určené zdánlivé konstanty stability jsou platné pouze pro daný systém, jsou

nižší než konstanty termodynamické a mohou poskytovat zcela mylnou informaci o síle interakce.

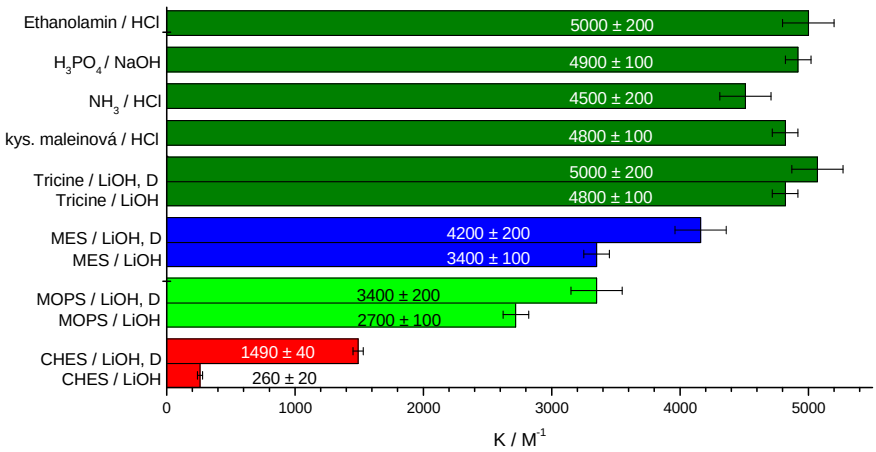

Obr. 7 Komplexační konstanty[§] R-flurbiprofenu s β-CD určené v různých pufrech. Pufr označený písmenem D je 5x zředěný. Přesné složení pufrů a experimentální podmínky jsou uvedeny v *Table 1* v Publikaci VI.

Abychom ověřili sílu interakce jednotlivých složek pufrů s β-CD, provedli jsme sérii experimentů, ve kterých jsme neutrální β-CD nadávkovali v daném pufru a určili jeho efektivní mobilitu. Výsledky jsou shrnuty na Obr. 8. V tricinovém pufru byla mobilita β-CD takřka nulová, nejvyšší mobilitu jsme naopak naměřili v pufru CHES. Toto zjištění plně koresponduje s rozdíly v určených komplexačních konstantách i výsledky měření NMR.

Abychom dokázali, že interakce komplexačního činidla se složkami pufru je hlavní příčinou výše popsaného chování, simulovali jsme ACE experimenty v CHES a tricinovém pufru simulačním programem Simul 5 Complex (nezbytnými vstupními daty byly i komplexační parametry CHES s β-CD, které byly stanoveny pomocí nezávislých měření). Na Obr. 9A je uvedeno srovnání experimentálních a simulovaných dat. Experimentální a simulované body jsou v perfektní shodě, což dokonale podporuje naši hypotézu, že interakce komplexačního činidla se složkami pufru je jediným důvodem výše popsaného chování.

[§]Komplexační parametry použité v tomto oddílu práce jsou korigovány na iontovou sílu, jedná se o parametry termodynamické. Pro přehlednost je uvádíme s jednotkou $(\text{mol dm}^{-3})^{-1}$.

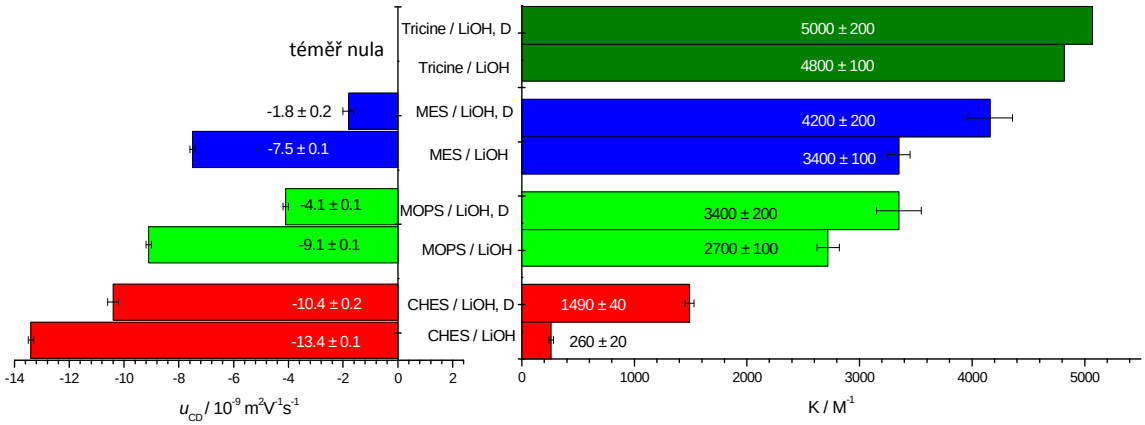

Obr. 8 Efektivní mobilita neutrálního β-CD v různých pufrech v porovnání s hodnotou komplexační konstanty R-flurbiprofenu a β-CD určené metodou ACE v daném pufru. Přesné složení pufrů a experimentální podmínky jsou uvedeny v *Table 1* v Publikaci VI.

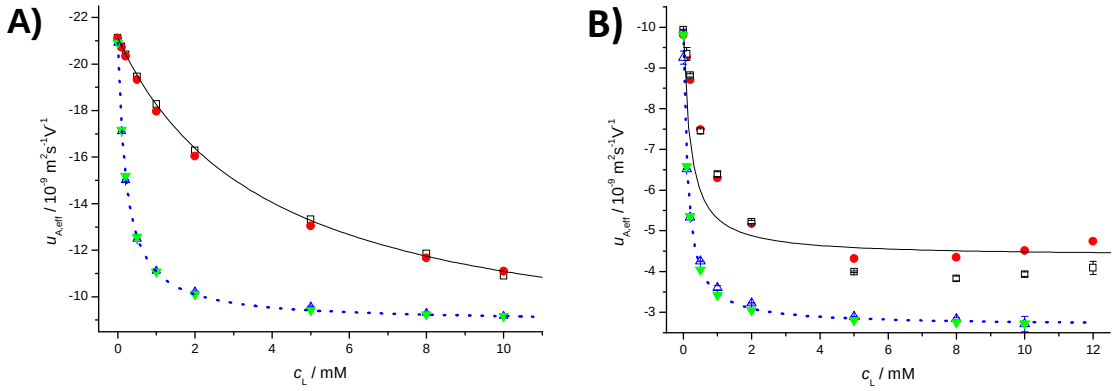

Obr. 9 A: Závislost efektivní mobility plně nabitého R-flurbiprofenu na koncentraci β-CD. ● a □ představují experimentální a simulované body v CHES pufru. ▵ a ▼ představují experimentální a simulované body v tricinovém pufru. Křivky odpovídají regresní analýze regresní funkcí (15). B: Závislost efektivní mobility částečně disociovaného R-flurbiprofenu na koncentraci β-CD. ● a □ představují experimentální a simulované body v pufru s kyselinou benzoovou. ▵ a ▼ představují experimentální a simulované body v acetátovém pufru. Křivky odpovídají regresní analýze regresní funkcí (16).

Významně složitější situace nastává při určování konstanty stability nabité a nenabité formy analytu (slabý elektrolyt). Konstanta stability nenabité formy se určuje při hodnotě pH, kdy je analyt pouze částečně disociován (pH ≐ pK_A). K proložení experimentálních dat se použije následující regresní funkce:

$$\mu_{A,eff} = \mu_A \frac{1 + \frac{\mu_{AC}}{\mu_A} K_{XAc}[C]}{1 + K_{XAc}[C] + \frac{[H_3O^+]}{K_{HA}}(1 + K_{XAn}[C])}, \quad (16)$$

kde K_{XAn} a K_{XAc} jsou komplexační konstanty neutrální a nabité formy analytu, K_{HA} je disociační konstanta analytu. Velmi důležité je v průběhu experimentů držet konstantní experimentální podmínky, především pH. Ovšem interakce složek pufru s komplexačním činidlem může významně pH pufru změnit a tím stanovení konstanty stability neutrální formy analytu znemožnit. K potvrzení této domněnky jsme provedli dvě sady ACE experimentů s R-flurbiprofenem a β-CD v pufrech tvořených kyselinou octovou nebo kyselinou benzoovou a hydroxidem lithným. pH obou pufrů bylo 3,98, R-flurbiprofen je v nich tedy částečně disociovaný (pK_A = 4,16). Pomocí nezávislých experimentů jsme ukázali, že kyselina octová s β-CD nijak významně neinteraguje, zatímco kyselina benzoová interaguje silně. Získané závislosti jsou zobrazeny na Obr. 9B. Experimentální hodnoty získané v acetátovém pufru byly proloženy regresní funkcí (16), komplexační konstanta neutrální formy 11 100 ± 200 (mol dm^{-3})$^{-1}$. Avšak data získaná v pufru s kyselinou benzoovou nevykazují očekávaný hyperbolický průběh a není možné je proložit regresní funkcí (16). Na Obr. 9B jsou zároveň vidět data získaná simulací obou těchto systémů v programu Simul 5 Complex. V případě pufru obsahujícím kyselinu benzoovou je zohledněna komplexace jak analytu, tak kyseliny benzoové s β-CD (příslušné komplexační parametry kyseliny benzoové s β-CD byly stanoveny pomocí nezávislých ACE experimentů). Je zřejmé, že experimentální a simulovaná data jsou v dobré shodě.

Je tedy možno shrnout, že komplexační konstanty určené metodou ACE v pufrech, které interagují s komplexačním činidlem, mohou být zcela nesprávné, poskytovat naprosto mylnou informaci o síle komplexace nebo stanovení úplně znemožnit. Proto by měla být možnost interakce komplexačního činidla se složkami pufru prověřena před samotnými experimenty.

Závěr

Předkládaná dizertační práce byla zaměřena na matematický popis komplexačních systémů v kapilární elektroforéze a možnosti predikce výsledků enantioseparací.

Byl odvozen kompletní teoretický model kapilární elektroforézy s komplexačními rovnováhami. Tento model byl implementován do dynamického simulátoru Simul 5 Complex, který umožňuje simulovat všechny běžně používané metody k určení konstant stability i výsledky enantioseparací. Platnost tohoto modelu a simulátoru byla ověřena pomocí experimentů ve třech různých enantioselektivních systémech. Simulované a experimentální elektroforegramy byly ve výborné shodě, co se týče amplitudy, polohy i tvaru píků analytu (jak z UV, tak vodivostní detekce). Simul 5 Complex je tedy vhodným nástrojem k predikci výsledků enantioseparace a optimalizaci separačního systému.

Zároveň byl odvozen model elektromigrační disperze pro systémy obsahující neutrální komplexační činidlo a plně nabitý analyt. Tento model byl implementován do simulačního programu PeakMaster 5.3 Complex. Nově odvozený model byl ověřen jak experimentálně, tak pomocí simulací v programu Simul 5 Complex. Ke kvantitativnímu popisu deformace píku elektromigrační disperzí byly zvoleny veličiny S_X, *relative velocity slope*, a $S_{EMD,A}$, *the nonlinear mobility slope of the analyte zone*. Předpovězené hodnoty byly v dobré shodě s hodnotami vypočítanými z experimentálních a simulovaných elektroferogramů. Zároveň byl PeakMaster 5.3 Complex použit k vysvětlení vlivu charakteru interakce mezi analytem a komplexačním činidlem na tvar píku. PeakMaster 5.3 Complex tak byl ukázán jako vhodný nástroj k optimalizaci separačních podmínek vedoucí k eliminaci EMD.

Třetí část práce je věnována stanovení konstant stability v systémech, ve kterých složky základního pufru interagují s komplexačním činidlem. Taková interakce může změnit vlastnosti základního elektrolytu jako pH, vodivost či iontovou sílu. Bylo ukázáno, že konstanty stability určené v takových systémech mohou poskytovat zcela mylnou informaci o síle interakce mezi analytem a komplexačním činidlem. Takto určené komplexační parametry závisí nejen na analytu a komplexačním činidle ale také na výběru pufru a dokonce i jeho koncentraci. Stanovení konstanty stability neutrální a nabité formy slabého elektrolytu může být interakcí složek základního elektrolytu s komplexačním činidlem zcela znemožněno. Studované systémy byly nasimulovány

pomocí dynamického simulátoru Simul 5 Complex. Výborná shoda experimentálních a simulovaných dat potvrdila, že interakce komplexačního činidla se složkami základního elektrolytu je jedinou příčinou výše popsaného chování.

Literatura

[1] Vacik J., Fidler V., *Collect. Czech. Chem. Commun.* **1971**, *36*, 2123-2129

[2] Vacik J., Fidler Z., Collect. Czech. Chem.Commun. 1971, *36*, 2343-2346

[3] Moore G. T., *Journal of Chromatography*. **1975**, *106*, 1-16

[4] Gas B., Diplomová práce, Univerzita Karlova v Praze, Praha **1975**

[5] Ryser P., Dissertation, University of Bern, Bern **1976**

[6] Saville D. A., Palusinski O. A., *AIChE J* **1986**, *32*, 207-214

[7] Bier M., Palusinski O. A., Mosher R. A., Saville D. A., *Science* **1983**, *219*, 1281-1287

[8] Palusinski O. A., Graham A., Mosher R. A., Bier M., Saville D. A., *AIChE J* **1986**, *32*, 215-223

[9] Radi P., Schumacher E., *Electrophoresis* **1985**, *6*, 195-200

[10] Roets G. O., Rhodes P. H., Snyder R. S., *Journal of Chromatography* **198**9, *480*, 35-67

[11] Stedry M.,Jaros M.,Gas B., *Journal of Chromatography A* **2002**, *960*, 187-198

[12] Gebauer P., Mala Z., Bocek P., *Electrophoresis* **2009**, *30*, 866-874

[13] Gas B.,Vacik J., Zelensky I., *Journal of Chromatography* **1991**, *545*, 225-237

[14] Thormann W., Firestone M. A., Sloan J. E., Long T. D., Mosher R. A., *Electrophoresis* **1990**, *11*, 298-304

[15] Thormann W., Mosher R. A., *Electrophoresis* **2008**, *29*, 1676-1686

[16] Thormann W., Mosher R. A., *Electrophoresis* **2008**, *29*, 1036-1047

[17] Hruska V., Gas B., Vigh G., *Electrophoresis* **2009**, *30*, 433-443

[18] Thormann W., Caslavska J., Breadmore M. C., Mosher R. A., *Electrophoresis* **2009**, *30*, S16-S26

[19] Thormann W., Breadmore M. C., Caslavska J., Mosher R. A., *Electrophoresis* **2010**, *31*, 726-754

[20] Gas B., *Electrophoresis* **2009**, *30*, S7-S15

[21] Thormann W., Zhang C. X., Caslavska J., Gebauer P., Mosher R. A., *Analytical Chemistry* **1998**, *70*, 549-562

[22] Mao Q., Pawliszyn J., Thormann W., *Analytical Chemistry* **2000**, *72*, 5493-5502

[23] Breadmore M. C., Mosher R. A., Thormann W., *Analytical Chemistry* **2006**, *78*, 538-546

[24] Hruska V., Jaros M., Gas B., *Electrophoresis* **2006**, 27, 984-991

[25] Bercovici M., Lele S. K., Santiago J. G., *Journal of Chromatography A* **2009**, *1216*, 1008-1018

[26] Bercovici M., Lele S. K., Santiago J. G., *Journal of Chromatography A* **2010**, *1217*, 588-599

[27] Mosher R. A., Breadmore M. C., Thormann W., *Electrophoresis* **201**1, *32*, 532-541

[28] Schwer C., Gas B., Lottspeich F., Kenndler E., *Analytical Chemistry* **1993**, *65*, 2108-2115

[29] Hirokawa T., Kiso Y., *Journal of Chrotmatography* **1982**, *248*, 341-362

[30] Hirokawa T., Nishimo M., Aoki N., Kiso Y., Sawamoto Y., Yagi T., Akiyama J., *Journal of Chromatography* **1983**, *271*, D1-D106

[31] Hirokawa T., Gojo T., Kiso Y., *Journal of Chromatography* **1986**, *369*, 59-81

[32] Hirokawa T., Gojo T., Kiso Y., *Journal of Chromatography* **1987**, *390*, 201-223

[33] Hirokawa T., Kiso Y., Gas B., Zuskova I., Vacik J., *Journal of Chromatography* **1993**, *628*, 283-308

[34] Onsager L., Fuoss R. M., *Journal of Physical Chemistry* **1932**, *36*, 2689-2778

[35] Jaros M., Vcelakova K., Zuskova I., Gas B., *Electrophoresis* **2002**, *23*, 2667-2677

[36] Dubrovcakova E., Gas B., Vacik J., Smolkova – Keulemansova E., *Journal of Chromatography* **1992**, *623*, 337-344

[37] Busch M. H. A., Kraak J. C., Poppe H., *Journal of Chromatograpfy A* **1997**, 777, 329-353

[38] Dubsky P., Tesarova E., Gas B., *Electrophoresis* **2004**, *25*, 733-742

[39] Dubsky P., Svobodova J., Gas B., *Journal of Chromatography B* **2008**, *875*, 30-34

[40] Dubsky P., Svobodova J., Tesarova E., Gas B., *Journal of Chromatography B* **2008**, *875*, 35-41

[41] Tesarova E., Sevcik J., Gas B, Armstrong D. W., *Electrophoresis* **2004**, *25*, 2693-2700

[42] Fang N, Chen D. D. Y., *Analytical Chemistry* **2005**, *77*, 840-847

[43] Chen D. D. Y., Fang N., Sun Y., Zheng J.Y., *Electrophoresis* **2007**, *28*, 3214-3222

[44] Righletti P. G., Andreev V. P., Pliss N. S., *Electrophoresis* **2002**, *23*, 889-895

[45] Breadmore M. C., Quirino J. P., Thormann W., *Electrophoresis* **2009**, *30*, 570-578

[46] Breadmore M. C., Kwan H. Y., Caslavska J., Thormann W., *Electrophoresis* **2012**, *33*, 960-971

[47] Rundlett K. L., Armstrong D. W., *Electrophoresis* **2001**, *22*, 1419-1427

[48] Gas B., Zuska J., Coufal P., van der Goor T., *Electrophoresis* **2002**, *23*, 3520-3527

[49] Williams B. A., Vigh G., *Analytical Chemistry* **1996**, *68*, 1174-1180

[50] Williams B. A., Vigh G., *Analytical Chemistry* **1997**, *69*, 4445-4451

[51] Svobodová J., Benes M., Dubsky P., Vigh G., Gas B., *Electrophoresis* **2012**, *33*, 3012-3020

[52] Gas B., Stedry M., Kenndler E., *Electrophoresis* **1997**, *18*, 2123-2133

[53] Gas B., Kenndler E., *Electrophoresis* **2000**, *21*, 3888-3897

[54] Gas B., Kenndler E., *Electrophoresis* **2002**, *23*, 3817-3826

[55] Erny G. L., Bergstrom E. T., GYoodall D. M., *Analytical Chemistry* **2001**, *73*, 4862-4872

[56] Erny G. L., Bergstrom E. T., Goodall D. M., *Journal of Chromatography A* **2002**, *959*, 229-239

[57] Haarhoff P. H., Van der Linde H. J., *Analytical Chemistry* **1966**, *38*, 573-582

[58] Xu X., Kok W. T., Poppe H., *Journal of Chromatography A* **1996**, *741*, 211-227

[59] Gebauer P., Bocek P., *Analytical Chemistry* **1997**, *69*, 1557-1563

[60] Gebauer P., Caslavska J., Thormann W., Bocek P., *Journal of Chromatography A* **1997**, *772*, 63-71

[61] Gebauer P., Borecka P., Bocek P., *Analytical Chemistry* **1998**, *70*, 3397-3406

[62] Gebauer P., Desiderio C.,Fanali S., Bocek P., *Electrophoresis* **1998**, *19*, 701-706

[63] Horka M., Slais K., *Electrophoresis* **2000**, *21*, 2814-2827

[64] Gebauer P., Bocek P., *Electrophoresis* **2000**, *21*, 2809-2813

[65] Gebauer P., Pantuckova P., Bocek P., *Journal of Chromatography A* **2000**, *894*, 89-93

[66] Gas B., Coufal P., Jaros M., Muzikar J., Jelinek I., *Journal of Chromatography A* **2001**, *905*, 269-279

[67] Poppe H., *Journal of Chromatography* **1990**, *506*, 45-60

[68] Poppe H., *Analytical Chemistry* **1992**, *64*, 1908-1919

[69] Stedry M., Jaros M., Gas B., *Journal of Chromatography A* **2002**, *960*, 187-198

[70] Stedry M., Jaros M., Vcelakova K., Gas B., *Electrophoresis* **2003**, *24*, 536-547

[71] Stedry M., Jaros M., Hruska V., Gas B., *Electrophoresis* **2004**, *25*, 3071-3079

[72] Jaros M., Hruska V., Stedry M., Zuskova I., Gas B., *Electrophoresis* **2004**, *25*, 3080-3085

[73] Jaros M., Soga T., van der Goor T., Gas B., *Electrophoresis* **2005**, *26*, 1948-1953

[74] Hruska V., Stedry M., Vcelakova K., Lokajova J., Tesarova E., Jaros M., Gas B., *Electrophoresis* **2006**, *27*, 4610-4617

[75] Hruska V., Riesova M., Gas B., *Electrophoresis* **2012**, *33*, 923-930

[76] Riesova M., Hruska V., Gas V., *Eletrophoresis* **2012**, *33*, 931-937

[77] Houghton G., *Journal of Physical Chemistry* **1963**, *67*, 84-88

[78] Rundlett K. L., Armstrong D. W., *Electrophoresis* **2001**, *22*, 1419-1427

[79] Tanaka Y., Terabe S., *Journal of Chromatography B* **2002**, *768*, 81-92

[80] Jiang C. X., Armstrong D. W., *Electrophoresis* **2010**, *31*, 17-27

[81] Rundlett K. L., Armstrong D. W., *Electrophoresis* **1997**, *18*, 2197-2202

[82] Bowser M. T., Chen D. D. Y., *Journal of Physical Chemistry A* **1998**, *102*, 8063-8071

[83] Bowser M. T., Chen D. D. Y., *Journal of Physical Chemistry A* **1999**, *103*, 197-202

[84] Uselova-Vcelakova K., Zuskova I., Gas B., *Electrophoresis* **2007**, *28*, 2145-2152

[85] Koval D., Kasicka V., Jiracek J., Colinnsova M., *Electrophoresis* **2003**, *24*, 774-781

[86] Koval D., Kasicka V., Jiracek J., Colinnsova M., *Electrophoresis* **2006**, *27*, 4648-4657

[87] Evenhuis C. J., Guijt R. M., Macka M., Marriott P. J., Haddad P. R., *Analytical Chemistry* **2006**, *78*, 2684-2693

[88] Evenhuis C. J., Hruska V.,Guijt R. M., Macka M., Gas B., Marriott P. J., Haddad P. R., *Electrophoresis* **2007**, *28*, 3759-3766

[89] Bowser M. T., Sternberg E.D., Chen D. D. Y., *Electrophoresis* **1997**, *18*, 82-91

[90] Kawaoke J., Gomez F. A., *Journal of Chromatography A* **1998**, *715*, 203-210

[91] Wren S. A. C., Rowe R. C., *Journal of Chromatography* **1992**, *603*, 235-241

[92] Shibukawa A., Lloyd D. K., Wainer I. W., *Chromatographia* **1993**, *35*, 419-429

[93] Ehala S., Dybal J., Makrlik E., Kasicka V., *Journal of Separation Science* **2009**, *32*, 597-604

[94] Ehala S., Makrlik E., Toman P., Kasicka V., *Electrophoresis* **2010**, *31*, 702-708

[95] Benes M., Zuskova I., Svobodova J., Gas B., *Electrophoresis* **2012**, *33*, 1032-1039

[96] Rawjee Y.Y., Williams R. L., Vigh G., *Analytical Chemistry* **1994**, *66*, 3777-3781

[97] Chen Y. R., Ju D. D., Her G. R., *Journal of High Resolution Chromatography* **2000**, *23*, 409-412

[98] Fang L., Yin X. B., Wang E., *Analytical Letters* **2007**, *40*, 3457-3471

[99] Evans C. E., Stalcup A. M., *Chirality* **2003**, *15*, 709-723

Přílohy

A. Seznam publikací

1. Methods for determination of all binding parameters in systems with simultaneous borate and cyclodextrin complexation
J. Svobodová, P. Dubský, E. Tesařová, **M. Beneš**, B. Gaš
Journal of Chromatography A 2011, 1218, 7211-7218

2. Determination of stability constants of complexes of neutral analytes with charged cyclodextrins by capillary zone electrophoresis
M. Beneš, I. Zusková, J. Svobodová, B. Gaš
Electrophoresis 2012, 33, 1032-1039

Publikace I:
3. Simulation of the effects of complex-formation equilibria in electrophoresis: I. Mathematical model
V. Hruška, **M. Beneš**, J. Svobodová, I. Zusková, B. Gaš
Electrophoresis 2012, 33, 938-947

Publikace II:
4. Simulation of the effects of complex-formation equilibria in electrophoresis: II. Experimental verification
J. Svobodová, **M. Beneš**, V. Hruška, K. Ušelová, B. Gaš
Electrophoresis 2012, 33, 948-957

5. Simulation of the effects of complex formation equilibria in electrophoresis: III. Simultaneous effects of chiral selector concentration and background electrolyte pH
J. Svobodová, **M. Beneš**, P. Dubský, G. Vigh, B. Gaš
Electrophoresis, 2012, 33, 3012-3020

Publikace III:
6. A nonlinear electrophoretic model for PeakMaster: Part III. Electromigration dispersion in systems that contain a neutral complex-forming agent and a fully charged analyte. Theory
V. Hruška, J. Svobodová, **M. Beneš**, B. Gaš
Journal of Chromatography A, 2012, 1267, 102-108

Publikace IV:

7. A nonlinear electrophoretic model for PeakMaster: Part IV. Electromigration dispersion in systems that contain a neutral complex-forming agent and a fully charged analyte. Experimental verification
M. Beneš, J. Svobodová, V. Hruška, M. Dvořák, I. Zusková, B. Gaš
Journal ofChromatography A, 2012, 1267, 109-115

8. Applicability and limitations of affinity capillary electrophoresis and vacancy affinity capillary electrophoresis methods for determination of complexation constants
M. Dvořák, J. Svobodová, **M. Beneš**, B. Gaš
Electrophoresis, 2013, 34, 761-767

Publikace V:

9. Complexation of Buffer Constituents with Neutral Complexation Agents: Part I. Impact on Common Buffer Properties
M. Riesová, J. Svobodová, Z. Tošner, **M. Beneš**, E. Tesařová, B. Gaš
Analytical Chemistry, 2013, 85, 8518-8525

Publikace VI:

10. Complexation of Buffer Constituents with Neutral Complexation Agents: Part II. Practical Impact in Capillary Zone Electrophoresis
M. Beneš, M. Riesová, J. Svobodová, E. Tesařová, P. Dubský, B Gaš
Analytical Chemistry, 2013, 85, 8526-8534

B. Seznam konferenčních příspěvků

Přednášky

1. Simul 5 – Let´s Simulate Chiral Separations
M. Beneš, J. Svobodová, V. Hruška, I. Zusková, B. Gaš
11th International Symposium and Summer School on Bioanalysis, září 2011, Graz, Rakousko

2. Electrophoretical Systems with Complexation Agents: Prediction of Electromigration Dispersion
M. Beneš, V. Hruška, J. Svobodová, I. Zusková, B. Gaš
12th Symposium and Summer School on Bioanalysis, červenec 2012, Cluj Napoca, Rumunsko

3. Prediction of Electromigration Dispersion in Electrophoretical Systems with Neutral Complexation Agents
M. Beneš, V. Hruška, J. Svobodová, I. Zusková,B.Gaš
CECE 2012, 9th International Interdisciplinary Meeting on Bioanalysis, listopad 2012, Brno, Česká republika.

4. Complexation with Buffer Constituents: Impact on Determination of Stability Constants
M. Beneš, M. Riesová, J.Svobodová, I.Zusková, B. Gaš
13th Symposium and Summer School on Bioanalysis, červenec 2013, Debrecen, Maďarsko

Postery

1. Determination of Stability Constants of Charged Cyclodextrin Complexes by Capillary Electrophoresis
M. Beneš, J. Svobodová, I. Zusková, B. Gaš
10th Symposium and Summer School on Bioanalysis, červenec 2010, Záhřeb, Chorvatsko

2. Simul 5 – Complexation Equilibria in Simulations of Electrophoresis
M. Beneš, J. Svobodová, V. Hruška, I. Zusková, B. Gaš
Nordic Separation Science Society 6th Conference, srpen 2011, Riga, Lotyšsko

3. Factors Influencing Determination of Stability Constants of Charged Cyclodextrin Complexes by Capillary Electrophoresis
M. Beneš, J. Svobodová, I. Zusková, B. Gaš
ITP 2011, 18th International Symposium on Electro- and Liquid Phase-separation Techniques, srpen 2011, Tbilisi, Gruzie

4. Methods for Determination of All Binding Parameters in Systems with Simultaneous Borate and Cyclodextrin Complexation
M. Beneš, J. Svobodová, P. Dubský, E. Tesařová, B. Gaš
11th International Symposium and Summer School of Bioanalysis, září 2011, Graz, Rakousko

5. Stability Constants of Charged Cyclodextrins with Neutral Analytes – Determination by CE
M. Beneš, J. Svobodová, I. Zusková, B. Gaš
CECE, 8th International Interdisciplinary Meeting on Bioanalysis, listopad 2011, Brno, Česká republika:

6. Prediction of Electromigration Dispersion in Electrophoretical Systems with Complexation Agents
M. Beneš, V. Hruška, J. Svobodová, I. Zusková, B. Gaš
24th International Symposium on Chirality, červen 2012, Fort Worth, TX, USA

7. Complexation of the Buffer Constituents with Complexation Agents Impact on Determination of Stability Constants
M. Beneš, M. Riesová, J. Svobodová, I. Zusková, E. Tesařová, B. Gaš
ITP 2013 – 20th International Symposium on Electro- and Liquid Phase- Separation Techniques, říjen 2013, Tenerife, Kanárské ostrovy (Španělsko)

I.

Simulation of the effects of complex-formation equilibria in electrophoresis: I. Mathematical model

V. Hruška, M. Beneš, J. Svobodová, I. Zusková, B. Gaš
Electrophoresis 2012, 33, 938-947

Vlastimil Hruška[1,2]
Martin Beneš[1]
Jana Svobodová[1]
Iva Zusková[1]
Bohuslav Gaš[1]

[1] Faculty of Science, Department of Physical and Macromolecular Chemistry, Charles University in Prague, Prague, Czech Republic
[2] Agilent Technologies GmbH, Waldbronn, Germany

Received October 6, 2011
Revised October 19, 2011
Accepted October 19, 2011

Research Article

Simulation of the effects of complex-formation equilibria in electrophoresis: I. Mathematical model

Simul 5 Complex is a one-dimensional dynamic simulation software designed for electrophoresis, and it is based on a numerical solution of the governing equations, which include electromigration, diffusion and acid–base equilibria. A new mathematical model has been derived and implemented that extends the simulation capabilities of the program by complexation equilibria. The simulation can be set up with any number of constituents (analytes), which are complexed by one complex-forming agent (ligand). The complexation stoichiometry is 1:1, which is typical for systems containing cyclodextrins as the ligand. Both the analytes and the ligand can have multiple dissociation states. Simul 5 Complex with the complexation mode runs under Windows and can be freely downloaded from our web page http://natur.cuni.cz/gas. The article has two separate parts. Here, the mathematical model is derived and tested by simulating the published results obtained by several methods used for the determination of complexation equilibrium constants: affinity capillary electrophoresis, vacancy affinity capillary electrophoresis, Hummel–Dreyer method, vacancy peak method, frontal analysis, and frontal analysis continuous capillary electrophoresis. In the second part of the paper, the agreement of the simulated and the experimental data is shown and discussed.

Keywords:
Complex-formation equilibria / Continuity equations / Dynamic simulation / Simul 5

DOI 10.1002/elps.201100529

1 Introduction

The development of various mathematical models of electrophoresis and their implementation in computer programs has been in progress for more than 30 years. In the last few years, thanks to the boom in computation power, computer simulations of electromigration started to play a significant role in common laboratory practice. Dynamic simulations enable a better understanding of and better insight into the process of electromigration and allow the determination of the optimum separation conditions without making experiments thus saving experimental time and money. Mathematical models that describe the electromigration separation systems are based on (i) the distribution equations of all forms of constituents undergoing acid–base and complexation equilibria, (ii) the electroneutrality condition, and (iii) the continuity equations. The continuity equations are nonlinear partial differential equations that have no analytical solution but can be solved in time and space numerically by dynamic simulations.

Many mathematical models and computer simulators have been described so far. The list of accessible dynamic simulators, their historical overview, applicability, and information about how the simulations performed are shown in comprehensive reviews [1, 2]. Applications of the three most widely used dynamic simulators (Simul 5, GENTRANS, and SPRESSO) were compared by Thormann et al. [3]. Our laboratory developed the publicly available software Simul 5 [4] and PeakMaster 5 [5, 6] (http://natur.cuni.cz/gas) that enable the prediction of the results of electrophoretic separations and understanding of the behavior of electrophoretic systems. PeakMaster 5 is based on linearized continuity equations and enables the users to calculate the parameters of the background electrolyte (BGE; pH, ionic strength, buffer capacity), the parameters of the separated analytes (effective mobility, relative velocity slope, detector response), and the parameters of the system zones. Simul 5 is a powerful dynamic simulator suitable for the exploration of various electrophoretic systems. Typically, Simul 5 is utilized for the optimization of

Correspondence: Prof. Bohuslav Gaš, Faculty of Science, Charles University in Prague, Albertov 2030, CZ-128 40 Prague 2, Czech Republic
E-mail: gas@natur.cuni.cz
Fax: +420224919752

Abbreviations: FA, frontal analysis; **FACCE**, frontal analysis continuous capillary electrophoresis; **HD**, Hummel–Dreyer method; **VACE**, vacancy affinity capillary electrophoresis; **VP**, vacancy peak method

Colour Online: See the article online to view Figs. 1 in colour.

separation systems, the inspection of various electrophoretic phenomena and various experimental setups, and for educational purposes.

Many dynamic simulators, including Simul 5, can be utilized to simulate isotachophoresis (ITP) [7, 8], isoelectric focusing (IEF) [9, 10], capillary zone electrophoresis (CZE) [11, 12], or isoelectric trapping [13]. However, mathematical models that include complexation equilibria were described only in a few articles and exhibit significant approximations. In 1992, a mathematical model and its numerical solution applicable only for complexation with a neutral additive (β-cyclodextrin) were presented [14]. Later, Busch et al. [15] introduced a simplified model for systems that contain a complexing agent (ligand) to demonstrate the principles and limitations of the methods available for the determination of binding constants by means of capillary electrophoresis (CE). Dubsky et al. [16] presented a simulation program, SimulChir, which is based on a simplified model of electromigration but includes full dynamics of the interconversion of enantiomers in a chiral separation system, so it can be used for the determination of the rate constants of interconversion. In the same year, Tesarova et al. [17] established a mathematical model and the simulator SimulMic. The model was used to describe the separation of neutral analytes in a system that contained a neutral cyclodextrin together with a charged surfactant (SDS). This model is able to simulate separations by micellar electrokinetic capillary chromatography (MEKC). Fang et al. [18, 19] and Righetti et al. [20] introduced programs allowing the simulation of affinity capillary electrophoresis (ACE) experiments but under simplified electromigration conditions. Recently, Breadmore et al. [21] presented a new version of the program GENTRANS that includes complexation equilibria. It allows the simulation of both MEKC with a charged surfactant and the separation of enantiomers with neutral or charged complexing agents (cyclodextrins). However, this is achieved at the cost of some simplifications: the mobilities of the complex and the ligand are assumed to be the same, and the dissociation states of the analytes and the ligand are limited. The latest version of GENTRANS [22] was modified to allow different mobilities for the complex and the ligand and it was used for simulation of ITP and CZE in complexation systems with neutral cyclodextrins.

We introduce a new mathematical model of electromigration, which includes complexation equilibria of analytes with a ligand (typically cyclodextrin) and implement it in our dynamic simulator, Simul 5 Complex. The article is split into two parts. In this first part, we will describe the mathematical model in detail and use it to simulate several standard methods used for the determination of complex formation constants. In the second part, we will show the agreement of the simulated results with our experimental data [23]. Since the theory presented in the text will require the use of many symbols, we list them in Table 1.

Table 1. Table of symbols used.

Symbol	Meaning
subscript i	index over all complex-formation constituents ($i = 1..N_x$)
subscript L	complex-formation agent (ligand)
subscript k	index over all constituents including ligand
subscript f	denotes all free and complexed forms of k-th constituent
subscript x	denotes quantity related to complexation equilibria
z and subscript z	charge number of ionic forms of all constituents except ligand
l and subscript l	charge number of ionic forms of ligand
subscripts H, OH	quantity related to hydronium and hydroxide ions, respectively
N_x	number of constituents complexed by ligand
n_i, n_L	the most negative charge number
p_i, p_L	the most positive charge number
$K_{i,z}$, $K_{L,l}$	acid–base equilibrium constant
$K_{x,i,z,l}$	complex formation equilibrium constant
K_w	ionic product of water
$L_{i,z}$, $L_{L,l}$	cumulative acid–base equilibrium constant
c_i, c_L	total concentration
$c_{i,z}$, $c_{L,l}$	ionic concentration
$c_{x,i,z,l}$	ionic concentration of complex
$\alpha_{i,z}$, $\alpha_{x,i,z,l}$, $\alpha_{L,i,z,l}$	molar fraction
α_0, B_i	auxiliary quantities defined by Eqs. (23) and (24)
J	molar flux
D	diffusion coefficient
u	electrophoretic mobility (unsigned value)
u_{eff}	effective electrophoretic mobility
v_{EOF}	velocity of electroosmotic flow
j, j_{diff}	current density and diffusion current density
κ	electric conductivity
F	faraday constant
λ	molar fraction of the most negative form of the ligand
Z, b	substituting some summation (defined in Table 2)
L	function derived from total concentration of ligand for determination of c_H and λ
G	electroneutrality function for determination of c_H and λ

2 Theory

2.1 Definition of acid–base and complexation equilibria for Simul 5 Complex

We adopted a general model of complex-formation systems in solutions. We assume that the electrophoretic system contains only one constituent, the ligand, which can form complexes with other constituents. The only allowed ratio of complexation is 1:1. The continuity equations consider only the electromigration and diffusion flux and the electroosmotic flow. We do not consider any other features or effects such as the dependence of ionic mobilities and equilibrium constants on the ionic strength or temperature of the BGE. Therefore,

simulations should use the input parameters that correspond to the actual experimental conditions.

The complex-forming agent will be referred to as the ligand and in equations it will be denoted with a subscript *L*. The number of complexed constituents, N_x, is not limited. There is no limitation on the acid–base type of any of the complexed constituents: they can be neutral, weak bases, or acids or ampholytes. Their most negative and most positive charge numbers are denoted by n_i and p_i, respectively ($n_i \leq 0$, $p_i \geq 0$), where subscript i represents the complexed constituents ($i = 1, \ldots, N_x$). Note that the expression "ionic forms" includes not only the charged forms, but also the neutral form of a given constituent. We allowed acid–base equilibria for the ligand as well, so it can be a general ampholyte and its limiting charge numbers are n_L and p_L. To decrease the number of input constants needed for the simulation, we introduced a special feature for the ligand: all ionic forms of the ligand need not be defined, so both n_L and p_L can be positive, negative, or even equal to each other, which would stand for a strong electrolyte ion. A typical example where this feature can be used is the case of highly sulfated cyclodextrins, which behave as strong electrolyte ions, e.g., with a charge number −7, so $n_L = -7$ and $p_L = -7$. There is no need to specify complexation constants and mobilities for the ionic states 0 to −6.

2.2 Acid–base equilibrium

Acid–base equilibrium constants, $K_{i,z}$, are defined as [24]

$$K_{i,z} = \begin{cases} z < 0 & \dfrac{c_{i,z} c_H}{c_{i,z+1}} \\ z = 0 & 1 \\ z > 0 & \dfrac{c_{i,z-1} c_H}{c_{i,z}} \end{cases} \tag{1}$$

where c stands for the (ionic) concentration of the noncomplexed ionic forms in solution, subscript H for the hydronium ions, and z for the charge number of an ionic form. $K_{i,0}$ is 1 since there is no acid–base equilibrium. For all constituents, which are present also in a neutral form (all except the ligand), we can group the equilibrium constants into the cumulative form, $L_{i,z}$ [24]

$$c_{i,z} = c_{i,0} L_{i,z} c_H^z \tag{2}$$

$$L_{i,z} = \begin{cases} z < 0 & \displaystyle\prod_{z'=z}^{-1} \frac{1}{K_{i,z'}} \\ z = 0 & 1 \\ z > 0 & \displaystyle\prod_{z'=1}^{z} K_{i,z'} \end{cases} \tag{3}$$

Note that for the cumulative constants we adopted the notation from our previous paper [24], so here the letter 'L' in $L_{i,z}$ does not mean the ligand. When defining the cumulative constants for the ligand, $L_{L,l}$, where l stands for the charge number of the ionic form of the ligand, we reformulated Eq. 2 for the most negative form with charge number n_L, because it is always defined

$$c_{L,l} = c_{L,n_L} L_{L,l} c_H^{l-n_L} \tag{4}$$

$$L_{L,l} = \begin{cases} l < 0 & n_L < 0 & \displaystyle\prod_{z=n_L}^{l-1} K_{L,z} \\ l \geq 0 & n_L < 0 & \displaystyle\prod_{z=n_L}^{l} K_{L,z} \\ l > 0 & n_L \geq 0 & \displaystyle\prod_{z=n_L+1}^{l} K_{L,z} \\ l = n_L & & 1 \end{cases} \tag{5}$$

2.3 Complex formation equilibria

The complex formation equilibrium for the i-th complexed constituent in its ionic form with charge number z, A_i^z, and a ligand in its ionic form with charge number l, L^l, is described by the equilibrium constant $K_{x,i,z,l}$

$$A_i^z + L^l \overset{K_{x,i,z,l}}{\longleftrightarrow} \left(A_i^z L^l\right)^{z+l} \tag{6}$$

$$K_{x,i,z,l} = \frac{c_{x,i,z,l}}{c_{i,z} c_{L,l}} \tag{7}$$

where $c_{x,i,z,l}$ stands for the ionic concentration of the complex formed. The complex equilibria, together with the acid–base equilibria, help us to determine all unknown concentrations of the free and complexed ionic forms of all constituents as a function of the total (net) concentrations of all complexed constituents, c_i, and the ligand, c_L. The total concentration is a sum over all the free and complexed forms

$$c_i = \sum_{z=n_i}^{p_i} c_{i,z} + \sum_{z=n_i}^{p_i} \sum_{l=n_L}^{p_L} c_{x,i,z,l} \tag{8}$$

$$c_L = \sum_{l=n_L}^{p_L} c_{L,l} + \sum_{i=1}^{N_x} \sum_{z=n_i}^{p_i} \sum_{l=n_L}^{p_L} c_{x,i,z,l} \tag{9}$$

The last unspecified ionic species are the hydroxide and hydronium ions. The electroneutrality condition enables the determination of the unknown concentration of hydronium ions c_H

$$G = c_H - \frac{K_w}{c_H} + \sum_{i=1}^{N_x} \sum_{z=n_i}^{p_i} z c_{i,z} + \sum_{l=n_L}^{p_L} l c_{L,l} + \sum_{i=1}^{N_x} \sum_{z=n_i}^{p_i} \sum_{l=n_L}^{p_L} (z+l)\, c_{x,i,z,l} = 0 \tag{10}$$

where we substituted the concentration of hydroxide ions, c_{OH}, by the expression obtained from the ionic product of water (autoprotolysis), $K_w = c_H c_{OH}$. The only remaining total concentrations of the complexed constituents and the ligand,

c_i and c_L, are determined by solving the set of continuity equations [4, 25].

2.4 Continuity equations

Simul 5 Complex solves the set of one-dimensional partial differential continuity equations that express the evolution of the total concentrations in time and space [4]. A general notation for both the ligand and all the other constituents ($k = L, 1, \ldots, N_x$) is

$$\frac{\partial c_k}{\partial t} = -\sum_f \left(\frac{\partial J_{k,f}}{\partial x}\right) \tag{11}$$

where the summation variable f stands for all the free and complexed forms of the k-th constituent and the quantity $J_{k,f}$ is the molar flux, which consists of diffusion, electromigration, and electroosmotic flow with a velocity v_{EOF}

$$J_{k,f} = -D_{k,f}\frac{\partial c_{k,f}}{\partial x} + \frac{\mathrm{sgn}\left(z_{k,f}\right) c_{k,f} u_{k,f}}{\kappa}\left(j - j_{\mathrm{diff}}\right) + v_{EOF} c_{k,f} \tag{12}$$

where D is the diffusion coefficient, u is the ionic mobility, which is an unsigned quantity, j is the current density, j_{diff} is the diffusion current density, and κ is the electric conductivity

$$j_{\mathrm{diff}} = -F\left[\sum_k \sum_f \left(z_{k,f} D_{k,f}\frac{\partial c_{k,f}}{\partial x}\right) + D_{\mathrm{H}}\frac{\partial c_{\mathrm{H}}}{\partial x} - D_{\mathrm{OH}}\frac{\partial c_{\mathrm{OH}}}{\partial x}\right] \tag{13}$$

$$\kappa = F\left[\sum_k \sum_f \left(\left|z_{k,f}\right| u_{k,f} c_{k,f}\right) + u_{\mathrm{H}} c_{\mathrm{H}} + u_{\mathrm{OH}} c_{OH}\right] \tag{14}$$

Here, F is the Faraday constant. The diffusion current density, j_{diff}, or diffusion potential (j_{diff}/κ) originates from a potential formed by the diffusive transport of charged ions with different velocities. Our approach for the numerical solution of the continuity equations is described in the section A.1 of Appendix.

A.5 Rearrangement of the coupled acid–base and complexation equilibrium equations for use in the multivariate Newton–Raphson method

Prior to solving the set of continuity equations (11), we have to solve the acid–base equilibria together with the complex formation equilibria given by set of Eqs. (1–10). It is advantageous for further calculations to introduce a molar fraction α for each form of all of the complexed constituents and of the ligand. Then, we can express the ionic concentrations as a product of the total concentration and the molar fraction

$$c_{i,z} = c_i \alpha_{i,z} \tag{15}$$

$$c_{L,l} = c_L \alpha_{L,l} \tag{16}$$

$$c_{x,i,z,l} = c_{i,z} c_{L,l} K_{x,i,z,l} = c_i \alpha_{x,i,z,l} = c_L \alpha_{L,i,z,l} \tag{17}$$

Note that Eq. (17) expresses the dual meaning of the molar fraction for the complexed forms, because it is treated both as the molar fraction of the forms of the complexed constituents ($\alpha_{x,i,z,l}$) and of the ligand forms ($\alpha_{L,i,z,l}$). It follows from Eq. (17) that

$$\alpha_{x,i,z,l} = c_L \alpha_{i,z} \alpha_{L,l} K_{x,i,z,l} \tag{18}$$

$$\alpha_{L,i,z,l} = c_i \alpha_{i,z} \alpha_{L,l} K_{x,i,z,l} \tag{19}$$

Solving the set of equations for the coupled equilibria can be reduced to the calculation of two characteristic unknown variables, which we have to choose—one for the acid–base equilibria and one for complexation equilibria. For the acid–base equilibria, it is obvious to choose the hydronium ion concentration, c_{H} [24]. For the complexation equilibria, we utilize the molar fraction of the most negative form of the ligand, α_{L,n_L}, which will be denoted for simplicity as λ

$$\lambda \equiv \alpha_{L,n_L} \tag{20}$$

Using Eq. (4), the molar fraction of the free ligand forms, $\alpha_{L,l}$, can be obtained as

$$\alpha_{L,l} = L_{L,l} c_H^{l-n_L} \lambda \tag{21}$$

Combination of Eqs. (2) and (8) allows us to express the molar fraction of the free forms in a solution, $\alpha_{i,z}$, as

$$\alpha_{i,z} = \alpha_{0,i,z} B_i \tag{22}$$

where $\alpha_{0,i,z}$ is an auxiliary quantity

$$\alpha_{0,i,z} = \frac{L_{i,z} c_H^z}{\sum_{z'=n_i}^{p_i} L_{i,z'} c_H^{z'}} \tag{23}$$

The quantity B_i is a factor between 0 and 1 that expresses the degree of complexation, i.e., it is zero for complete complexation and 1 for complete lack of complexation of the i-th constituent

$$B_i = \frac{1}{1 + b_{0,i} c_L \lambda} \tag{24}$$

The term $b_{0,i}$, together with the other summations, are defined in Table 2. The summations help the simplification of the equations and reduce size of the source code of the software. The values c_{H} and λ can be found from the total balance of all forms of the ligand, Eq. (9), and from the electroneutrality condition, Eq. (10). These equations are

Table 2. Substitution of some common summations.

$Z_{0L} = \sum_{l=n_L}^{p_L} L_{L,l} c_H^{l-n_L}$	$(Z_{0,i} = 1)$	$b_{0,i} = \sum_{z=n_i}^{p_i} \sum_{l=n_L}^{p_L} L_{L,l} c_H^{l-n_L} K_{x,i,z,l} \alpha_{0,i,z}$
$Z_{1L} = \sum_{l=n_L}^{p_L} l L_{L,l} c_H^{l-n_L}$	$Z_{1,i} = \sum_{z=n_i}^{p_i} z\alpha_{0,i,z}$	$b_{1,i} = \sum_{z=n_i}^{p_i} \sum_{l=n_L}^{p_L} (z+l) L_{L,l} c_H^{l-n_L} K_{x,i,z,l} \alpha_{0,i,z}$
$Z_{2L} = \sum_{l=n_L}^{p_L} l^2 L_{L,l} c_H^{l-n_L}$	$Z_{2,i} = \sum_{z=n_i}^{p_i} z^2\alpha_{0,i,z}$	$b_{2,i} = \sum_{z=n_i}^{p_i} \sum_{l=n_L}^{p_L} (z+l)^2 L_{L,l} c_H^{l-n_L} K_{x,i,z,l} \alpha_{0,i,z}$

The number in the subscript represents the exponent of the charge number in the summation. $\alpha_{0,i,z}$ defined in Eq. (23).

nonlinear in c_H and λ so one has to use an adequate numerical method to solve them. We have chosen a method with fast convergence, the multivariate Newton–Raphson method, which is described in the Section A.2 of Appendix. The substitutions in Table 2 enable us to formulate Eqs. (9) and (10) in compact forms

$$G = c_H - \frac{K_w}{c_H} + c_L \lambda Z_{1L} + \sum_{i=1}^{N_x} c_i B_i (Z_{1,i} + c_L \lambda b_{1,i}) \quad (25)$$

$$L = -1 + Z_{0L}\lambda + \lambda \sum_{i=1}^{N_x} c_i B_i b_{0,i} \quad (26)$$

The multivariate Newton–Raphson method iteratively finds the c_H and λ values to obtain zero G and L.

3 Results and discussion

3.1 Simulation of various experimental setups used for determination of the complexation parameters

Simul 5 Complex with the implemented complexation mode is a powerful tool that can be used for the simulation of electrophoretic systems that contain compounds that undergo complexation, e.g., enantiomer separation systems. We demonstrate the use of Simul 5 Complex for the simulation of several experimental setups that were applied for the determination of complexation parameters: ACE, vacancy affinity capillary electrophoresis (VACE), Hummel–Dreyer method (HD), vacancy peak method (VP), frontal analysis (FA), and frontal analysis continuous capillary electrophoresis (FACCE). The principles of these methods are summarized in several papers [15, 19, 26–29]. As already mentioned in the section 2, complexation ratio 1:1 is considered during the simulations. Although 1:1 complexation ratio is the most common for analyte–cyclodextrin complexes, there are also other ratios mentioned in the literature [30].

Simulations of the experimental setups of the methods were performed based on the actual experimental data [23]. The analyte is fully negatively charged (R-flurbiprofen: pKa = 4.19, limiting mobility 24.5×10^{-9} m^2 s^{-1} V^{-1}) and the chiral selector is a neutral cyclodextrin (6-*O*-α-maltosyl-β-cyclodextrin hydrate). The running buffer consists of 50 mM Tris and 50 mM Tricine. The samples were injected directly in the running buffer, only in the case of ACE method the buffer was diluted in the sample zone (48 mM Tris and 48 mM Tricine). The concentrations of analyte and chiral selector in the sample zone and in the BGE are shown in Table 3. The complexation parameters were determined by ACE experiments: the complexation constant is 3610 ± 123 dm^3 mol^{-1} and the mobility of the complex is 7.60 ± 0.03× 10^{-9} m^2 s^{-1} V^{-1}. Simulations for each method were performed at two different cyclodextrin concentrations in order to discuss the effects of the chiral selector concentration on the studied parameters in the electropherograms. The parameters used for the simulations are shown in Table 3. The electroosmotic flow (EOF) movement was imitated by the movement of the detector, which was initially situated outside the capillary. The voltage was adjusted to keep the same electric field strength as during the experiments. The number of nodes in the x axis was 50 000. The simulations were performed by the computer with Intel® Core™ i7-960 Processor 3.20 GHz. The simulation time was in the range of hours.

Simul 5 Complex can be downloaded as freeware from our web page http://www.natur.cuni.cz/gas together with the configuration files for easy setup of the methods as discussed next.

3.2 Affinity capillary electrophoresis (ACE)

ACE is the most frequently used method for the determination of the complexation parameters of interacting compounds by capillary electrophoresis [31]. The ligand is usually present in the BGE and its concentration is varied in a series of experiments while the analyte is injected as the sample. The complexation parameters are calculated from the dependence of the effective mobility of the analyte, u_{eff}, on the concentration of the chiral selector, c_L, in the BGE. For the simple but common case of a monovalent analyte complexing with a neutral ligand, we used the effective mobility dependence as follows

$$u_{eff} = \frac{u_i + K_{x,i} c_L u_{x,i}}{1 + K_{x,i} c_L} \quad (27)$$

where u_i and $u_{x,i}$ are the mobilities of the free analyte and of the complex, respectively, and $K_{x,i}$ is the complexation constant. The actual experiments need to be performed at constant ionic strength in order to avoid the dependence of parameters on the ionic strength. Increasing the ligand concentration results in the decrease of the effective mobility of

Table 3. Simulations parameters for the different experimental setups used in the methods designed for the determination of the complexation parameters.

Method	c_A(mM)		c_L(mM)		u_{EOF}(10^{-9} m^2 s^{-1} V^{-1})	U(V)	l_{TOT}(mm)	l_{DET}(mm)	l_{inj}(mm)	Peak width(mm)	Peak edge width(mm)
	c(inj)	c	c(inj)	c							
ACE	0.3	0	2	2	52.8	10 261	220	651	200	0.4	0.2
VACE	0	0.3	0	2	52.8	10 261	220	651	200	0.4	0.2
FA	0.3	0	2	0	52.8	13 993	300	741	290	15	0.2
FA (short capillary)	0.3	0	2	0	52.8	13 993	300	331	290	15	0.2
FACCE	0.3	0	2	0	–52.8	–13 993	300	451	0	15	0.2

c_A and c_L is the concentration of analyte (R-flurbiprofen) and chiral selector, respectively, c(inj) is the concentration in the sample zone, c is the concentration in the BGE, u_{EOF} is the electroosmotic flow mobility, l_{TOT} is the total length of capillary, l_{DET} is the position of detector, and l_{inj} is the injection site.

the analyte due to the formation of the analyte–cyclodextrin complex, which has a lower mobility than the free analyte. As an example, the simulations of the ACE experiments for two cyclodextrin concentrations are shown in Fig. 1A. Clearly, at higher concentration of the ligand (cyclodextrin), the analyte peak appears closer to that of the EOF marker, so its mobility in absolute value is lower than in the system where the concentration of the cyclodextrin is lower.

The experimental setup used in the simulations of ACE is also applicable for the HD method, the only difference is in the data evaluation. The complexation constants are determined from the height or the area of the peak related to the

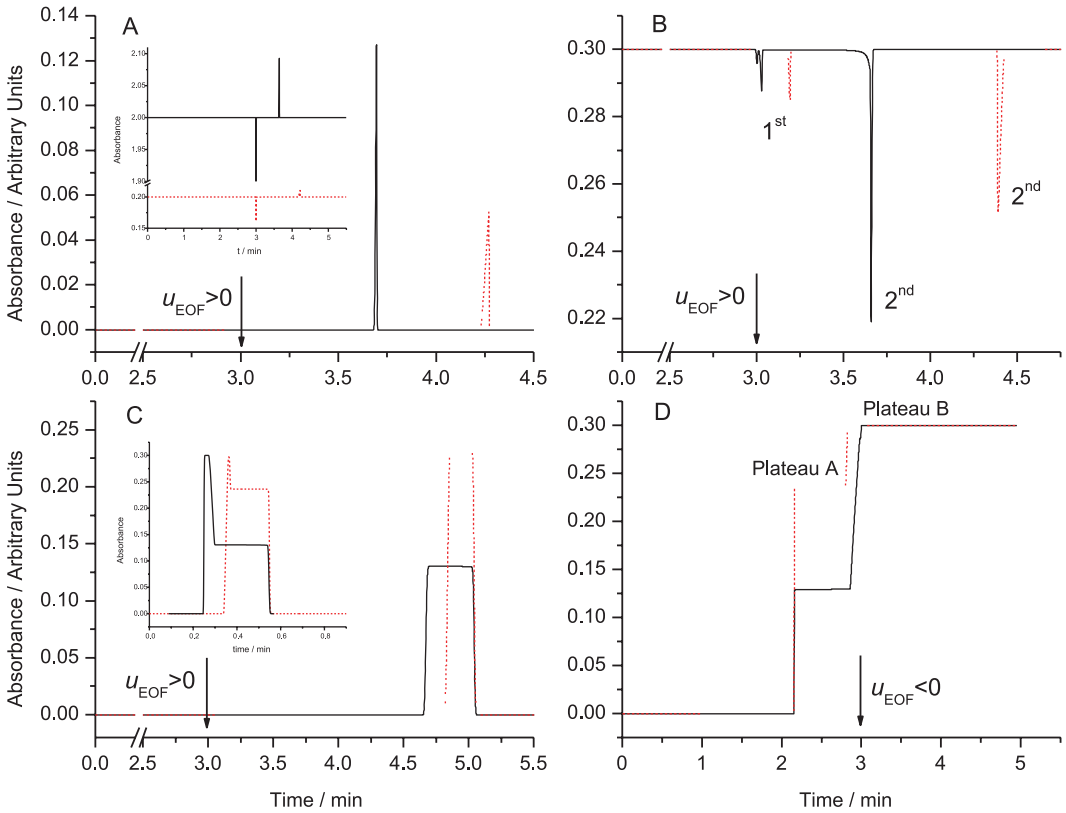

Figure 1. Simulated electropherograms of different experimental setups used in the methods designed for the determination of the complexation parameters: ACE (A), HD (A insert), VACE/VP (B), FA (C), FACCE (D). Insert C: FA with shorter capillary. The parameters of the simulations are based on the actual experimental data for the analyte (R-flurbiprofen) and the ligand (6-*O*-α-maltosyl-β-cyclodextrin hydrate), see Table 3. Complexation parameters: complexation constant is 3610 ± 123 dm^3 mol^{-1} and the mobility of the complex is 7.60 ± 0.03 × 10^{-9} m^2 s^{-1} V^{-1}. The record of UV direct detection (corresponding to the concentration of the analyte) is shown for majority of the methods, UV indirect detection (corresponding to concentration of the ligand) is presented for the HD and VACE methods. Simulations for each method were performed at two different concentrations of cyclodextrin: 0.2 mM (dashed line) and 2 mM (solid line). The position of the EOF marker peak is indicated by an arrow and its polarity is denoted by $u_{EOF} < 0$ or > 0.

ligand, therefore, the HD method requires an external calibration as discussed in Reference [32]. In Fig. 1A (inserted graph), the simulated concentration profile of the ligand is shown. The positive peak is associated with the complex, the negative one with the ligand. The height/area of the negative peak is related to the amount of the ligand bounded in the complex. The higher the concentration of the ligand in the BGE, the larger the amount of the complex formed, the simulated profiles show a larger negative peak.

3.3 Vacancy affinity capillary electrophoresis (VACE)

In the VACE method, both the analyte and the ligand are constituents of the BGE and the BGE without the analyte or the ligand is injected as a sample. Two negative system peaks (related to the analyte and the ligand) appear in the electropherogram. The presence of both the ligand and the analyte in the BGE ensures a sufficient background signal that facilitates the detection of these peaks. The concentration of one of the constituents in the BGE (either the ligand or the analyte) is varied while the concentration of the other one is fixed. The mobilities of the system peaks are determined as a function of the concentration of the constituent in the BGE, and the complexation parameters are evaluated by a similar procedure as in the ACE method as discussed in References [33, 34]. The simulated electropherograms for the VACE/VP experiments shown in Fig. 1B indicate that two negative system peaks and a small system peak with zero mobility appear. The mobilities of the system peaks are related to the fraction of the complexed analyte and the complexed ligand. The mobility of the slower system peak (the first peak after the peak of the EOF marker) is related to the fraction of the ligand that is complexed with the analyte. The dependence of the fraction of the complexed ligand on concentration of the ligand can be described for our particular system by the following equation

$$\alpha_L = \frac{2Kc_A}{K(c_A + c_L) + 1 + \sqrt{[K(c_A + c_L) + 1]^2 - 4K^2 c_A c_L}} \quad (28)$$

This dependence is shown in Fig. 2. When the concentration of the ligand is increased, the fraction of the complexed ligand and, consequently, the mobility of this system peak decrease. The mobility of the second system peak (the second peak after the peak of the EOF marker) depends mainly on the fraction of the complexed analyte and decreases as the concentration of the ligand is increased, similarly to the ACE experiments. This system peak is generally used for the determination of the complexation parameters, because usually its mobility depends on the ligand concentration more significantly than the mobility of the first system peak.

The same experimental setup is used for VP as well. In contrast to the VACE experiment, in the VP method the complexation parameters are determined from the height/area of the system peaks. An external calibration and a different data evaluation procedure are required.

3.4 Frontal analysis (FA)

The FA method is often utilized for the determination of the complexation parameters in systems where the complexation constants are high, e.g., for the binding of a drug to a protein [35]. In the setup of the FA experiment, the running buffer is used as the BGE and a large plug of the preequilibrated mixture of the analyte and the ligand is injected as the sample. Since the mobilities of the free analyte and the analyte–ligand complex are different, the free analyte migrates out of the sample plug after voltage is applied. In the resulting electropherogram, there is a plateau that corresponds to the free analyte and another peak/plateau that corresponds to the equilibrated mixture of the free analyte, the ligand, and the analyte–ligand complex. Thus, using a calibration curve, the concentration of the free analyte can be determined from the height of the free analyte plateau. Consequently, the complexation parameters are calculated from the experimentally determined free analyte concentration and known total analyte concentration. This method is especially useful when the complexation constants are in the range of 10^3–10^8 dm^3 mol^{-1} [36].

As shown in Fig. 1C, there is no plateau/peak for the equilibrated mixture connected to the plateau of the free analyte in the simulated electropherograms. The reason is that the complexation constant in our particular system is rather low, 3610 dm^3 mol^{-1}, so the entire amount of the analyte leaked out from the sample plug during the separation. To reveal that Simul 5 Complex is able to predict the typical elution profile for FA experiments, the simulation was performed with the same complexation parameters but with a shorter capillary (see Table 3)-–see Fig. 1C insert. During the shorter analysis time, a fraction of the analyte still remains complexed in the sample plug so there are two plateaus, or rather, there is a plateau connected to the peak of the equilibrated mixture. It is obvious from the simulations that the last boundary of the analyte plateau migrates with a mobility that is independent

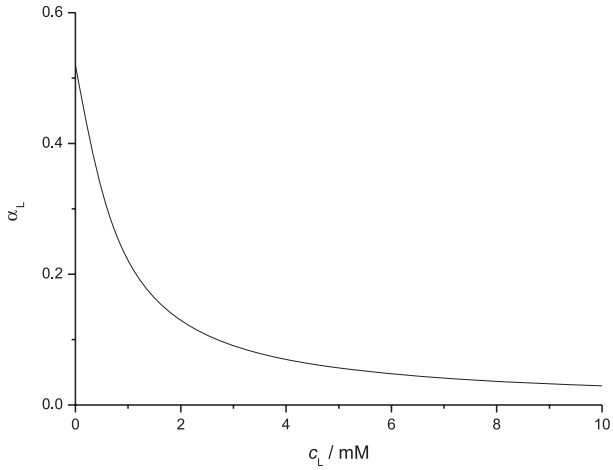

Figure 2. Fraction of the ligand complexed with the analyte as a function of the ligand concentration (Eq. 28) used for the explanation of the VACE method.

of the ligand concentration. This fully agrees with the expectation that the last boundary corresponds to the free analyte that migrates out of the sample plug immediately after the beginning of the separation. Thus, it has to move with the same mobility regardless of the concentration of the ligand. Only the height of the free analyte plateau is necessary for the evaluation of complexation parameters. The simulations clearly show that the height of the plateau decreases with increasing concentration of the ligand. This is expected, because when the ligand concentration is lower, a larger fraction of analyte is not complexed and can migrate out of the sample.

3.5 Frontal analysis continuous capillary electrophoresis (FACCE)

FACCE is analogous to FA but exhibits better reproducibility and lower detection limits [37]. The capillary is filled with a buffer solution and the capillary inlet is immersed in a vial that contains the pre-equilibrated mixture of the analyte and the ligand. Thus, the sample is continuously added to the capillary during the separation process. Usually, two detectable plateaus appear in the electropherogram. One plateau corresponds to the free analyte, the other to the equilibrated mixture. The complexation parameters are usually calculated from the height of the analyte plateau, similarly to the FA method, with the help of a calibration curve.

Unfortunately, the FACCE method is not applicable for our experimental setup. In the previously mentioned methods, the negatively charged analyte is dragged through the capillary to the detector by a fast EOF, while its own effective mobility is in the opposite direction. Since the absolute value of the mobility of the complex is lower than that of the free analyte, and because the sample continuously flows into the capillary, the complex moves to the detector faster than the analyte and continuously overlaps with it. For this reason, we have to use both a voltage with negative polarity and a reverse EOF. This simulates a coating of the capillary wall, which would be necessary for the actual experiment to be performed.

In the simulated electropherogram (Fig. 1D), there are two plateaus. Plateau A corresponds to the free analyte, plateau B to the equilibrated mixture. Analogously to the FA method, the first boundary moves with the mobility of the free analyte, regardless of the ligand concentration. The second boundary moves with the effective mobility of the complex. The complexation parameters are again evaluated from the height of the plateau of the free analyte. As in FA, the plateau height decreases with increasing concentration of the ligand.

4 Conclusions

We have introduced a mathematical model for the simulation of electrophoresis in complex formation systems with 1:1 complexation ratio. The model enables the consideration of individual complexation equilibrium constants and mobilities for every ionic form of the analytes and ligands. We have shown in detail how to get the solution of the coupled acid–base and complexation equilibria and how to solve numerically the corresponding continuity equations. The mathematical model is implemented in a new version of the Simul software, Simul 5 Complex. We have simulated several experimental methods, which are used for the determination of complexation equilibrium constants.

The support of the Grant Agency of the Czech Republic, grant no. 203/08/1428; Grant agency of Charles University, grant no. 101309, grant no. 323611; and the long-term research plan of the Ministry of Education of the Czech Republic (MSM0021620857) are gratefully acknowledged.

The authors declare no conflict of interest.

6 References

[1] Thormann, W., Breadmore, M. C., Caslavska, J., Mosher, R. A., *Electrophoresis* 2010, *31*, 726–754.

[2] Thormann, W., Caslavska, J., Breadmore, M. C., Mosher, R. A., *Electrophoresis* 2009, *30*, S16–S26.

[3] Thormann, W., Mosher, R. A., Breadmore, M. C., *Electrophoresis* 2011, *32*, 532–541.

[4] Hruska, V., Jaros, M., Gas, B., *Electrophoresis* 2006, *27*, 984–991.

[5] Gas, B., Jaros, M., Hruska, V., Zuskova, I., Stedry, M., *LC GC EUR.* 2005, *18*, 282–288.

[6] Jaros, M., Hruska, V., Stedry, M., Zuskova, I., Gas, B., *Electrophoresis* 2004, *25*, 3080–3085.

[7] Gas, B., Vacik, J., Zelensky, I., *J. Chromatogr.* 1991, *545*, 225–237.

[8] Thormann, W., Firestone, M. A., Sloan, J. E., Long, T. D., Mosher, R. A., *Electrophoresis* 1990, *11*, 298–304.

[9] Thormann, W., Mosher, R. A., *Electrophoresis* 2008, *29*, 1676–1686.

[10] Thormann, W. F., Mosher, R. A., *Electrophoresis* 2008, *29*, 1036–1047.

[11] Stedry, M., Jaros, M., Gas, B., *J. Chromatogr. A* 2002, *960*, 187–198.

[12] Gebauer, P., Mala, Z., Bocek, P., *Electrophoresis* 2009, *30*, 866–874.

[13] Hruska, V., Gas, B., Vigh, G., *Electrophoresis* 2009, *30*, 433–443.

[14] Dubrovcakova, E., Gas, B., Vacik, J., Smolkovakeulemansova, E., *J. Chromatogr.* 1992, *623*, 337–344.

[15] Busch, M. H. A., Kraak, J. C., Poppe, H., *J. Chromatogr. A* 1997, *777*, 329–353.

[16] Dubsky, P., Tesarova, E., Gas, B., *Electrophoresis* 2004, *25*, 733–742.

[17] Tesarova, E., Sevcik, J., Gas, B., Armstrong, D. W., *Electrophoresis* 2004, *25*, 2693–2700.

[18] Fang, N., Chen, D. D. Y., *Anal. Chem.* 2005, *77*, 840–847.

[19] Chen, D. D. Y., Fang, N., Sun, Y., Zheng, J. Y., *Electrophoresis* 2007, *28*, 3214–3222.

[20] Righetti, P. G., Andreev, V. P., Pliss, N. S., *Electrophoresis* 2002, *23*, 889–895.

[21] Breadmore, M. C., Quirino, J. P., Thormann, W., *Electrophoresis* 2009, *30*, 570–578.

[22] Breadmore, M. C., Kwan, H. Y., Caslavska, J., Thormann, W., *Electrophoresis* 2012, *33*, 960–971.

[23] Svobodová, J., Beneš, M., Hruška, V., Zusková, I., Gaš, B., *Electrophoresis* 2012, *33*, 940–949.

[24] Stedry, M., Jaros, M., Hruska, V., Gas, B., *Electrophoresis* 2004, *25*, 3071–3079.

[25] Chatterjee, A., *J. Micromech. Microeng.* 2003, *13*, 758–767.

[26] Busch, M. H. A., Carels, L. B., Boelens, H. F. M., Kraak, J. C., Poppe, H., *J. Chromatogr. A* 1997, *777*, 311–328.

[27] Armstrong, D. W., Rundlett, K. L., *Electrophoresis* 2001, *22*, 1419–1427.

[28] Armstrong, D. W., Jiang, C. X., *Electrophoresis* 2010, *31*, 17–27.

[29] Tanaka, Y., Terabe, S., *J. Chromatogr. B* 2002, *768*, 81–92.

[30] Asztemborska, M., Nowakowski, R., Sybilska, D., *J. Chromatogr. A* 2000, *902*, 381–387.

[31] Uselova-Vcelakova, K., Zuskova, I., Gas, B., *Electrophoresis* 2007, *28*, 2145–2152.

[32] Timerbaev, A. R., Rudnev, A. V., Aleksenko, S. S., Semenova, O., Hartinger, C. G., Keppler, B. K., *J. Sep. Sci.* 2005, *28*, 121–127.

[33] Busch, M. H. A., Boelens, H. F. M., Kraak, J. C., Poppe, H., *J. Chromatogr. A* 1997, *775*, 313–326.

[34] Erim, F. B., Kraak, J. C., *J. Chromatogr. B* 1998, *710*, 205–210.

[35] Fung, Y. S., Sun, D. X., Yeung, C. Y., *Electrophoresis* 2000, *21*, 403–410.

[36] McDonnell, P. A., Caldwell, G. W., Masucci, J. A., *Electrophoresis* 1998, *19*, 448–454.

[37] Gao, J. Y., Dubin, P. L., Muhoberac, B. B., *Anal. Chem.* 1997, *69*, 2945–2951.

[38] Hamming, R. W., *J. Acm.* 1959, *6*, 37–47.

[39] Ralston, A., Rabinowitz, P., *A First Course in Numerical Analysis*, Dover Publications, Mineola, NY 2001.

Appendix

A.1 Numerical solution of the continuity equations

Simul 5 Complex uses the same numerical scheme as Simul 5 in its standard mode [4]. Spatial differentiation is calculated by a central finite difference formula using a maximum of three points and the time problem is solved by the predictor–corrector method of Hamming [38, 39]. The predictor–corrector method uses for its calculation five time points: three past time points, one actual, and one future. The first four time points require an initialization by the Runge–Kutta method [39].

To avoid a nested differentiation, Eq. (12) is substituted into Eq. (11) and the electromigration term is partly differentiated

$$\frac{\partial c_k}{\partial t} = \sum_f \frac{\partial}{\partial x}\left(D_{k,f}\frac{\partial c_{k,f}}{\partial x}\right) - (j - j_{\text{diff}})\sum_f \times \frac{\partial}{\partial x}\left(\frac{\text{sgn}\left(z_{k,f}\right)c_{k,f}u_{k,f}}{\kappa}\right) + \frac{\partial j_{\text{diff}}}{\partial x}\sum_f\left(\frac{\text{sgn}\left(z_{k,f}\right)c_{k,f}u_{k,f}}{\kappa}\right) - v_{EOF}\frac{\partial c_k}{\partial x} \quad \text{(A29)}$$

$$\frac{\partial j_{\text{diff}}}{\partial x} = -F\left(\sum_k\sum_f\left[z_{k,f}\frac{\partial}{\partial x}\left(D_{k,f}\frac{\partial c_{k,f}}{\partial x}\right)\right] + \frac{\partial}{\partial x}\left(D_{\text{H}}\frac{\partial c_{\text{H}}}{\partial x}\right) - \frac{\partial}{\partial x}\left(D_{\text{OH}}\frac{\partial c_{\text{OH}}}{\partial x}\right)\right) \quad \text{(A30)}$$

The first-order central finite difference is used for the second and the last term in the right-hand side of Eq. (A29)

$$\frac{\partial g_x}{\partial x} = \frac{1}{2\Delta x}\left(g_{x+\Delta x} - g_{x-\Delta x}\right) \quad \text{(A31)}$$

where g is an arbitrary function and Δx is a width of a discrete axial segment (point).

Assuming a constant diffusion coefficient D, the second-order central difference can be applied

$$\frac{\partial}{\partial x}\left(D\frac{\partial c}{\partial x}\right)_x = \left(D\frac{\partial^2 c}{\partial x^2}\right)_x = \frac{D}{\Delta x^2}\left(c_{x+\Delta x} - 2c_x + c_{x-\Delta x}\right) \quad \text{(A32)}$$

The border points of the simulated channel require special attention. We apply the boundary condition using the sign of the total molar flux $J_k = \sum_f J_{k,f}$ based on Eq. (12)

$$\left(\frac{\partial c_k}{\partial t}\right)_{left} = \begin{cases} J_k < 0 & \left(\frac{\partial c_k}{\partial t}\right)_{left+\Delta x} \quad \text{constituent is leaving the channel} \\ J_k \geq 0 & 0 \quad\quad\quad\quad\quad\quad\quad\quad\quad\quad \text{constituent is entering the channel} \end{cases} \quad \text{(A33)}$$

$$\left(\frac{\partial c_k}{\partial t}\right)_{right} = \begin{cases} J_k \leq 0 & 0 \quad\quad\quad\quad\quad\quad\quad\quad\quad\quad \text{constituent is entering the channel} \\ J_k > 0 & \left(\frac{\partial c_k}{\partial t}\right)_{right-\Delta x} \quad \text{constituent is leaving the channel} \end{cases} \quad \text{(A34)}$$

A.2 Solution of the coupled acid–base and complexation equilibria by the multivariate Newton–Raphson method

The multivariate Newton–Raphson method is an iteration algorithm

$$\vec{x}_{n+1} = \vec{x}_n + \Delta\vec{x}_n \tag{A35}$$

where n expresses the n-th iteration, $\vec{x}$ is a column vector of values of the solved variables, and $\Delta\vec{x}_n$ is a determined difference based on the following matrix equation

$$\Delta\vec{x}_n = -\mathbf{J}_n^{-1} \times \vec{R}_n \tag{A36}$$

where $\mathbf{J}$ is the Jacobi matrix of the partial derivations of G and L by c_H and λ and $\vec{R}$ is a vector of the residues (i.e., the values of G and L functions for a certain c_H and λ)

$$\mathbf{J} = \begin{pmatrix} \dfrac{\partial G}{\partial c_H} & \dfrac{\partial G}{\partial \lambda} \\ \dfrac{\partial L}{\partial c_H} & \dfrac{\partial L}{\partial \lambda} \end{pmatrix} \tag{A37}$$

$$\vec{R} = \begin{pmatrix} G \\ L \end{pmatrix} \tag{A38}$$

Both $\mathbf{J}$ and $\vec{R}$ are evaluated for the actual values of c_H and λ in the n-th iteration. By inverting $\mathbf{J}$ and multiplying it with $\vec{R}$, we can derive analytical equations for our unknowns

$$(c_H)_{n+1} = (c_H)_n - \left(\frac{\dfrac{\partial L}{\partial \lambda} G - \dfrac{\partial G}{\partial \lambda} L}{\det(\mathbf{J})} \right)_n \tag{A39}$$

$$(\lambda)_{n+1} = (\lambda)_n - \left(\frac{\dfrac{\partial G}{\partial c_H} L - \dfrac{\partial L}{\partial c_H} G}{\det(\mathbf{J})} \right)_n \tag{A40}$$

$$\det(\mathbf{J}) = \frac{\partial G}{\partial c_H}\frac{\partial L}{\partial \lambda} - \frac{\partial G}{\partial \lambda}\frac{\partial L}{\partial c_H} \tag{A41}$$

Partial derivatives of G and L are determined from Eqs. (25) and (26)

$$\frac{\partial G}{\partial c_H} = 1 + \frac{K_w}{c_H} + \frac{c_L \lambda}{c_H}(Z_{2L} - n_L Z_{1L}) + \frac{1}{c_H}\sum_{i=1}^{N_x} c_i B_i^2 \left[-(Z_{1,i} + c_L \lambda b_{1,i})^2 + c_L \lambda n_L (Z_{1,i} b_{0,i} - b_{1,i}) + \frac{1}{B_i}(Z_{2,i} + c_L \lambda b_{2,i}) \right] \tag{A42}$$

$$\frac{\partial G}{\partial \lambda} = c_L Z_{1L} - c_L \sum_{i=1}^{N_x} c_i B_i^2 (Z_{1,i} b_{0,i} - b_{1,i}) \tag{A43}$$

$$\frac{\partial L}{\partial c_H} = \frac{\lambda}{c_H}(Z_{1L} - n_L Z_{0L}) - \frac{\lambda}{c_H}\sum_{i=1}^{N_x} c_i B_i^2 (Z_{1,i} b_{0,i} - b_{1,i} + n_L b_{0,i}) \tag{A44}$$

$$\frac{\partial L}{\partial \lambda} = Z_{0L} + \sum_{i=1}^{N_x} c_i B_i^2 b_{0,i} \tag{A45}$$

We assume that the equilibrium constants are true constants independent of the concentrations. This simplification implies that their derivations by c_H and λ are zero. The identity for differentiation of c_H^z by c_H, $\partial(c_H^z)/\partial c_H = z c_H^{z-1}$ is valid for every charge state including $z = 0$. Using this identity substantially simplifies the differentiating of the summations in Table 2.

II.

Simulation of the effects of complex-formation equilibria in electrophoresis: II. Experimental verification

J. Svobodová, M. Beneš, V. Hruška, K. Ušelová, B. Gaš
Electrophoresis 2012, 33, 948-957

Jana Svobodová[1]
Martin Beneš[1]
Vlastimil Hruška[1,2]
Kateřina Ušelová[1]
Bohuslav Gaš[1]

[1]Charles University in Prague Faculty of Science, Department of Physical and Macromolecular Chemistry, Prague, Czech Republic
[2]Agilent Technologies GmbH, Waldbronn, Germany

Received September 23, 2011
Revised October 11, 2011
Accepted October 12, 2011

Research Article

Simulation of the effects of complex-formation equilibria in electrophoresis: II. Experimental verification

The complete mathematical model of electromigration in systems with complexation agents introduced in the Part I of this article (V. Hruška et al., *Eletrophoresis*, 2012, *33*, this issue), which was implemented into our simulation program Simul 5, was verified experimentally. Three different chiral selector (CS) systems differing in the type of the CS, the magnitude of the complexation constants as well as in the experimental conditions were selected for verification. The experiments and simulations were performed at various concentrations of the CSs in order to discuss the influence of the concentration of the CS on the separation. The simulated and experimental electropherograms show very good agreement in the position, shape and amplitude of the analyte peaks. The new Simul 5 Complex offers a deep insight into electrophoretical separations that take place in systems containing complexing agents, for example into enantiomer separations. Using Simul 5 Complex we were able to predict and explain the significant electromigration dispersion of analyte peaks. It was clarified that the electromigration dispersion in these systems results directly from complexation. The new Simul 5 Complex was also shown to be a useful and powerful tool for the prediction of the results of enantioseparations.

Keywords:
Complex-formation equilibria / Dynamic simulation / Enantiomer separations / Simul 5

DOI 10.1002/elps.201100503

1 Introduction

Capillary zone electrophoresis (CZE) is an excellent technique for the separation of chiral analytes. The significant advantage of electromigration techniques in enantiomer separations is the possibility to add a chiral selector (CS) directly to the background electrolyte (BGE). Thus, the CS can be easily altered and a wide range of CSs can be investigated and used. Recent progress in the separation of enantiomers by CZE and the variety of CSs used has been discussed in several review articles [1–7].

The complexation equilibrium between the chiral analyte A and the ligand (or CS) L can be characterized by the complexation constant K, which can be determined directly by CZE. Many authors [8–11] summarize suitable experimental techniques for determination of the complexation constants. The most commonly used method is affinity capillary electrophoresis (ACE). In ACE, the complexation constants are determined from the dependence of the effective mobility of the analyte on the concentration of the CS.

In 2007, Uselova-Vcelakova et al. pointed out the problems connected with determination of the accurate complexation constant values by ACE [12]. Changes in the ionic strength, viscosity, or temperature of the BGE caused by the addition of different concentrations of CS to the BGE may significantly influence the obtained complexation constants. Therefore, all these factors have to be suitably corrected. Recently, Benes et al. proposed suitable procedures and corrections necessary for the determination of accurate complexation constants in BGE systems that contain charged CSs [13], where all effects mentioned above are especially significant. Correctly determined complexation constants can further be used for prediction of the results of enantiomer separations or even modelling as already mentioned by Williams and Vigh [14].

In 1992, Wren and Rowe proposed a basic model describing the separation of enantiomers in electrophoresis [15]. They showed that the results of the separation depended on the concentration of the neutral chiral additive (β-cyclodextrin), and proposed a simple approximate

Correspondence: Professor Bohuslav Gaš, Charles University in Prague, Faculty of Science, Albertov 2030, CZ-128 40 Prague 2, Czech Republic
E-mail: gas@natur.cuni.cz
Fax: +420224919752

Abbreviations: **CS**, chiral selector; **MAL-β-CD**, 6-*O*-α-maltosyl-β-cyclodextrin hydrate; **PA-β-CD**, 6-monodeoxy-6-mono(3-hydroxy) propylamino-β-cyclodextrin chloride; **R-BMP**, R-3-bromo-2-methylpropan-1-ol; **R-flurbiprofen**, (R)-(-)-2-fluoro-α-methyl-4-biphenylacetic acid; **S-BMP**, S-3-bromo-2-methylpropan-1-ol; **TM-β-CD**, heptakis(2,3,6-tri-*O*-methyl)-β-cyclodextrin

Colour online: See the article online to view Figs. 2–6 in colour.

equation for determination of the optimum concentration of the CS to achieve the best separation,

$$c_L^{opt} = \frac{1}{\sqrt{K_R K_S}} \quad (1)$$

where K_R and K_S are the complexation constants for the R and S enantiomer, respectively. The equation is a result of simplifications and does not take into account the effect of ionic strength. Later, they modified the model for BGE systems that contain organic solvents [16]. In 2010, Dubsky et al. extended the model for systems with multiple CSs [17]. The authors showed that in BGEs that contain multiple CSs not only the difference in complexation constants, but also the difference in the mobilities of the analyte–CS complexes have to be considered. In such cases, the Wren and Rowe model for determination of the optimum selector concentration can provide misleading values.

Numerous authors focused on the theoretical description of enantioseparation in CZE and discussed the effects of the various experimental parameters such as pH and CS concentration on the results of enantioseparation, especially on separation selectivity and efficiency [14–16, 18–29]. Theoretical models were established at first for systems with neutral CSs [15, 16, 18–25]. In 1997, Williams and Vigh proposed the theoretical model CHARM (charged resolving agent migration) which is suitable for systems with a charged CS and various analytes (nonelectrolytes, weak or strong electrolytes) [14]. This model is based on simultaneous protonation and 1:1 complexation equilibria and enables the calculation of the effective charges and effective mobilities of the complexes, along with the resulting separation selectivity and efficiency. They discussed how these parameters depend on the concentration of the CS, the pH of the BGE, and the electroomostic flow. The CHARM model was also verified experimentally [26–29].

There were also several attempts to model the separation of enantiomers, but all the models proposed until now are based on significant simplifications. In 1992, Dubrovcakova et al. presented the first theoretical model of electromigration including complexation of strong electrolyte analytes with neutral chiral additives [30]. The model was applied for the simulation of the dynamics of the electrophoretic separations, for the calculation of the isotachophoretic steady state and even for the determination of the binding constant. In 2004, Dubsky et al. [31] presented the simulation program SimulChir. This program is based on the simplified model of electromigration, but includes full dynamics of interconversion of the enantiomers in the separation systems and enables the determination of the interconversion rate constants. This model and the simulation program was later extended to systems with multiple CSs [32, 33] and was validated with different CS systems [34]. At the same time, Tesarova et al. [35] presented the mathematical model of micellar electrokinetic chromatography (MEKC) for systems combining both sodium dodecyl sulfate (SDS) micelles and CSs. This model was implemented in the dynamic simulator SimulMic. The authors focused on the effects of the SDS concentration in the presence of hydroxypropyl-β-cyclodextrin and the effects of the different electrolyte compositions that exist in different parts of the capillary used for the enantioselective separation. The model also used several simplifications, e.g., it could only be applied for systems in which a single charged analyte interacted with a neutral ligand and, simultaneously, with micelles. In 2009, Breadmore et al. [36] presented a new version of GENTRANS software allowing the simulation of both MEKC with charged surfactants and CZE separation of enantiomers with neutral or charged complexation agents. They used the approximation that the complex mobilities and the ligand mobilities were the same, so the model is useful only for a limited number of cases. The authors obtained good agreement between the simulated results and the experimental data, the simulated migration times were within the range of 7% error around the experimental ones. Simultaneously with our paper, Thormann and Breadmore [37] presents a new version of the simulation program GENTRANS, which enables the simulation of the electromigration process in complex CS systems.

Although the complexation equilibria are widely discussed, almost all presented models apply some simplifications and a complete model of electromigration in systems that contain a complexing ligand has not been published yet. Here we introduce a complete theoretical model of electromigration, which was described in detail in Part I of this article [38]. The model was implemented in the new version of Simul 5–Simul 5 Complex. This paper, Part II of the series shows experimental verification of this model. The model was tested with three different CS systems, including both neutral and charged cyclodextrins. These systems also differ in the extent of complexation. The results offer a deep insight into the enantiomer separation process, so we will discuss some unexpected effects such as electromigration dispersion caused by complexation. We will also discuss the applicability of Simul 5 Complex for the prediction of the results of enantiomer separations.

2 Mathematical model

A complete mathematical model used in the simulation tool Simul 5 Complex is described in detail in Part I of this article [38]. The model is applicable for any number of multivalent constituents (acids, bases, ampholytes) and one multivalent complexing agent, which we will call ligand. The ligand is allowed to form complexes with all other constituents, regardless whether analytes or BGE constituents. The model we propose considers the most common complexation stoichiometry, 1:1.

The complexation equilibrium of the i-th constituent in the ionic form with charge number z with a ligand in the ionic form with charge number l is characterized by the complexation constant $K_{x,i,z,l}$,

$$K_{x,i,z,l} = \frac{c_{x,i,z,l}}{c_{i,z} c_{L,l}}, \quad i = 1, \ldots, N \quad (2)$$

where $c_{i,z}$, $c_{L,l}$ are the concentrations of the corresponding ionic form of the analyte and ligand, respectively, $c_{x,i,z,l}$ is concentration of respective complex, N is the number of constituents. The total concentrations of all constituents, c_i, and the ligand, c_L, can be expressed as the sum of all neutral, ionic, free, and complexed forms of the appropriate constituent:

$$c_i = \sum_{z=n_i}^{p_i} c_{i,z} + \sum_{z=n_i}^{p_i} \sum_{l=n_L}^{p_L} c_{x,i,z,l} \tag{3}$$

$$c_L = \sum_{l=n_L}^{p_L} c_{L,l} + \sum_{i=1}^{N} \sum_{z=n_i}^{p_i} \sum_{l=n_L}^{p_L} c_{x,i,z,l} \tag{4}$$

Here n_i and p_i are the minimum negative and maximum positive charge numbers of the i-th constituent, respectively, n_L and p_L are the minimum negative and maximum positive charge numbers of the ligand. The concentration of hydronium ions, c_H, is set by the electroneutrality condition:

$$c_H - \frac{K_w}{c_H} + \sum_{z=n_i}^{p_i} z c_{i,z} + \sum_{l=n_L}^{p_L} l c_{L,l} + \sum_{i=1}^{N} \sum_{z=n_i}^{p_i} \sum_{l=n_L}^{p_L} (z+l) c_{x,i,z,l} = 0 \tag{5}$$

where the concentration of hydroxide ions, c_{OH}, is calculated from the equation for the ionic product of water. All ionic concentrations of the free and complexed forms of the analytes and ligand are determined by combining Eqs. (2–5) and the respective acid–base equilibria.

Electromigration is described by a mathematical model, which is based on the set of one-dimensional continuity equations. These partial differential equations express the development of the total concentrations of the constituents in time and space. The equation valid for both the ligand and all analytes ($k = L, 1,..., N$) is:

$$\frac{\partial c_k}{\partial t} = -\sum_f \left(\frac{\partial J_{k,f}}{\partial x} \right) \tag{6}$$

The subscript f stands for all ionic forms of both the free and the complexed forms of the k-th constituent and the quantity $J_{k,f}$ is the mass flux density, which consists of the diffusion flux, the electromigration flux and the electroosmotic flow (EOF) with velocity v_{EOF}:

$$J_{k,f} = -D_{k,f} \frac{\partial c_{k,f}}{\partial x} + \frac{\mathrm{sgn}\left(z_{k,f}\right) c_{k,f} u_{k,f}}{\kappa} \left(j - j_{diff}\right) + v_{EOF} c_{k,f} \tag{7}$$

where $D_{k,f}$ is the diffusion coefficient, $u_{k,f}$ the ionic mobility, j the current density, j_{diff} the diffusion current density

$$j_{diff} = -F \left[\sum_k \sum_f \left(z_{k,f} D_{k,f} \frac{\partial c_{k,f}}{\partial x} \right) + D_H \frac{\partial c_H}{\partial x} - D_{OH} \frac{\partial c_{OH}}{\partial x} \right] \tag{8}$$

and κ is the electric conductivity:

$$\kappa = F \left[\sum_k \sum_f \left(\left| z_{k,f} \right| u_{k,f} c_{k,f} \right) \right] + u_H c_H + u_{OH} c_{OH} \tag{9}$$

F is the Faraday constant.

To find a numeric solution for the sets of nonlinear differential equations and nonlinear algebraic equations we used the same approach as in the previous version of Simul 5 [39]. The model does not take into account the effect of ionic strength; however, all input parameters (e.g. pKa, ionic mobilities) can be corrected for the initial ionic strength before the simulation starts.

3 Materials and methods

3.1 Chemicals

All chemicals were of analytical grade purity. Tri(hydroxymethyl)aminomethane (Tris), *N*-[Tris(hydroxymethyl)methyl]glycine (Tricine), lithium hydroxide monohydrate were purchased from Lachema (Brno, Czech Republic), and acetic acid from Penta (Prague, Czech Republic). The EOF marker dimethyl sulfoxide (DMSO) and the analytes (R)-(-)-2-fluoro-α-methyl-4-biphenylacetic acid (R-flurbiprofen), S-3-bromo-2-methylpropan-1-ol (S-BMP), R-3-bromo-2-methylpropan-1-ol (R-BMP) were obtained from Sigma Aldrich (Prague, Czech Republic). 6-*O*-α-Maltosyl-β-cyclodextrin hydrate (MAL-β-CD) from Sigma Aldrich (Prague, Czech Republic), heptakis(2,3,6-tri-*O*-methyl)-β-cyclodextrin (TM-β-CD) from Sigma Aldrich (Prague, Czech Republic), and 6-monodeoxy-6-mono(3-hydroxypropylamino)-β-cyclodextrin hydrochloride (PA-β-CD) from CycloLab Ltd. (Budapest, Hungary), served as CSs. Water used for preparation of all solutions was purified by a Milli-Q water purification system (Millipore, Bedford, MA, USA).

3.2 Instrumentation

All experiments were performed using Agilent 3D^{CE} capillary electrophoresis equipment operated under ChemStation software (Agilent Technologies, Waldbronn, Germany) control. Fused silica capillaries (50 μm id, 375 μm od) were provided by Polymicro Technologies (Phoenix, AZ, USA). The experiments in Examples 1 and 2 were performed in bare fused silica capillary with a total length and effective length to the detector (DAD/contactless conductivity detector) of 53.6 cm and 45.1/38.2 cm, respectively. The total length and the effective length to the detector of the capillary used in Example 3 were 64.4 cm and 53.9 cm, respectively. The PHM 220 instrument (Radiometer, Copenhagen, Denmark) calibrated with standard IUPAC buffers, pH 1.679, pH 7.000, and pH 10.012 (Lyon, France) was used for pH measurements.

3.3 Experimental conditions

Running voltage and parameters of the capillaries were chosen to keep the electric current low (the current was always lower than 13 μA), and thus to avoid the effects of excessive Joule heating. New capillaries were flushed with 0.1 M sodium hydroxide for 30 min and three times for 3 min with H_2O before use. Then, a voltage of 20 kV was applied on the capillary filled with the BGE for 20 min. The capillaries were rinsed with the actual BGE for 3 min before each experiment. Every measurement was repeated four times. All solutions used in the experiments were filtered with a syringe filter, pore size 0.2 μm, and degassed for 5 min in an ultrasonic bath.

The running buffer (BGE) in Examples 1 and 2 was 50 mM Tris and 50 mM Tricine, experimental pH 8.15. The ionic strength of the BGE was 25.76 mM. The CSs MAL-β-CD, concentration range 0 mM to 10 mM, and TM-β-CD, concentration range 0 mM to 50 mM, were dissolved directly in the running buffer. The injected sample was 0.3 mM analyte (R-flurbiprofen) and 0.15 mM dimethyl sulfoxide, which served as the EOF marker, both dissolved directly in the running buffer. Detection was performed with the diode-array detector (DAD) at the detection wavelength of 214 nm and a contactless conductivity detector of our construction [40]. The samples were injected hydrodynamically for 450 mbar·s. The applied voltage was 15 kV (cathode at the detector side). The operating temperature was 25°C.

The BGE in Example 3 was composed of acetic acid and lithium hydroxide in 2:1 ratio, experimental pH 4.70. The ionic strength was kept constant at 40 mM by changing the concentration of acetic acid and lithium hydroxide to compensate the contribution of the charged CS to the ionic strength. The ligand, PA-β-CD, was dissolved directly in the buffer, its concentration varied from 1 mM to 30 mM. The sample was composed of 0.5 mM solution of either the analyte S-BMP or both analytes S-BMP and R-BMP and 2.8 mM dimethyl sulfoxide, which served as the EOF marker, all dissolved directly in the running buffer. Detection was performed with the DAD at the detection wavelength of 214 nm. The samples were injected hydrodynamically for 100 mbar·s. The applied voltage was 20 kV (cathode at the detector side). The average temperature was kept constant at 25°C. All experiments in Example 3 were performed by the PreMCE method described by Williams and Vigh [41, 42], which enables the determination of low effective mobilities of analytes in the systems with slow electroosmotic flow and avoids problems that compromise the determination of accurate effective mobilities. In the two-band PreMCE method used, the sample zone (containing the analyte and the EOF marker) is injected first and pushed by constant pressure into the thermostated part of the capillary filled with the actual BGE, then voltage is applied for time $t_{migr.}$ Finally, the zone containing the EOF marker is injected by the same conditions as the sample zone and the whole content of capillary is pushed by the same constant pressure into the detector. The effective mobility of the analyte is calculated from the distance which the analyte migrates during the time when voltage is applied. This distance is calculated from the velocity of the pressure-induced movement and the time difference between the analyte and the EOF marker peak on the resulting detector trace. The mobility of EOF can be only roughly estimated by the two-band PreMCE method. The exact setup of measurements and the procedure of data evaluation is described in our parallel paper [13].

Shapes of all enantiomer peaks in electropherograms were fitted by the Haarhoff–Van der Linde function [43, 44] to determine the accurate position of the peak. The Origin Ver. 8.1 software (OriginLab, Northhampton, NH, USA) was used for data evaluation.

4 Results and discussion

4.1 Simul 5 Complex

All simulations were performed by means of our simulation program Simul 5 Complex with implemented complexation mode. In the first step, the software requires the entry of the name, pKa, ionic mobility, and concentration in both the BGE and the injected zone of each constituent. A database containing the pKa values and limiting mobilities of a number of constituents is included, thus, the constituents can be easily selected from the database so only the concentrations of the constituent in the BGE and sample zone must be entered. The complexation mode requires that the ligand is entered as the first constituent in the constituents list: the ligand is marked with L.

In the next step the experimental conditions have to be specified, namely, the capillary length, detector position, temperature, driving voltage, and mobility of the electroosmotic flow. The basic setup of the simulation is the same as in the previous version of Simul 5 (without the complexation mode), as described in details in our previous paper [39] and in the program Help. The complexation mode is activated by clicking on the button Complex in the main menu bar. If the complexation mode is on, the red sign COMPLEXATION MODE appears in the main window. The program automatically creates and opens the Complex table with default values for all the complexation parameters. The characteristics of the ligand − pKa and ionic mobilities − should be modified to reflect the desired actual values. If a neutral compound is used as the ligand, no pKa value is required; however, the estimated mobility of the neutral form of the ligand must be entered, which is used for calculation of the diffusion coefficient of the ligand. In the case of a strong electrolyte ligand, such as a sulfated cyclodextrin, the software allows one to modify the ligand charge numbers (the Ligand nL and/or pL values) in the Complex table. For example, by setting both nL and pL as −7, the ligand is regarded as the strong electrolyte constituent with a charge number of −7. Again, only the mobility of the free ligand has to be entered. In the next step, the complexation parameters are specified. All constituents of the BGE and all analytes are allowed to form a complex with the ligand. This requires the entry of complexation

constants and mobilities for all complexes of all constituents which form complexes with the ligand. We recommend the use of the default minimum values of complexation parameters for the analytes and the BGE constituents, which do not form a known complex with the ligand. The complexation mode also enables one to apply ionic strength correction for the input data. By clicking on the button Apply IS, pKa values and mobilities of all compounds in the constituent list, the parameters of the ligand and the water ion product in the Complex table are recalculated for the actual ionic strength according to the Debey–Hückel and the Onsager–Fuoss theory. The software does not perform ionic strength correction during the simulation, the correction occurs on the input parameters.

4.2 Conditions of simulations

The experimental conditions used in the simulations were set the same as in the measurements but we had in mind minimizing simulation time also: (i) the EOF movement was imitated by the movement of the detector, which was initially situated outside the capillary. Thus, only the part of the capillary, which the analyte passed through by its own effective mobility, was simulated, (ii) the shorter capillary length was compensated by the reduction of voltage to keep the intensity of electric field the same as in the experiment. These two simplifications did not influence principally the result of simulation.

The length of the capillary in the Example 1 and 2 ranged from 150 to 370 mm. The width of the injection zone was 0.4 mm and the zone edge 0.2 mm. The intensity of the electric field was 46.64 kVm^{-1}. The current in both Examples 1 and 2 was 11.3 μA. The number of nodes in the *x*-axis was always 50 000. The length of the capillary in Example 3 was in the range from 50 to 350 mm. The width of the injection zone was 0.8 mm and the peak edge 0.4 mm. The intensity of the electric field was kept constant at 31.06 kVm^{-1}. The current varied, during the simualtion according to the actual composition of the BGE in the capillary, between 17.5 and 17.8 μA. The number of nodes in the *x*-axis was 30 000.

The simulations were performed by computer with Intel® Core™ i7-960 Processor 3.20 GHz. The simulation time was in the range of hours.

4.3 Experiments

The new Simul 5 Complex software was tested by real "wet" experiments using three different CS systems (Instead of the term "ligand", the term chiral selector, which is generally used in enantiomer separations, will be used in the rest of the paper.). The systems were chosen to differ in the CS used and in the experimental conditions. The experiments in Examples 1 and 2 were designed to have the same analyte, R-flurbiprofen, which was completely charged at the actual pH, and to differ in the choice of the CS, which was neutral in both examples.

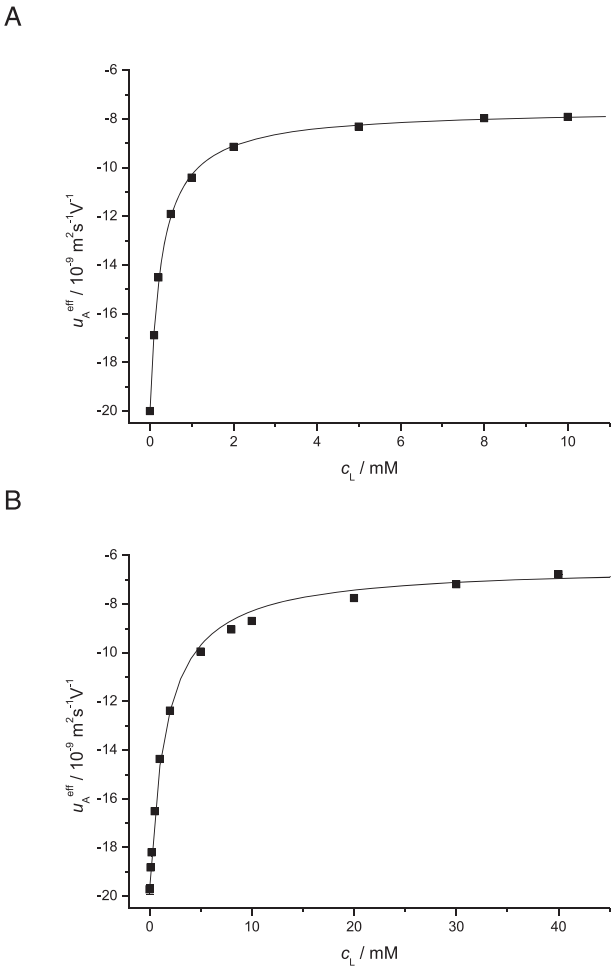

Figure 1. The dependences of the effective mobility of R-flurbiprofen on the concentration of (A) MAL-β-CD, (B) TM-β-CD in the BGE. Squares: experimental data; Solid line: fitted curve; Error bars present standard error.

MAL-β-CD and TM-β-CD were used in Examples 1 and 2, respectively. These two CSs were selected because of their significantly different complexation with R-flurbiprofen. In Example 3, a neutral analytes, S-BMP and R-BMP, and a completely charged CS, a well defined single-isomer cyclodextrin, PA-β-CD, were used. Only the complexation of analytes with the CS was supposed to be significant in the separation process, complexation of the constituents of the running buffer with the CSs was not considered.

First, the complexation constants and mobilities of complexes for individual systems were determined by performing a series of ACE experiments at various concentrations of the CS. The complexation constants and the mobilities of the complexes were used as the input data to be entered for the simulation runs. In the next step, the simulations were performed and the simulated profiles for the UV and the conductivity detector were compared with those obtained experimentally.

Table 1. Complexation constants and mobilities of complexes with standard error.

	Example 1	Example 2	Example 3 R- BMP	Example 3 S-BMP
K/(mol.dm^{-3})$^{-1}$	3610 ± 123	614 ± 43	110.9 ± 6.3	113.6 ± 6.5
u_A/10^{-9} m^{2}s^{-1}V^{-1}	−7.60 ± 0.03	−6.43 ± 0.11	7.08 ± 0.16	7.01 ± 0.16

Example 1: chiral selector – 6-*O*-α-maltosyl-β-cyclodextrin hydrate, analyte – R-flurbiprofen; Example 2: chiral selector – heptakis(2,3,6-tri-*O*-methyl)-β-cyclodextrin, analyte – R-flurbiprofen; Example 3: chiral selector – 6-monodeoxy-6-mono(3-hydroxypropylamino)-β-cyclodextrin hydrogen chloride, analytes – S-BMP and R-BMP

4.3.1 Example 1

In Example 1, neutral MAL-β-CD was used as the CS and fully charged R-flurbiprofen served as the analyte. The complexation constants were determined from the dependence of the effective mobility of the analyte on the concentration of the CS, see Fig. 1A. The resulting complexation constants summarized in Table 1 were used as input data in simulations. The simulations were performed at different concentration levels of the CS to show the influence of complexation on the position, shape, and amplitude of the analyte zone. The experimental conditions used in the simulation (e.g., length of the capillary, position of the detector, voltage, EOF mobility, width of the injected zone) are described in the Section 4.1. The experimental and simulated profiles for the conductivity and UV detectors are compared in Fig. 2A and Fig. 2B, respectively. The simulated profiles show very good agreement with the experimental electropherograms. As follows from Fig. 2A, the addition of a small amount of CS reverts the polarity of the conductivity detector signal for the analyte peak. While the peak has positive amplitude in the BGE system without CS, it becomes negative when CS has a concentration of about 0.1 mM and its amplitude increases with increasing concentration of CS. The difference in the amplitude results from the complexation of the analyte with CS in BGE.

The shape of the analyte peak changes significantly when the CS complexes with the analyte. The conductivity (Fig. 2A) and especially the UV detection (Fig. 2B) electropherograms show that the analyte peak has almost Gaussian profile in the BGE free of CS. Interestingly, at a CS concentration of 0.1 mM, the peak shape is significantly distorted by electromigration dispersion but when the concentration of the CS is increased, distortion diminishes. At concentrations of about 2 mM and higher the peak is again almost symmetrical.

Electromigration dispersion occurs if the velocity of the analyte in its own zone significantly depends on its concentration and is characterized by the relative velocity slope, which is defined by

$$S_X = \lim_{c_A^{in} \to 0} \frac{\kappa}{\boldsymbol{v}_A} \left(\frac{\partial \boldsymbol{v}_A}{\partial c_A} \right), \tag{10}$$

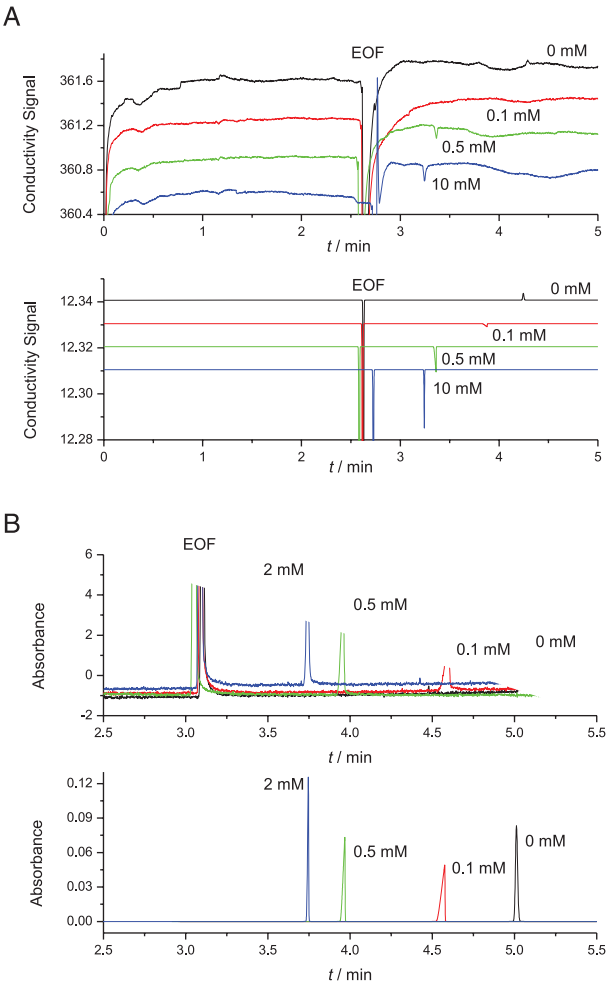

Figure 2. The comparison of the experimental (upper) and simulated (lower) profiles for the analyte R-flurbiprofen and the chiral selector MAL-β-CD. (A) Conductivity, (B) UV detection. The curves/analyte peaks are marked by the corresponding concentrations of the chiral selector. The experimental and simulated conductivity signals were shifted along the *y*-axis for better visibility, thus the *y*-axis is only a relative measure of the conductivity signal.

where c_A is the concentration of the analyte and v_A is the analyte velocity. Usually, the relative velocity slope is a function of the conductivity and pH of the BGE. However, this cannot explain the distortion of the analyte peak in our system, because the analyte peak in the absence of the CS is not distorted by dispersion and the conductivity or pH of the BGE are not changed when the neutral CS is added to the BGE in a low concentration. Here, electromigration dispersion is caused by complexation, i.e., complexation influences S_X.

The effective mobility u_A^{eff} of the analyte in the systems where complexation occurs depends on the fraction of the complexed analyte $\alpha_{X,A}$as follows:

$$u_A^{eff} = \alpha_{x,A} u_A + (1 - \alpha_{x,A})\, u_A^0, \tag{11}$$

where u_A is the mobility of the analyte–CS complex and u_A^0 is the mobility of the free analyte. By combining the

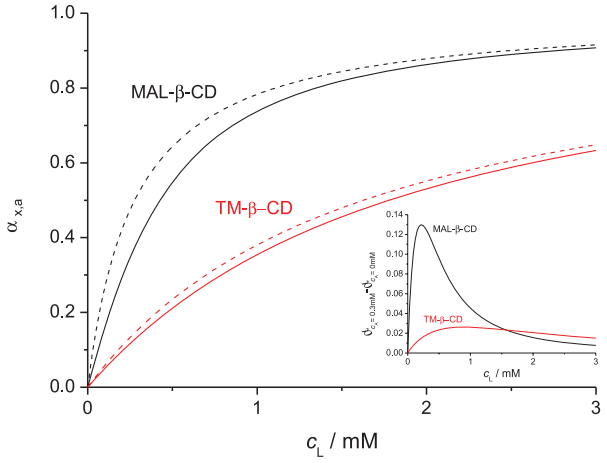

Figure 3. The theoretical dependences of the fraction of the complexed analyte R-flurbiprofen on concentration of MAL-β-CD and TM-β-CD. The dependence was plotted according to the Eq. (11) using the experimentally determined complexation constants. Solid: analytical concentration of analyte 0.3 mM; dashed: analytical concentration of analyte 0 mM. Insert: difference of the plotted curves of analyte for both chiral selector systems.

Eqs. (2, 3, 4) and (11), an expression for the fraction of the complexed analyte can be derived as follows:

$$\alpha_{x,A} = \frac{2Kc_L}{K(c_A + c_L) + 1 + \sqrt{[K(c_A + c_L) + 1]^2 - 4K^2 c_A c_L}}, \quad (12)$$

where c_A and c_L are the analytical (total) concentrations of the analyte and the ligand, respectively. Obviously, the fraction of the complexed analyte is a function of the analytical concentration of both the ligand and the analyte. This dependence for both Examples 1 and 2 is shown in Fig. 3. At low concentrations of the CS and within the range of concentrations of the analyte in the sample zone in the experiments (notice that the concentration of the analyte in the injected sample is 0.3 mM), the complexed fraction of the analyte depends on the concentration of the analyte. Therefore, the mobility of the analyte is not constant in the sample zone and electromigration dispersion must occur. This is especially obvious for Example 1 (curve MAL-β-CD in Fig. 3), in the CS concentration range of 0 mM $< c_L <$ 2 mM (with the maximum between 0.1 mM and 0.5 mM). When the concentration of the CS is higher than 2 mM, it is sufficient "to saturate" almost completely the injected analyte, depletion of the free ligand in the sample zone will be small and consequently, electromigration dispersion will be small. This behavior is clearly proved by simulations as well as by experimental data as shown in Fig. 2B.

4.3.2 Example 2

In the second example, the same analyte R-flurbiprofen, fully charged at the given pH, and a neutral CS TM-β-CD were used (the experimental conditions were the same as in Example 1). The complexation parameters were determined by ACE experiments. The experimental data and the fitted curve are shown in Fig. 1B, the resulting complexation parameters are summarized in Table 1. The complexation constant here is about six times lower than in Example 1, therefore, it can be expected that the behavior of the system will differ significantly from what was seen in the previous one.

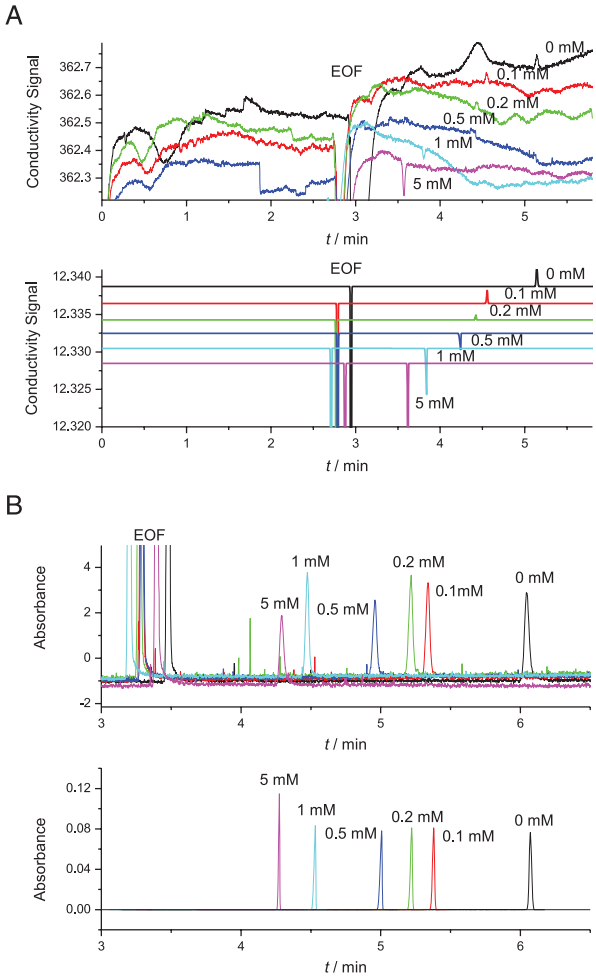

Figure 4. The comparison of experimental (upper) and simulated (lower) profiles for the analyte R-flurbiprofen and the chiral selector TM-β-CD. (A) Conductivity detection, (B) UV detection. All curves/analyte peaks are marked by individual concentrations of chiral selector. In panel A, the experimental and simulated conductivity signals were shifted along the *y*-axis for better visibility, thus the *y*-axis is only a relative measure of the conductivity signal.

The simulated and experimental electropherograms are shown in Fig. 4. They are in perfect agreement as regards the positions, shapes and amplitudes of the peaks. The R-flurbiprofen peak in the conductivity detector traces has a small positive amplitude not only in the absence of the complexation agent, but also at a CS concentrations of 0.1 mM and 0.2 mM. Simulation predicts the reversal of the amplitude of the analyte peak from positive to negative once the

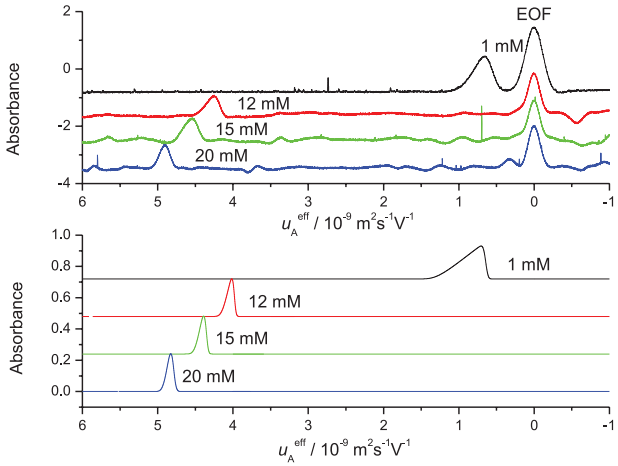

Figure 5. Comparison of the experimental (upper) and simulated (lower) profiles for the analyte S-BMP and the chiral selector PA-β-CD using UV detection. The curves/analyte peaks are marked by the corresponding concentrations of the chiral selector. The experimental and simulated UV detection signals were shifted along the *y*-axis for better visibility, thus the *y*-axis is only a relative measure of the absorbance signal.

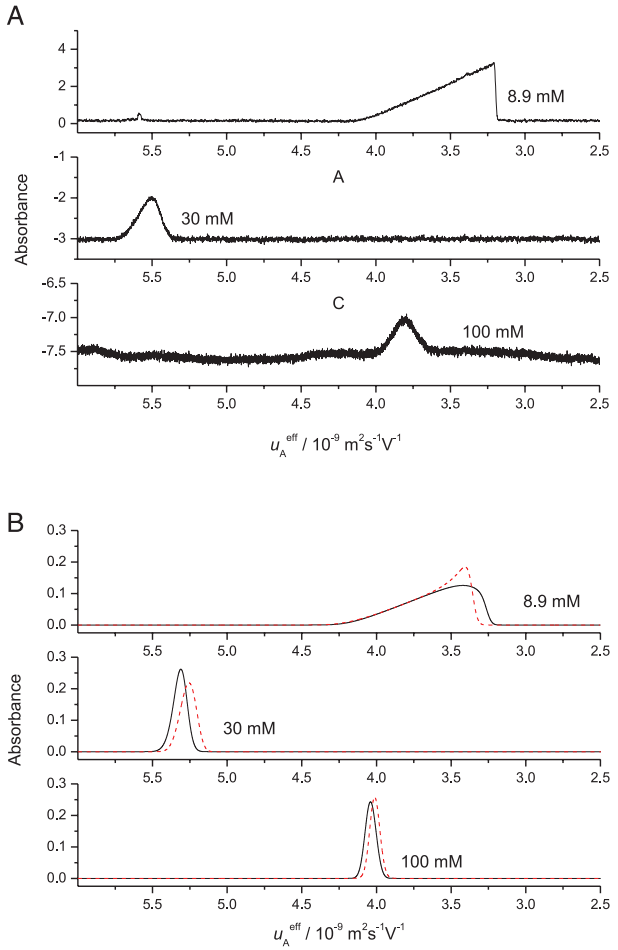

Figure 6. Experimental (A) and simulated (B) electropherograms of the separation of S-BMP and R-BMP using 8.9 mM, 30 mM, and 100 mM PA-β-CD in the BGE. Solid line: S-BMP; dashed line: R-BMP.

concentration of CS is about 0.5 mM, which is confirmed by the experiments.

The other difference when compared to the Example 1 is in the shape of analyte peaks, which are almost symmetrical here at every CS concentration. Because complexation of the analyte with the CS is weaker, the CS concentration is sufficient to provide the stoichiometric selector amount needed for the formation of the small amount of complexed analyte. Consequently, as is obvious from curve TM-β-CD in Fig. 3, the fraction of complexed analyte does not depend much on the concentration of the analyte over the whole CS concentration range. Therefore, the influence of complexation on the distortion of the analyte peak shape is negligible and electromigration dispersion is small.

4.3.3 Example 3

Example 3 differs from the previous ones not only in the choice of the CS but also in the experimental conditions and methods of measurements: a neutral analytes (S-BMP and R-BMP) and a charged CS (PA-β-CD) were used. The ACE experiments were performed at constant ionic strength (the buffer composition was varied to compensate the contribution of the charged CS to ionic strength). Determination of the complexation parameters in such a system is described in our parallel paper [13]. The determined complexation parameters used in the simulations are shown in Table 1.

Due to the low mobilities of the formed complexes all measurements were performed by using the PreMCE method of Williams and Vigh [41, 42], as discussed in Section 3.2. This method requires several steps including the application of pressure and changing the vials at the capillary inlet and outlet. The resulting native electropherograms are complicated to evaluate, therefore, we show the experimental and simulated profiles as detector signals in the mobility scale (instead of the time scale), which is easier to inspect.

The simulations were performed at the same conditions as used in experiments (see Section 4.1). In the PreMCE method, both the analyte and the EOF marker are moved through the detector by application of pressure. Simul 5 Complex has the ability to simulate pressurization of the content of the capillary and the velocity of this pressure-induced movement can be specified. Although the analyte peaks were pushed through the detector by the same velocity in the simulations and in the measurements, the simulated widths of the peaks has still to be considered as only approximate, because the Taylor–Aris dispersion is not implemented in the simulation causing the simulated peaks narrower than the experimental ones.

The experimental electropherograms obtained by UV detection and the simulation results are shown in Fig. 5. The positions and shapes of the analyte peaks are in good agreement. The analyte peaks at low concentrations of the CS are significantly influenced by electromigration dispersion, this effect decreases with increasing concentration of the CS. Both

the simulations and the experimental data show that at a CS concentration of 20 mM, the analyte peak appears almost Gaussian. It should be noted that not only the concentration of CS but also the composition of the BGE was altered during the measurements. This also has an influence on electromigration dispersion due to conductivity effects and will change the shape of analyte peak. Obviously, Simul 5 Complex is able to correctly consider peak shape distortion caused by both complexation and conductivity effects.

Example 3 was also used to predict the results of the separation of the R-BMP and S-BMP enantiomers. This is a difficult task in the given system, because the complexation constants of the enantiomers differ only slightly, 110.9 and 113.6 $(\text{mol.dm}^{-3})^{-1}$ for the R and S form, respectively, see Table 1. According to Wren and Rowe [15] we calculated the optimum concentration of the CS to be 8.9 mM for obtaining maximum separation. However, the real separation performance is very poor due to strong electromigration dispersion at this concentration, as is proved both by the simulations and the experiments; see Fig. 6. As found in previous examples, electromigration dispersion due to complexation is generally less when using higher concentration of ligand in the separation system. Therefore, we simulated the separation at higher CS concentrations as well: at 30 mM and 100 mM. Although there is much less electromigration dispersion, peak resolution is still not sufficient due to the fact that the concentration of the ligand is out of the optimum value. The experiments show exactly the same behavior. Obviously, the Wren and Rowe model [15] cannot take into account the influence of electromigration dispersion, and separation at the optimum ligand concentration is spoiled by high electromigration dispersion due to complexation. The CS system used does not offer sufficient separation selectivity to achieve adequate peak resolution. All these aspects are predicted by Simul 5 Complex.

5 Concluding remarks

The new Simul 5 Complex software with the implemented complexation mode enables one to simulate the process of electromigration in systems that contain a complexing agent and to predict the results of the separation, for example the results of enantiomer separations. The Simul 5 Complex was verified using three different CS systems. These systems differed in the choice of the CS and in the experimental conditions. Two systems contained a neutral CS and were used with a fully charged analyte. In the third system, a positively charged CS was utilized and neutral enantiomers were injected as the analyte. The experiments were performed by either classical electrophoresis or by the PreMCE method. With all CSs and experimental methods used, the simulated profiles for the UV and conductivity detectors are in very good agreement with those obtained experimentally. The positions, shapes, and amplitudes of the analyte peaks agree perfectly and show the same trends. The influence of complexation on the amplitude and shape of analyte peak was discussed. In addition, the new Simul 5 Complex is a useful tool to demonstrate the results of enantiomer separations and to optimize the separation conditions, enabling the saving of expensive CSs and experimental time.

The support of the Grant Agency of the Czech Republic, Grant No. 203/08/1428, Grant agency of Charles University, Grant No. 101309, Grant No. 323611 and the long-term research plan of the Ministry of Education of the Czech Republic (MSM 0021620857), are gratefully acknowledged. The authors want to express their gratitude to CycloLab Ltd. (Budapest, Hungary) for generous donation of 6-monodeoxy-6-mono(3-hydroxypropylamino)-β-cyclodextrin hydrogen chloride.

The authors have declared no conflict of interest.

6 References

[1] Rizzi, A., *Electrophoresis* 2001, *22*, 3079–3106.

[2] Gubitz, G., Schmid, M. G., *Electrophoresis* 2004, *25*, 3981–3996.

[3] Van Eeckhaut, A., Michotte, Y., *Electrophoresis* 2006, *27*, 2880–2895.

[4] Chankvetadze, B., *J. Chromatogr. A* 2007, *1168*, 45–70.

[5] Gubitz, G., Schmid, M. G., *Electrophoresis* 2007, *28*, 114–126.

[6] Scriba, G. K. E., *J. Sep. Sci.* 2008, *31*, 1991–2011.

[7] Gubitz, G., Schmid, M. G., *J. Chromatogr. A* 2008, *1204*, 140–156.

[8] Busch, M. H. A., Carels, L. B., Boelens, H. F. M., Kraak, J. C., Poppe, H., *J. Chromatogr. A* 1997, *777*, 311–328.

[9] Rundlett, K. L., Armstrong, D. W., *Electrophoresis* 2001, *22*, 1419–1427.

[10] Tanaka, Y., Terabe, S., *J. Chromatogr. B* 2002, *768*, 81–92.

[11] Jiang, C. X., Armstrong, D. W., *Electrophoresis* 2010, *31*, 17–27.

[12] Uselova-Vcelakova, K., Zuskova, I., Gas, B., *Electrophoresis* 2007, *28*, 2145–2152.

[13] Benes, M., Zuskova, I., Svobodova, J., Gas, B., *Electrophoresis* 2012, *33*, 1034–1042.

[14] Williams, B. A., Vigh, G., *J. Chromatogr. A* 1997, *777*, 295–309.

[15] Wren, S. A. C., Rowe, R. C., *J. Chromatogr.* 1992, *603*, 235–241.

[16] Wren, S. A. C., Rowe, R. C., *J. Chromatogr.* 1992, *609*, 363–367.

[17] Dubsky, P., Svobodova, J., Tesarova, E., Gas, B., *Electrophoresis* 2010, *31*, 1435–1441.

[18] Wren, S. A. C., Rowe, R. C., *J. Chromatogr.* 1993, *635*, 113–118.

[19] Rawjee, Y. Y., Staerk, D. U., Vigh, G., *J. Chromatogr.* 1993, *635*, 291–306.

[20] Rawjee, Y. Y., Williams, R. L., Vigh, G., *J. Chromatogr. A* 1993, *652*, 233–245.

[21] Rawjee, Y. Y., Williams, R. L., Vigh, G., *J. Chromatogr. A* 1994, *680*, 599–607.

[22] Rawjee, Y. Y., Vigh, G., *Anal. Chem.* 1994, *66*, 619–627.

[23] Rawjee, Y. Y., Williams, R. L., Buckingham, L. A., Vigh, G., *J. Chromatogr. A* 1994, *688*, 273–282.

[24] Williams, R. L., Vigh, G., *J. Chromatogr. A* 1995, *716*, 197–205.

[25] Biggin, M. E., Williams, R. L., Vigh, G., *J. Chromatogr. A* 1995, *692*, 319–325.

[26] Cai, H., Vigh, G., *J. Pharma. Biomed.* 1998, *18*, 615–621.

[27] Tacker, M., Glukhovskiy, P., Cai, H., Vigh, G., *Electrophoresis* 1999, *20*, 2794–2798.

[28] Maynard, D. K., Vigh, G., *Electrophoresis* 2001, *22*, 3152–3162.

[29] Busby, M. B., Maldonado, O., Vigh, G., *Electrophoresis* 2002, *23*, 456–461.

[30] Dubrovcakova, E., Gas, B., Vacik, J., Smolkova-Keulemansova, E., *J. Chromatogr.* 1992, *623*, 337–344.

[31] Dubsky, P., Tesarova, E., Gas, B., *Electrophoresis* 2004, *25*, 733–742.

[32] Dubsky, P., Svobodova, J., Gas, B., *J. Chromatogr. B* 2008, *875*, 30–34.

[33] Dubsky, P., Svobodova, J., Tesarova, E., Gas, B., *J. Chromatogr. B* 2008, *875*, 35–41.

[34] Svobodova, J., Dubsky, P., Tesarova, E., Gas, B., *Electrophoresis* 2011, *32*, 595–603.

[35] Tesarova, E., Sevcik, J., Gas, B., Armstrong, D. W., *Electrophoresis* 2004, *25*, 2693–2700.

[36] Breadmore, M. C., Quirino, J. P., Thormann, W., *Electrophoresis* 2009, *30*, 570–578.

[37] Breadmore, M. C., Kwan, H. Y., Caslavska, J., Thormann, W., *Electrophoresis* 2012, *33*, 960–971.

[38] Hruska, V., Benes, M., Svobodova, J., Zuskova, I., Gas, B, *Electrophoresis* 2012, *33*, 940–949.

[39] Hruska, V., Jaros, M., Gas, B., *Electrophoresis* 2006, *27*, 984–991.

[40] Gas, B., Zuska, J., Coufal, P., van de Goor, T., *Electrophoresis* 2002, *23*, 3520–3527.

[41] Williams, B. A., Vigh, G., *Anal. Chem.* 1996, *68*, 1174–1180.

[42] Williams, B. A., Vigh, G., *Anal. Chem.* 1997, *69*, 4445–4451.

[43] Haarhoff, P. C., van der Linde, H. J., *Anal. Chem.* 1966, *38*, 573–582.

[44] Erny, G. L., Bergstrom, E. T., Goodall, D. M., *Anal. Chem.* 2001, *73*, 4862–4872.

III.

A nonlinear electrophoretic model for PeakMaster: Part III. Electromigration dispersion in systems that contain a neutral complex-forming agent and a fully charged analyte. Theory

V. Hruška, J. Svobodová, M. Beneš, B. Gaš
Journal of Chromatography A, 2012, 1267, 102-108

Journal of Chromatography A, 1267 (2012) 102–108

Contents lists available at SciVerse ScienceDirect

Journal of Chromatography A

journal homepage: www.elsevier.com/locate/chroma

A nonlinear electrophoretic model for PeakMaster: Part III. Electromigration dispersion in systems that contain a neutral complex-forming agent and a fully charged analyte. Theory

Vlastimil Hruška[a,b,*], Jana Svobodová[a], Martin Beneš[a], Bohuslav Gaš[a]

[a] Charles University in Prague, Faculty of Science, Department of Physical and Macromolecular Chemistry, Prague, Czech Republic
[b] Agilent Technologies GmbH, Waldbronn, Germany

ARTICLE INFO

Article history:
Available online 2 July 2012

Keywords:
Complex-forming equilibrium
Electromigration dispersion
Electrophoresis
Nonlinear electromigration
PeakMaster 5.3 Complex
Simul 5 Complex

ABSTRACT

We introduce a new nonlinear electrophoretic model for complex-forming systems with a fully charged analyte and a neutral ligand. The background electrolyte is supposed to be composed of two constituents, which do not interact with the ligand. In order to characterize the electromigration dispersion (EMD) of the analyte zone we define a new parameter, the nonlinear electromigration mobility slope, $S_{EMD,A}$. The parameter can be easily utilized for quantitative prediction of the EMD and for comparisons of the model with the simulated and experimental profiles. We implemented the model to the new version of PeakMaster 5.3 Complex that can calculate some characteristic parameters of the electrophoretic system and can plot the dependence of $S_{EMD,A}$ on the concentration of the ligand. Besides $S_{EMD,A}$, also the relative velocity slope, S_X, can be calculated. It is commonly used as a measure of EMD in electrophoretic systems. PeakMaster 5.3 Complex software can be advantageously used for optimization of the separation conditions to avoid high EMD in complexing systems. Based on the theoretical model we analyze the $S_{EMD,A}$ and reveal that this parameter is composed of six terms. We show that the major factor responsible for the electromigration dispersion in complex-forming electrophoretic systems is the complexation equilibrium and particularly its impact on the effective mobility of the analyte. To prove the appropriateness of the model we showed that there is a very good agreement between peak shapes calculated by PeakMaster 5.3 Complex (plotted using the HVLR function) and the profiles simulated by means of Simul 5 Complex. The detailed experimental verification of the new mode of PeakMaster 5.3 Complex is in the next part IV of the series.

1. Introduction

Capillary electrophoresis is the analytical separation method very well described theoretically. Already in 1897 Kohlrausch introduced the basic set of continuity equations describing the electrophoretic movement as well as the conservation law now called Kohlrausch regulation function [1]. Later Dismukes and Alberty [2] and also Jovin [3] presented the additional conservation functions for some electrophoretic systems. The overview of different conservation laws and their applicability can be found in the review paper of Hruska and Gas [4]. However, the continuity equation is nonlinear, and thus, it cannot be solved analytically without certain approximations. One of the possibilities to study the process of electrophoretic separation is to solve the continuity equations numerically by simulation. There are several simulation programs available, such as SIMUL 5 [5], GENTRANS [6,7] or SPRESSO [8]. The simulations offer detailed insight into the process of electrophoretic separation, however, the simulation is often time consuming. Also, the result of numerical solution is only graphical representation of concentration, pH or conductivity profiles. Simulations do not provide exact values of mobilities, amplitudes or other parameters of studied systems.

Because of the special experimental setup of capillary zone electrophoresis (CZE) its governing equations can be solved by linearization. In CZE analytes are injected in a sample zone into a certain position in the capillary that creates disturbances in the background electrolyte (BGE). Such a setup can be first treated as a linear problem by the perturbation theory regardless of the magnitude of disturbances and in a next step the nonlinearity can be taken into account. In 90s Poppe [9] showed that solving the corresponding linearized equations leads to the matrix eigenvalue problem. Our group adopted and generalized this approach. We presented a linearized model of electromigration, which was implemented into the program PeakMaster 5.2 [10–12]. Simultaneously, we established the new term – the system eigenmobility,

* Corresponding author at: Agilent Technologies GmbH, Hewlett-Packard-Straße 8, 76337 Waldbronn, Germany. Fax: +49 7243 602 2414.
E-mail address: vlastimilhruska@gmail.com (V. Hruška).

0021-9673/$ – see front matter © 2012 Elsevier B.V. All rights reserved.
http://dx.doi.org/10.1016/j.chroma.2012.06.086

which is the mobility of the system zone emerging during the separation that directly equals to one eigenvalue of the Jacobian matrix that describes the linearized system. PeakMaster 5.2 also enables to predict the characteristics of separation systems such as pH, ionic strength, conductivity of BGE and mobility, amplitude and shape of the analyte or system zone. Electromigration dispersion (EMD) is expressed as the relative velocity slope established in 1997 by Gebauer and Bocek [13] and later by Horka and Slais [14].

Recently we introduced a simplified nonlinear model of electromigration, which can still be solved by the perturbation approach using matrix notation. The model was implemented into the new version of PeakMaster software, PeakMaster 5.3 [15,16], which enables plotting shapes of the system zones distorted by EMD. The extent of EMD of a system zone is characterized by the nonlinear electromigration mobility u_{EMD}, which experimentally corresponds to the difference between the mobility at the maximum (apex) of the peak and at its base as long as composition in the maximum remains close to initial conditions, i.e., until it becomes significantly dispersed. PeakMaster 5.3 can present the separation result in a form of the electropherogram.

Simultaneously, we presented the new version of our simulation program, Simul 5 Complex [17,18], which is especially useful for prediction of results of enantiomer separation [19] and offers a deep insight into the chiral separation. We developed the complete model of electrophoretic separation in systems with a complexation agent. The model is suitable for any number of analytes with any number of charge states and one ligand. We suppose the complexation ratio of 1:1, which is the mostly expected for system with cyclodextrins, although there are also other ratios mentioned in the literature [20]. The program Simul 5 Complex was verified experimentally and simulations together with experiments pointed out the unusual behavior of EMD, which was found to be closely related to the complexation.

In this paper we introduce the linearized model of EMD for particular electrophoretic systems with one neutral ligand and one strong (fully charged) analyte which can form a complex. Such systems are often used in the analytical practice. The model enables us to calculate the commonly used quantity characterizing EMD, the relative velocity slope, S_X. We also introduce a new similar quantity, the nonlinear electromigration mobility slope, $S_{EMD,A}$, as a slope of the nonlinear electromigration mobility, u_{EMD}, on the analyte concentration in the sample, which can be easily used to describe EMD in any electrophoretic system. We implement the model into the program PeakMaster 5.3 Complex, which now enables to predict EMD of one strong analyte that forms a complex with a neutral ligand present in the background electrolyte. We also discuss different contributions of EMD and prove the significant role of complexation on the shape of analyte peaks.

2. Theory

2.1. Linearization of continuity equations and nonlinear model

Electrophoretic evolution of a total concentration, c_i, in time, t, and one dimensional space coordinate, x, is described by a set of continuity equations for all N constituents where only electromigration is taken into account:

$$\frac{\partial c_i}{\partial t} = -\frac{\partial(v_i c_i)}{\partial x}, \quad i = 1, \ldots, N \tag{1}$$

where $v_i = u_{eff,i} j/\kappa$ is the velocity and $u_{eff,i}$ is the effective mobility of the ith constituent, j is the electric current density and κ is the conductivity. Information about the system is obtained by linearization of continuity equations [10,21]. The linearization is possible thanks to a special experimental setup of the capillary zone electrophoresis and analogous techniques where the separation space is filled by an undisturbed BGE solution and in the beginning of the experiment a sample zone is introduced, which creates a set of initial disturbances in all constituents. These disturbances develop in time and space and appear as system and analyte zones [10].

The solution of the set of continuity equations (1) are concentration profiles c_i, which can be expressed as a sum of a concentration of the ith constituent in the BGE, C_i, and a function $\tilde{c}_i$ that describes development of all disturbances in ith concentration profile in time and space: $c_i(x, t) = C_i + \tilde{c}_i(x, t)$. Initial conditions are $c_i(x, t = 0) = C_i + \tilde{c}_i^{in}(x)$ for all constituents i where $\tilde{c}_i^{in}(x) = \Delta C_i^{in} \varphi^{in}(x)$, ΔC_i^{in} is the amplitude (concentration magnitude) of the initial disturbance [12] and the function φ^{in} describes a spatial shape of the sample zone [15]. Linearization of continuity equations results in the eigenvalue problem with the characteristic Jacobian matrix $\mathbf{M}_0$:

$$\frac{\partial \vec{\tilde{c}}}{\partial t} = -\frac{j}{\kappa_0}\mathbf{M}_0 \times \frac{\partial \vec{\tilde{c}}}{\partial x} \tag{2}$$

where κ_0 is the conductivity of the BGE, arrows denote column vectors and $\mathbf{M}_0$ elements have dimension of mobility. For our next considerations it is important to realize that the solution of the linearized matrix Eq. (2) is done by a transformation $\vec{\tilde{c}} = \mathbf{Q}_R \times \vec{\tilde{w}}$ that converts concentrations $\tilde{c}_i$ into characteristic variables $\tilde{w}_i$ that represent individual zones [10,15]. Such a transformation converts matrix $\mathbf{M}_0$ to a diagonal matrix $\mathbf{\Lambda}_0 = \mathbf{Q}_L \times \mathbf{M}_0 \times \mathbf{Q}_R$ that contains mobilities of all zones. $\mathbf{Q}_R$ is a matrix composed of column eigenvectors in a way that the first column of $\mathbf{Q}_R$ corresponds to the first eigenvalue (zone mobility) in $\mathbf{\Lambda}_0$. $\mathbf{Q}_L$ is an inverse matrix to $\mathbf{Q}_R$. By matrix multiplication of the ith column of $\mathbf{Q}_R$ with the ith row of $\mathbf{Q}_L$ we get a matrix of amplitudes for the ith zone, $\mathbf{P}_i$, that provides information about individual disturbances in each concentration profile [12]: $\Delta\vec{C}^i = \mathbf{P}_i \times \Delta\vec{C}^{in}$ where superscripts 'i' and 'in' indicate the ith zone and the initial disturbance in the sample zone, respectively. A shape of the ith zone is described by the shape function $\varphi_i(x, t)$ [15]. In the linearized case of electromigration it is identical to the initial shape and it is moving with the mobility of the ith zone [10]. In the nonlinear case where diffusion and the first nonlinear mobility term are included into the model, the shape function reflects a non-symmetrical shape induced by the nonlinearity [15].

We described in detail a combined approach of the linearization and nonlinear model in Ref. [15]. The set of continuity equations (1) is rearranged to a matrix $\mathbf{M}(\tilde{c}_1, \ldots, \tilde{c}_N)$, which is further expanded by the Taylor matrix expansion to the first nonlinear matrix, which provides nonlinear information about individual zones for sufficiently small disturbances in the sample zone. The transformation of nonlinear matrices from the concentration (c) to the zone (w) domain is the same as transformation of $\mathbf{M}_0$ to $\mathbf{\Lambda}_0$, i.e., by a multiplication by eigenvector matrices $\mathbf{Q}_R$ and $\mathbf{Q}_L$, which are determined by the linearization.

2.2. Velocity of sample zone

Our goal in this paper is to describe nonlinear behavior of the analyte zone denoted as A, which undergoes a complex-forming equilibrium with a neutral ligand (L). Adding the complex-forming equilibrium to the same general nonlinear model as was used in the latest version of PeakMaster 5.3 [15] is a complicated problem, which may be addressed in future. Here we will restrict our consideration to a more specific and simpler case where a fully charged analyte forms a complex with a neutral ligand. First we determine the velocity of the analyte zone, $v_{zone,A}(x, t)$, in a non-linearized form and in the next step we will derive information about the nonlinear behavior of the analyte zone.

We will rearrange the set of continuity equations (1) into a vector form and transform such a vector equation to characteristic variables w, first by multiplying both sides of the equation

Table 1
Example of matrices $\mathbf{M}_0$, $\mathbf{Q}_R$ and $\mathbf{Q}_L$ and $\mathbf{P}_A$ (matrix of amplitudes for the zone of the analyte) of linearized system. System composed of two BGE constituents 1 and 2 and one analyte with subscript $3 \equiv A$. Elements m, r and l stand for general values.

$$\mathbf{M}_0 = \begin{pmatrix} m_{11} & m_{12} & m_{13} \\ m_{21} & m_{22} & m_{23} \\ 0 & 0 & u_{\mathrm{eff,A,0}} \end{pmatrix} \qquad \mathbf{Q}_R = \begin{pmatrix} 1 & 1 & 1 \\ r_{21} & r_{22} & r_{23} \\ 0 & 0 & r_{33} \end{pmatrix}$$

$$\mathbf{Q}_L = \begin{pmatrix} l_{11} & l_{12} & l_{13} \\ l_{21} & l_{22} & l_{23} \\ 0 & 0 & \frac{1}{r_{33}} \end{pmatrix} \qquad \mathbf{P}_A = \begin{pmatrix} 0 & 0 & \frac{1}{r_{33}} \\ 0 & 0 & \frac{r_{23}}{r_{33}} \\ 0 & 0 & 1 \end{pmatrix}$$

by $\mathbf{Q}_L$, which transforms the left-hand side to $\tilde{w}$, $\vec{\tilde{w}} = \mathbf{Q}_L \times \vec{\tilde{c}}$, and then using $\vec{\tilde{c}} = \mathbf{Q}_R \times \vec{\tilde{w}}$ to transform individual c_i in the right-hand side. This transforms continuity equations from concentrations (c) to zone functions (w). The transformed continuity equation of the analyte A is:

$$\frac{\partial w_A}{\partial t} = -\sum_{j=1}^{N} (\mathbf{Q}_L)_{A,j} \frac{\partial}{\partial x} \left[v_j \left(C_j + \sum_k (\mathbf{Q}_R)_{j,k} \tilde{w}_k \right) \right] \tag{3}$$

To simplify the equation we suppose that all zones move independently on each other, which means that mutual influence of overlapping zones is neglected. This implies that within the sample zone all $w_{k \neq A} = 0$:

$$\frac{\partial w_A}{\partial t} = -\sum_{j=1}^{N} (\mathbf{Q}_L)_{A,j} \frac{\partial}{\partial x} [v_j (C_j + (\mathbf{Q}_R)_{j,A} \tilde{w}_A)] \tag{4}$$

Second, since the analyte is present only in its own zone, its concentration in the BGE is zero, $C_A = 0$. It has a substantial impact on the above continuity equation as well as on the linearized matrix $\mathbf{M}_0$ and eigenvector matrices $\mathbf{Q}_R$ and $\mathbf{Q}_L$. Table 1 shows an example of matrices $\mathbf{M}_0$, $\mathbf{Q}_R$ and $\mathbf{Q}_L$ and $\mathbf{P}_A$ (the matrix of amplitudes for the analyte zone) for a system composed of two BGE constituents, 1 and 2, and one analyte, $3 \equiv A$. Elements of the third row in all matrices are zero due to $C_A = 0$ except the diagonal position that reduces the summation in Eq. (4). From matrices $\mathbf{Q}_R$ and $\mathbf{Q}_L$ in Table 1 is evident that the remaining product of $(\mathbf{Q}_L)_{A,A}$ and $(\mathbf{Q}_R)_{A,A}$ is 1 so Eq. (4) becomes:

$$\frac{\partial w_A}{\partial t} = -\frac{\partial (v_A \tilde{w}_A)}{\partial x} = -\frac{d(v_A \tilde{w}_A)}{d\tilde{w}_A} \frac{\partial \tilde{w}_A}{\partial x} \tag{5}$$

where the partial derivative of $v_A \tilde{w}_A$ by x was split into two terms. The character 'd' is the total derivative by $\tilde{w}_A$ and symbolizes the fact that $\tilde{w}_A$ is the only independent variable. The first term has a meaning of the velocity of the analyte zone, $v_{\mathrm{zone,A}} = \mathrm{d}(v_A \tilde{w}_A)/\mathrm{d}\tilde{w}_A$. The variable $\tilde{w}_A$ is in fact a function of the zone shape, φ_A, $\tilde{w}_A = \Delta W_A \varphi_A$ where ΔW_A is its amplitude. Similarly, $\tilde{c}_i = \Delta C_i^A \varphi_A$, where the amplitude ΔC_i^A is given by ith row of $\Delta \vec{C}^A = \mathbf{P}_A \times \Delta \vec{C}^{\mathrm{in}}$. We use it to rewrite $v_{\mathrm{zone,A}}$ from $\tilde{w}_A$ variable to c_A:

$$v_{\mathrm{zone,A}} = \frac{\mathrm{d}(v_A c_A)}{\mathrm{d}c_A} \tag{6}$$

2.3. Nonlinear electromigration mobility slope $S_{EMD,A}$

In the nonlinear model for PeakMaster 5.3 [15] we expressed nonlinearity of a zone by a nonlinear electromigration mobility, u_{EMD}. Due to zeros in the matrix $\mathbf{P}_A$, see Table 1, all disturbances in the analyte zone are dependent only on the analyte concentration in the sample, ΔC_A^{in}, which makes also $u_{\mathrm{EMD,A}}$ to be directly proportional to the analyte concentration. Therefore, the nonlinearity of the analyte zone can be expressed as the slope of $u_{\mathrm{EMD,A}}$ on ΔC_A^{in}, $S_{\mathrm{EMD,A}} = u_{\mathrm{EMD,A}}/\Delta C_A^{\mathrm{in}}$. For the analyte zone, $u_{\mathrm{EMD,A}}$ can be evaluated from the Taylor expansion of $v_{\mathrm{zone,A}}$ by c_A at the BGE composition (C_i) that is indicated by (0). The absolute term of the expansion is the linear velocity of the analyte zone, $v_{\mathrm{zone,A}}(0) = j/\kappa_0 \times u_{\mathrm{eff,A,0}}$, the linear term is $\mathrm{d}(v_{\mathrm{zone,A}})/\mathrm{d}c_A(0) \times c_A$. Since $c_A = \Delta C_A^{\mathrm{in}} \varphi_A$, the definition of $u_{\mathrm{EMD,A}}$ is based on the magnitude of the linear term:

$$u_{\mathrm{EMD,A}} = \frac{\kappa_0}{j} \frac{\mathrm{d}(v_{\mathrm{zone,A}})}{\mathrm{d}c_A}(0) \Delta C_A^{\mathrm{in}} \tag{7}$$

Application of $u_{\mathrm{EMD,A}}$ and subsequently $v_{\mathrm{zone,A}}$, Eq. (6), to $S_{\mathrm{EMD,A}}$ results in:

$$S_{\mathrm{EMD,A}} = \frac{\kappa_0}{j} \frac{\mathrm{d}^2(v_A c_A)}{\mathrm{d}c_A^2}(0) = 2\frac{\kappa_0}{j} \frac{\mathrm{d}v_A}{\mathrm{d}c_A}(0) \tag{8}$$

Obviously, in the equation for $S_{\mathrm{EMD,A}}$ the slope $\mathrm{d}v_A/\mathrm{d}c_A(0)$ is doubled. It is a consequence of our approach, where we consider the velocity of the analyte zone, $v_{\mathrm{zone,A}}$, determined from continuity equations and not the analyte velocity v_A, which is utilized for estimation of velocity slope [13] and relative velocity slope [14] in the previous approach. Advantageously, our approach offers us possibility to quantitatively compare theoretical calculations of $S_{\mathrm{EMD,A}}$ with degree of EMD evaluated from simulations or experiments, which we will perform in the next part (IV – Experimental verification) of this series.

In the general case, v_A is a function of all $\tilde{c}_i$, which are within the analyte zone functions only of c_A that can be expressed from $\tilde{c}_i = \Delta C_i^A \varphi_A = (\mathbf{P}_A)_{i,A} \Delta C_A^{\mathrm{in}} \varphi_A$ and that results in $\tilde{c}_i = (\mathbf{P}_A)_{i,A} c_A$. This can be used for the evaluation of $\mathrm{d}v_A/\mathrm{d}c_A(0)$:

$$\frac{\mathrm{d}v_A}{\mathrm{d}c_A}(0) = \sum_i \frac{\partial v_A}{\partial c_i}(0) \frac{\mathrm{d}c_i}{\mathrm{d}c_A}(0) = \sum_i \frac{\partial v_A}{\partial c_i}(0) (\mathbf{P}_A)_{i,A} \tag{9}$$

where the partial derivative $\partial v_A/\partial c_i(0)$ represents the first mentioned fact that v_A is the function dependent on all constituents. When applying $\mathrm{d}v_A/\mathrm{d}c_A(0)$ to the $S_{\mathrm{EMD,A}}$ and performing substitution $v_A = u_{\mathrm{eff,A}} j/\kappa$:

$$S_{\mathrm{EMD,A}} = 2 \sum_i (\mathbf{P}_A)_{i,A} \frac{\partial}{\partial c_i} \left(u_{\mathrm{eff,A}} \frac{\kappa_0}{\kappa} \right)(0) \tag{10}$$

Note that Eqs. (6) and (10) are valid in general for any model and experimental technique that can be described by the continuity Eq. (1) and can be linearized, i.e., is based on injection of a sample to a background electrolyte, such as capillary zone electrophoresis (CZE), affinity capillary electrophoresis (ACE), gel electrophoresis or even the isocratic mode of HPLC.

2.4. Complex-forming equilibrium

Our goal is to express the slope of nonlinearity of a complex-forming analyte by $S_{\mathrm{EMD,A}}$ in a specific simple setup: the BGE consists of two weak non-complexing constituents (denoted 1, 2) and the ligand (L), which is neutral and forms a complex only with the analyte (A). The analyte is strong, its charge number is z_A, its free (non-complexed) mobility is u_A, the complexed mobility is u_x and its complex-forming equilibrium constant, K_x, comes from the binding equation $K_x c_{A,f} c_{L,f} = c_{x,A}$ where $c_{x,A}$ is the concentration of the complex, $c_{A,f}$ is the concentration of the non-complexed analyte and $c_{L,f}$ is the concentration of the non-complexed ligand. The total concentration of the analyte is $c_A = c_{A,f} + c_{x,A}$ and that of the ligand is $c_L = c_{L,f} + c_{x,A}$. The molar fraction of the non-complexed ligand, λ, is the characteristic unknown quantity, which is determined by solving the complex equilibrium. It is defined as a relation between $c_{L,f}$ and c_L : $c_{L,f} = \lambda c_L$. The model is fully described by definitions of K_x, c_A and c_L. The molar fraction of the complexed analyte is $\alpha_x = K_x c_L \lambda/(1 + K_x c_L \lambda)$ and that of the complexed ligand is $\alpha_L = K_x c_A \lambda/(1 + K_x c_L \lambda)$. From their definition it follows that $c_A \alpha_A = c_L \alpha_L = c_{x,A}$ [17]. Using these equations we can also express

$c_{A,f} = c_A(1-\alpha_x)$. Again, similarly as shown in Ref. [17], the characteristic equation, L, for determination of λ is formulated from the rearranged definition of c_L : $L = -1 + \lambda + \alpha_L = 0$. Unlike the approach in Ref. [17], the complex-forming equilibrium here is not coupled with acid–base equilibria through molar fractions since both the analyte and the ligand do not dissociate – the analyte is fully dissociated and the ligand is neutral. The equation $L = 0$ can be rearranged to a quadratic equation, which can be solved analytically for the unknown λ:

$$\lambda = \frac{2}{1 + K_x(c_A - c_L) + \sqrt{[1 + K_x(c_A - c_L)]^2 + 4K_x c_L}} \tag{11}$$

2.5. Calculation of $S_{EMD,A}$ for complex-forming analyte

We will describe here a procedure how to calculate $S_{EMD,A}$ for the system of a strong analyte (A) forming a complex with a neutral ligand (L), which is present in the BGE together with two buffer constituents (1, 2), which do not interact with the ligand. For this purpose we use quantities calculated by the standard PeakMaster calculation of the setup without the ligand and combine it with the new scheme containing the complex-forming equilibrium. For the evaluation of $S_{EMD,A}$ the following quantities have to be expressed: $u_{eff,A,0}$, κ_0, $(\mathbf{P}_A)_{i,A}$ and $\partial(u_{eff,A}\kappa_0/\kappa)/\partial c_i(0)$ for $i = 1$, 2, A and L. The effective mobility of the complex-forming analyte $u_{eff,A}$ is:

$$u_{eff,A} = sgn(z_A)[u_A - (u_A - u_x)\alpha_x] \tag{12}$$

The linearized value of $u_{eff,A}$ in the BGE, $u_{eff,A,0}$, is then obtained simply by a change of α_x to $\alpha_{x,0}$ that is calculated first by evaluating λ in the BGE using Eq. (11): $\lambda(0) = 1$ and consequently applying it to the definition of α_x:

$$\alpha_{x,0} = \frac{K_x C_L}{1 + K_x C_L} \tag{13}$$

Similarly, $\alpha_{L,0} = 0$. The conductivity κ is defined as follows:

$$\kappa = \kappa_{orig} - F|z_A|c_A(u_A - u_x)\alpha_x \tag{14}$$

where κ_{orig} is the conductivity of the original system without any complex-forming equilibria consisting of BGE constituents 1 and 2, a strong (non-complexing) analyte A and H_3O^+ and OH^- ions. Since the additional term due to complexation is proportional to c_A, $\kappa_0 = \kappa_{orig}(0)$. The terms $\partial(u_{eff,A}\kappa_0/\kappa)/\partial c_i(0)$ for $i = 1$, 2, A and L can be further expanded using $u_{eff,A}$ from Eq. (12) and κ from Eq. (14):

$$\frac{\partial}{\partial c_i}\left(u_{eff,A}\frac{\kappa_0}{\kappa}\right)(0) = -\frac{u_{eff,A,0}}{\kappa_0}\left(\frac{\partial \kappa_{orig}}{\partial c_i}\right)(0) + \frac{u_{eff,A,0}}{\kappa_0}F|z_A|(u_A - u_x)\alpha_{x,0}\delta_{i,A} - sgn(z_A)(u_A - u_x)\left(\frac{\partial \alpha_x}{\partial c_i}\right)(0) \tag{15}$$

where $\delta_{i,A} = 0$ for $i = 1$, 2, L and $\delta_{A,A} = 1$. The term $(\partial\kappa_{orig}/\partial c_i)(0)$ comes from the conductivity and it is a constant calculated by the original PeakMaster model without the complex-forming equilibrium. It is zero for the ligand, $(\partial\kappa_{orig}/\partial c_L)(0) = 0$, since it is a neutral agent and, therefore, it cannot influence the original conductivity κ_{orig} by dissociation. Note that such a statement is just an approximation because in reality the ligand can interfere with other constituents by changes of viscosity of the solution. The effect is significant, e.g., for high concentrations of cyclodextrin [22], which we consider as a model ligand. The middle term comes form the complexing part of the conductivity that contains c_A therefore its derivative is nonzero only for the analyte due to $C_A = 0$. The last term in Eq. (15) comes from $u_{eff,A}$. The $(\partial\alpha_x/\partial c_i)(0)$ is evidently zero for constituents 1 and 2. For the analyte and the ligand it is $(\partial\alpha_x/\partial c_A)(0) = -K_x\alpha_{x,0}(1-\alpha_{x,0})^2$ and $(\partial\alpha_x/\partial c_L)(0) = K_x(1-\alpha_{x,0})^2$.

Finally, to calculate the last set of quantities we have to determine $(\mathbf{P}_A)_{i,A}$ for $i = 1$, 2 and L. The case $i = A$ is trivial since $(\mathbf{P}_A)_{A,A} = 1$ because it is a proportionality constant between concentration of the analyte in its own zone and its concentration in the sample zone. To do so we have to modify the original matrix $\mathbf{M}_0$ of non-complex-forming system (Table 1) to a matrix $\mathbf{M}_{x,0}$, which is extended by the presence of the ligand and modified by the complex-forming equilibrium of the ligand with the analyte:

$$\mathbf{M}_{x,0} = \begin{pmatrix} m_{11} & m_{12} & \frac{\kappa_0}{j}\frac{\partial J_1}{\partial c_A}(0) & 0 \\ m_{21} & m_{22} & \frac{\kappa_0}{j}\frac{\partial J_2}{\partial c_A}(0) & 0 \\ 0 & 0 & u_{eff,A,0} & 0 \\ 0 & 0 & \frac{\kappa_0}{j}\frac{\partial J_L}{\partial c_A}(0) & 0 \end{pmatrix} \tag{16}$$

In general, the element in the ith row and the kth column of matrices $\mathbf{M}_0$ and $\mathbf{M}_{x,0}$ is composed of a partial derivative of the molar flux of the ith constituent, $J_i = ju_{eff,i}c_i/\kappa$, by the kth total concentration, c_k, for i and $k = 1$, 2, A and L. Since these matrices are in mobility units (not velocity), every element is divided by the electric field strength in the BGE, $E_0 = j/\kappa_0$. Effective mobilities of BGE constituents 1 and 2 are not affected by the complex-forming equilibrium therefore they are calculated by the basic mode of PeakMaster, $u_{eff,A}$ is given by Eq. (12) and $u_{eff,L} = \mathrm{sgn}(z_A)u_x\alpha_L$. For the matrix $\mathbf{M}_{x,0}$ the elements m are identical to the original matrix $\mathbf{M}_0$ due to the mentioned independency of equilibria. The partial derivatives in Eq. (16) are as follows:

$$\frac{\kappa_0}{j}\frac{\partial J_i}{\partial c_A}(0) = m_{i3} + \frac{1}{\kappa_0}FC_i u_{eff,i,0}|z_A|(u_A - u_x)\alpha_{x,0}, \quad i = 1 \text{ and } 2 \tag{17}$$

$$\frac{\kappa_0}{j}\frac{\partial J_L}{\partial c_A}(0) = sgn(z_A)u_x\alpha_{x,0} \tag{18}$$

The matrix $\mathbf{M}_{x,0}$ has a simple structure and its four eigenvalues can be easily determined because it can be divided into two 2×2 characteristic matrices, which are located on the matrix's main diagonal. The first one is the top-left 2×2 matrix composed of elements m_{11}, m_{12}, m_{21} and m_{22}. This is identical to the matrix $\mathbf{M}_0$, therefore, the two resulting eigenvalues will be unchanged and are calculated by the original (non-complex-forming) PeakMaster calculation. The second bottom-right 2×2 matrix is a lower triangular matrix, so its eigenvalues are $u_{eff,A,0}$ due to the complex-forming analyte and 0 due to the neutral ligand in the BGE. The matrix $\mathbf{M}_{x,0}$ can be decomposed to eigenvector matrices $\mathbf{Q}_R$ and $\mathbf{Q}_L$ from which the elements of the matrix of amplitudes $(\mathbf{P}_A)_{i,A}$ for $i = 1$, 2 and L can be obtained:

$$(\mathbf{P}_A)_{1,A} = \frac{1}{B}\frac{\kappa_0}{j}\left[\frac{\partial J_1}{\partial c_A}(0)(u_{eff,A,0} - m_{22}) + \frac{\partial J_2}{\partial c_A}(0)m_{12}\right] \tag{19}$$

$$(\mathbf{P}_A)_{2,A} = \frac{1}{B}\frac{\kappa_0}{j}\left[\frac{\partial J_2}{\partial c_A}(0)(u_{eff,A,0} - m_{11}) + \frac{\partial J_1}{\partial c_A}(0)m_{21}\right] \tag{20}$$

$$B = u_{eff,A,0}^2 - (m_{11} + m_{22})u_{eff,A,0} + m_{11}m_{22} - m_{12}m_{21} \tag{21}$$

$$(\mathbf{P}_A)_{L,A} = \frac{1}{u_{eff,A,0}}\frac{\kappa_0}{j}\frac{\partial J_L}{\partial c_A}(0) \tag{22}$$

3. Results and discussion

In the theoretical section we have formulated the mathematical model for calculation of the nonlinear electromigration

mobility slope of the analyte ($S_{EMD,A}$) in the system containing non-complexing buffer constituents 1 and 2, a neutral ligand L and one fully dissociated analyte A that forms a complex with the neutral ligand L. The model was implemented in the latest version of PeakMaster 5.3 Complex that is available online at www.natur.cuni.cz/gas. In this section we will analyze the shape and contributions of $S_{EMD,A}$ by means of the model system that will be experimentally tested in the subsequent paper of this series (Part IV – Experimental verification) [23]. The non-complexing buffer is composed of 50 mM Tris (*Tris(hydroxymethyl)aminomethane*) and 50 mM Tricine (*N-[Tris(hydroxymethyl)methyl]glycine*). The analyte is negatively charged and its ionic (unsigned) mobility of the non-complexed form is $19.81 \times 10^{-9}\ m^2\ V^{-1}\ s^{-1}$. The complexation constant of the analyte with the neutral ligand is $K_x = 4037\ dm^3\ mol^{-1}$ and the mobility of the complex is $u_x = 8.82 \times 10^{-9}\ m^2\ V^{-1}\ s^{-1}$. The used values correspond to the experimental system containing the analyte R-flurbiprofen and the complex-forming agent β-cyclodextrin that will be discussed in Example 1 of the subsequent part IV of this series.

3.1. Shape and contributions of the nonlinear electromigration mobility slope ($S_{EMD,A}$) plot against ligand concentration

A calculated profile of the $S_{EMD,A}$ as the dependence on the ligand concentration in the BGE for the model system is plotted in Fig. 1A. It exhibits a specific shape of the curve. Initially, starting from $+0.11 \times 10^{-9}\ m^5\ V^{-1}\ s^{-1}\ mol^{-1}$ the value goes steeply down. At the concentration of the ligand of 0.10 mM it reaches the minimum of $-6.17 \times 10^{-9}\ m^5\ V^{-1}\ s^{-1}\ mol^{-1}$ (the highest absolute magnitude) and from this point turns back and approaches $-0.38 \times 10^{-9}\ m^5\ V^{-1}\ s^{-1}\ mol^{-1}$ for the infinite concentration of the ligand. The importance of the plot is that it can be used for optimization of the experimental conditions in order to avoid high electromigration dispersion (EMD) and, if needed, to use as low concentration of the ligand in the BGE as possible, e.g., due to its cost or solubility.

Eq. (10) defines $S_{EMD,A}$ as a sum over contributions of all constituents, therefore as we consider here four constituents, we have four main contributions to $S_{EMD,A}$. Further, Eq. (15) shows that each contribution is composed of three terms. For buffer constituents 1 and 2 only the first term is nonzero and for the ligand only the last one is nonzero. This gives us six contributions to $S_{EMD,A}$ in total and we will denote them by the s character with two subscripts – the first one denotes constituents (1, 2, A and L) and the second one relates to the position of the term in Eq. (15) where '0' relates to the first, 'c' to the middle and 'u' to the last term. As mentioned in Section 2, the first two terms in Eq. (15) originate from the derivative of the conductivity, $\partial\kappa/\partial c_i$, which has two components, see Eq. (14), the original conductivity κ_{orig} of the non-complexing system (subscript '0') and the second component that is due to complexation (subscript 'c'). The third term is derivative of the effective mobility (subscript 'u'), Eq. (12), or more specifically of the molar fraction of the complexed analyte, $\partial\alpha_x/\partial c_i$. The definition of the $S_{EMD,A}$, Eq. (10), can be then rewritten as $S_{EMD,A} = s_{1,0} + s_{2,0} + s_{A,0} + s_{A,c} + s_{A,u} + s_{L,u}$ and individual contributions are as follows:

$$s_{1,0} = -2(\mathbf{P}_A)_{1,A}\frac{u_{eff,A,0}}{\kappa_0}\left(\frac{\partial\kappa_{orig}}{\partial c_1}\right)(0) \tag{23}$$

$$s_{2,0} = -2(\mathbf{P}_A)_{2,A}\frac{u_{eff,A,0}}{\kappa_0}\left(\frac{\partial\kappa_{orig}}{\partial c_2}\right)(0) \tag{24}$$

$$s_{A,0} = -2\frac{u_{eff,A,0}}{\kappa_0}\left(\frac{\partial\kappa_{orig}}{\partial c_A}\right)(0) \tag{25}$$

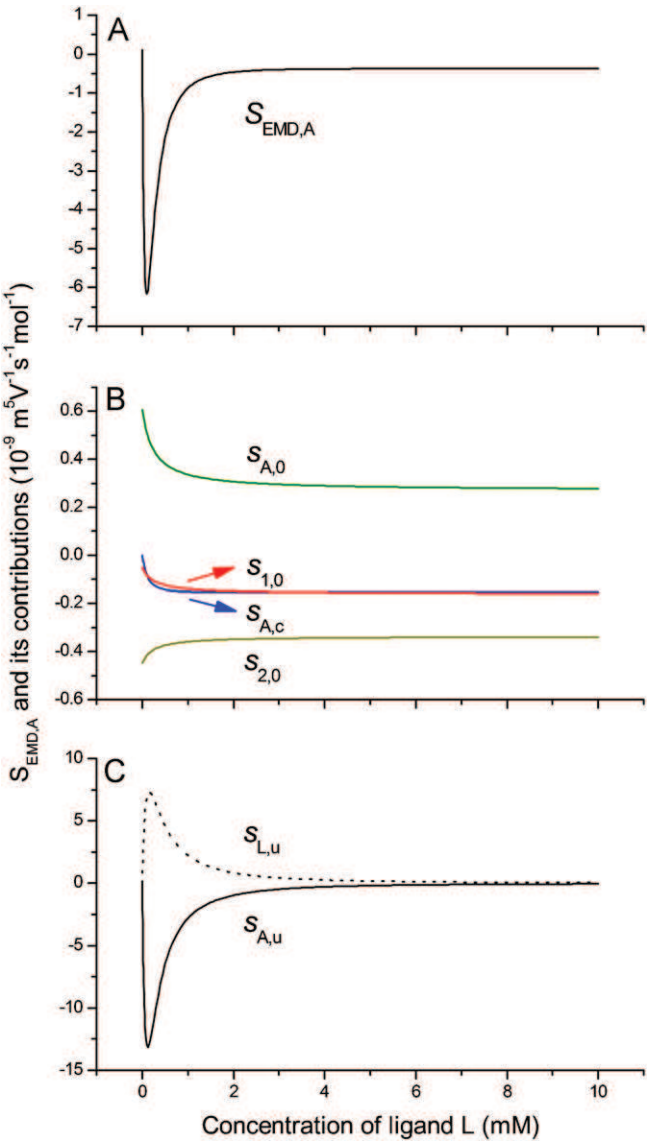

Fig. 1. Plot of $S_{EMD,A}$ and its contributions for the model system. (A) Plot of nonlinear electromigration mobility slope $S_{EMD,A}$. (B) $S_{EMD,A}$ contributions $s_{A,0}$ (green), $s_{1,0}$ (red), $s_{A,c}$ (blue) and $s_{2,0}$ (dark yellow). (C) $S_{EMD,A}$ contributions $s_{L,u}$ (dotted) and $s_{A,u}$ (solid). Model system: BGE 50 mM Tris and 50 mM Tricine; strong complex-forming analyte ($z_A = -1$, $u_A = 19.81 \times 10^{-9}\ m^2\ V^{-1}\ s^{-1}$); neutral complex-forming ligand ($K_x = 4037\ dm^3\ mol^{-1}$, $u_x = 8.82 \times 10^{-9}\ m^2\ V^{-1}\ s^{-1}$).

$$s_{A,c} = 2\frac{u_{eff,A,0}}{\kappa_0}F|z_A|(u_A - u_x)\alpha_{x,0} \tag{26}$$

$$s_{A,u} = 2sgn(z_A)(u_A - u_x)K_x\alpha_{x,0}(1 - \alpha_{x,0})^2 \tag{27}$$

$$s_{L,u} = -\frac{2u_x(u_A - u_x)K_x\alpha_{x,0}(1 - \alpha_{x,0})^2}{u_{eff,A,0}} \tag{28}$$

Here $(\mathbf{P}_A)_{1,A}$ and $(\mathbf{P}_A)_{2,A}$ are given by Eqs. (19) and (20), respectively. Contributions $s_{1,0}$, $s_{2,0}$, $s_{A,0}$ and $s_{A,c}$ are plotted in Fig. 1B. They all have a simple monotonous shape based on $\alpha_{x,0}$ – either directly, see $s_{A,c}$ Eq. (26), or through the effective mobility $u_{eff,A,0}$ that is a function of $\alpha_{x,0}$, see Eq. (12). Note that elements of matrix of amplitudes $(\mathbf{P}_A)_{1,A}$ and $(\mathbf{P}_A)_{2,A}$ are also functions of $u_{eff,A,0}$ and $\alpha_{x,0}$. Except $\alpha_{x,0}$, $u_{eff,A,0}$ and elements of matrix $\mathbf{P}_A$ all other quantities in Eqs. (23)–(28) are independent on complexation, therefore they are constants. The magnitude of plots in Fig. 1B is significantly lower compared to the maximum magnitude of the final $S_{EMD,A}$ plot.

Contributions $s_{A,u}$ and $s_{L,u}$ are plotted in Fig. 1C. Their curve shape is governed by derivatives of α_x by c_A and c_L, respectively, and their combination forms the specific shape of $S_{EMD,A}$. Interestingly, the magnitude of $s_{A,u}$ is even higher than the magnitude of $S_{EMD,A}$ and the magnitude of $s_{L,u}$ is counteractive to $s_{A,u}$ and $S_{EMD,A}$. The opposite sign of $s_{L,u}$ and $s_{A,u}$ is principal and it is given by the minus sign in Eq. (28) because $\mathrm{sgn}(z_A)$ and $u_{eff,A,0}$ have the same sign, u_x is an unsigned quantity (always positive) and all the other terms in Eqs. (27) and (28) are identical.

A further detailed discussion of dependences of $S_{EMD,A}$ on complex-forming parameters K_x and u_A is given in the subsequent paper (IV – Experimental verification) [23].

3.2. Simulation of model system by Simul 5 Complex and comparison with PeakMaster 5.3 Complex

Similarly as we did in the standard nonlinear model for PeakMaster 5.3 [15,16], we will test the validity of the model both by means of simulation by Simul 5 Complex and experimentally. Simulations and experiments for different types and concentrations of the ligand will be shown in the subsequent paper (IV – Experimental verification) [23]. Here, we focus on a basic correspondence of the model with simulations and the impact of $u_{EMD,A}$ on the non-symmetry of the peak.

Fig. 2 shows a comparison of calculations in PeakMaster 5 Complex (bold dashed blue curve) with simulations in Simul 5 Complex (solid black curve) of the model system (described above) with 0.1 mM neutral ligand in BGE for four different concentrations of the analyte in the sample. The parameters calculated by PeakMaster are plotted by means of the HVLR function [15], which is utilized in the standard version of PeakMaster 5.3 for plotting peaks in electropherograms. The HVLR function was originally derived by Houghton [24] for chromatography. It is suitable for plotting of nonsymmetrical peaks and it is more realistic version of the better known Haarhoff–van der Linde function (HVL) with improved shape of the injection zone, which is a rectangular pulse instead of an infinitely narrow band with an infinite height [15].

The concentration of the ligand we have chosen for simulations, 0.10 mM, corresponds to the maximum magnitude of the $S_{EMD,A}$ curve shown in Fig. 1A, $-6.17 \times 10^{-9}\ m^5\ V^{-1}\ s^{-1}\ mol^{-1}$. The four simulated electropherograms in Fig. 2A–D, are plotted for the four concentration of the analyte c_A: 0.005 mM, 0.025 mM, 0.1 mM, and 0.4 mM. Each electropherogram also shows the nonlinear electromigration mobility, $u_{EMD,A}$, which is the product of $S_{EMD,A}$ and the concentration of the analyte. With increasing concentration of the analyte the peaks become more and more distorted by EMD: from nearly symmetrical shape (Fig. 2A), the maximum of which almost coincides with the ideal peak center that is marked by the vertical dotted line, to a strongly triangulating peak in Fig. 2D. The HVLR plot used by the PeakMaster calculation is in all cases very close to the simulated curve obtained by Simul 5 Complex. A bit more significant deviation of the PeakMaster calculation from the simulation in Fig. 2D is due to the fact that the PeakMaster model uses only the first nonlinear term of zone velocity in the Taylor expansion.

Fig. 2D clearly demonstrates one important feature of EMD – its dependence on analyte actual concentration. The maximum (apex) of the peak is at the position of 7.2 min and it is 0.3 min before the ideal peak center (vertical dotted line) at 7.5 min. However, for the corresponding $u_{EMD,A} = -2.47 \times 10^{-9}\ m^2\ V^{-1}\ s^{-1}$ the apex of the peak should be around 1 min before the ideal peak center so it traveled only 30% of the theoretical distance. This is due to the continuous decrease of the concentration maximum caused by diffusion and EMD from 0.4 mM at the beginning to about 0.12 mM (30% of initial concentration). Obviously, during the run the actual

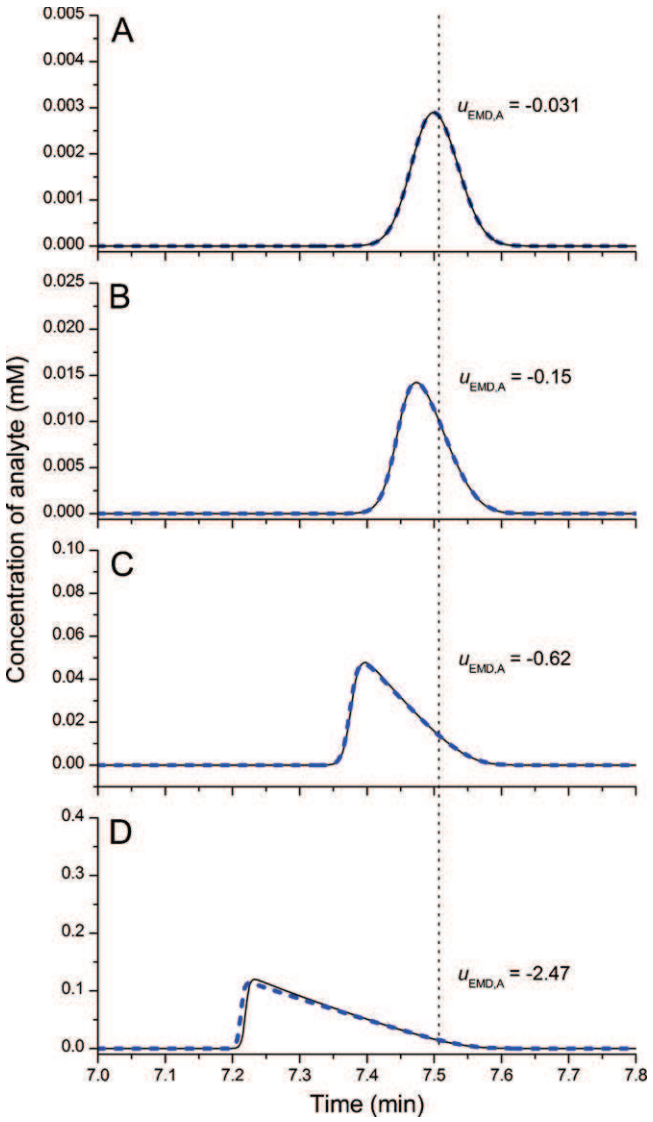

Fig. 2. Comparison of calculations by PeakMaster 5.3 Complex and simulations by Simul 5 Complex. Model system as in Fig. 1. Composition of BGE: 50 mM Tris, 50 mM Tricine and 0.1 mM ligand. Composition of injected sample: the BGE with varying concentration of analyte: (A) 0.005 mM; (B) 0.025 mM; (C) 0.1 mM; (D) 0.4 mM. Curves: simulations by Simul 5 Complex (black solid); HVLR function plot based on parameters calculated by PeakMaster 5.3 Complex (blue dashed bold). Label shows calculated $u_{EMD,A}$ by PeakMaster in $10^{-9}\ m^2\ V^{-1}\ s^{-1}$. Simulated setup: total capillary length 200 mm; length to detector 150 mm; voltage −4000 V (anode at detector side); simulation nodes 40,000; sample zone width 1 mm with smoothed edge width 0.05 mm. Calculated parameters of analyte by PeakMaster: ideal peak center (non-dispersed) in detector 7.5 min ($u_{eff,A,0} = -16.54 \times 10^{-9}\ m^2\ V^{-1}\ s^{-1}$) indicated in graph by vertical dotted line; $S_{EMD,A} = -6.17 \times 10^{-9}\ m^5\ V^{-1}\ s^{-1}\ mol^{-1}$; effective diffusion coefficient $D = 4.28 \times 10^{-10}\ m^2\ s^{-1}$. Front of peaks (direction of migration) is on left side of electropherogram.

EMD is proportional to the concentration. The HVLR function has a very good ability to depict the peak shapes dispersed by diffusion and distorted by electromigration dispersion.

Also a detailed look to the simulation of the 0.4 mM concentration of analyte (Fig. 2D) shows that all constituents and quantities that are supposed to have a minor effect to EMD indeed differ from the BGE values negligibly: the difference in pH is −0.001, the relative difference in conductivity is −0.02%, Tris −0.06% and Tricine −0.3%. On the other hand for the ligand, which is together with the analyte strongly influenced by the complexation, the simulation shows that its amplitude in the analyte zone differs by +0.12 mM

(+16%), which is two orders of magnitude higher than differences of the others.

4. Conclusions

We have formulated a mathematical model for a calculation of the nonlinear electromigration mobility slope of the analyte ($S_{EMD,A}$) in the complex-forming systems containing two non-complexing buffer constituents, a neutral ligand (complex-forming agent) and a fully charged complexing analyte. We implemented the model to the latest version of PeakMaster, PeakMaster 5.3 Complex, that is available online at www.natur.cuni.cz/gas. We based our derivation of $S_{EMD,A}$ on the velocity of the analyte zone determined from its continuity equation. Such an approach enables us to quantitatively compare theoretical calculations with simulations or experiments.

Dependence of $S_{EMD,A}$ on the ligand concentration has a specific shape with the high absolute maximum at which the electromigration dispersion is the highest. The knowledge of the curve shape allows us to optimize experimental conditions in order to minimize electromigration dispersion and eventually to minimize consumption of the ligand for the BGE.

We found six contributions of $S_{EMD,A}$ based on derivatives of the conductivity and effective mobility and showed that contributions based on derivatives of effective mobility are the most significant ones. The effective mobility of the analyte is solely dependent on the complex-forming equilibrium, as there are no acid–base equilibria in the case of the strong analyte and neutral ligand.

For validation of the model which is implemented in PeakMaster 5.3 Complex we compared the calculated peak shapes based on HVLR functions with numerical simulations done by means of Simul 5 Complex, which solves the more general model of continuity equations coupled with acid–base and complex equilibria. The comparison of the two different approaches exhibited a very good correspondence even for significantly dispersed peaks. It proves that HVLR function has a very good ability to describe the correct peak shape.

In the subsequent paper (IV – Experimental) [23] we analyze $S_{EMD,A}$ for various values of complex-forming parameters K_X and u_A and compare simulations and experiments for different types and concentrations of the ligand.

Acknowledgements

The support of the Grant Agency of the Czech Republic, Grant No. 203/08/1428, Grant agency of Charles University, Grant Nos. 323611 and 669412, and the long-term research plan of the Ministry of Education of the Czech Republic (MSM 0021620857), are gratefully acknowledged.

References

[1] F. Kohlrausch, Ann. Phys. (Leipzig) 62 (1897) 209.
[2] E.B. Dismukes, R.A. Alberty, J. Am. Chem. Soc. 76 (1954) 191.
[3] T.M. Jovin, Biochemistry – US 12 (1973) 871.
[4] V. Hruska, B. Gas, Electrophoresis 28 (2007) 3.
[5] V. Hruska, M. Jaros, B. Gas, Electrophoresis 27 (2006) 984.
[6] R.A. Mosher, D. Dewey, W. Thormann, D.A. Saville, M. Bier, Anal. Chem. 61 (1989) 362.
[7] W. Thormann, C.X. Zhang, J. Caslavska, P. Gebauer, R.A. Mosher, Anal. Chem. 70 (1998) 549.
[8] M. Bercovici, S.K. Lele, J.G. Santiago, J. Chromatogr. A 1216 (2009) 1008.
[9] H. Poppe, Anal. Chem. 64 (1992) 1908.
[10] M. Stedry, M. Jaros, V. Hruska, B. Gas, Electrophoresis 25 (2004) 3071.
[11] M. Jaros, V. Hruska, M. Stedry, I. Zuskova, B. Gas, Electrophoresis 25 (2004) 3080.
[12] V. Hruska, M. Stedry, K. Vcelakova, J. Lokajova, E. Tesarova, M. Jaros, B. Gas, Electrophoresis 27 (2006) 4610.
[13] P. Gebauer, P. Bocek, Anal. Chem. 69 (1997) 1557.
[14] M. Horka, K. Slais, Electrophoresis 21 (2000) 2814.
[15] V. Hruska, M. Riesova, B. Gas, Electrophoresis 33 (2012) 923.
[16] M. Riesova, V. Hruska, B. Gas, Electrophoresis 33 (2012) 931.
[17] V. Hruska, M. Benes, J. Svobodova, I. Zuskova, B. Gas, Electrophoresis 33 (2012) 938.
[18] J. Svobodova, M. Benes, V. Hruska, K. Uselova, B. Gas, Electrophoresis 33 (2012) 948.
[19] B. Chankvetadze, Capillary Electrophoresis in Chiral Analysis, 1st ed., John Wiley & Sons, Chichester, 1997.
[20] M. Asztemborska, R. Nowakowski, D. Sybilska, J. Chromatogr. A 902 (2000) 381.
[21] H. Poppe, J. Chromatogr. 506 (1990) 45.
[22] M. Benes, I. Zuskova, J. Svobodova, B. Gas, Electrophoresis 33 (2012) 1032.
[23] M. Benes, J. Svobodova, V. Hruska, M. Dvorak, I. Zuskova, B. Gas, J. Chromatogr. A 1267 (2012) 109.
[24] G. Houghton, J. Phys. Chem. – US 67 (1963) 84.

IV.

A nonlinear electrophoretic model for PeakMaster: Part IV. Electromigration dispersion in systems that contain a neutral complex-forming agent and a fully charged analyte. Experimental verification

M. Beneš, J. Svobodová, V. Hruška, M. Dvořák, I. Zusková, B. Gaš
Journal of Chromatography A, 2012, 1267, 109-115

Journal of Chromatography A, 1267 (2012) 109–115

Contents lists available at SciVerse ScienceDirect

Journal of Chromatography A

journal homepage: www.elsevier.com/locate/chroma

A nonlinear electrophoretic model for PeakMaster: Part IV. Electromigration dispersion in systems that contain a neutral complex-forming agent and a fully charged analyte. Experimental verification

Martin Beneš [a], Jana Svobodová [a,*], Vlastimil Hruška [a,b], Martin Dvořák [a], Iva Zusková [a], Bohuslav Gaš [a]

[a] Charles University in Prague, Faculty of Science, Department of Physical and Macromolecular Chemistry, Prague, Czech Republic
[b] Agilent Technologies GmbH, Waldbronn, Germany

ARTICLE INFO

Article history:
Available online 23 June 2012

Keywords:
Complex-formation equilibria
Enantiomer separations
PeakMaster 5.3
Electrophoresis
Nonlinear electromigration

ABSTRACT

The complete mathematical model of electromigration dispersion in systems that contain a neutral complex forming agent and a fully charged analyte was introduced in the previous part of this series of papers (Part III – Theory). The model was implemented in the newest version of our simulation program PeakMaster 5.3 that calculates the effective mobility of the analyte and its nonlinear electromigration mobility slope, S_{EMD}, in the presence of a complex forming agent in the background electrolyte. The mathematical model was verified by both experiments and simulations, which were performed by our dynamic simulator Simul 5 Complex. Three separation systems differing in the chiral selector used (having different values for the complexation constant and the mobility of the complex) were chosen for the verification. The nonlinear electromigration mobility slope values were calculated from the simulations and the experiments that were performed at different complex forming agent concentrations. These data agree very well with those predicted by the mathematical model and provided the foundation for the discussion and explanation of the electromigration dispersion process that occurs in systems which contain a complex forming agent. The new version of PeakMaster 5.3 was shown to be a powerful tool for optimization of the separation conditions by minimizing electromigration dispersion which improves the symmetry of the analyte peaks and their resolution.

1. Introduction

Capillary zone electrophoresis is an excellent separation technique suitable for the separation of a variety of analytes, including enantiomers, because it provides high separation efficiency and can utilize a wide variety of chiral selectors. However, the quality of an electrophoretic separation can be easily ruined by excessive peak broadening. Several review papers [1–3] detail the causes of peak broadening (*e.g.*, longitudinal diffusion, Joule heating, electromigration dispersion, wall adsorption, laminar flow, *etc.*). One of the most severe ones is electromigration dispersion (EMD), which is an inherently nonlinear phenomenon that leads to characteristic triangular peak shapes. EMD has been intensively studied for a long time. Already in 1979, Mikkers et al. [4,5] observed that the EMD of strong electrolyte analytes can be eliminated by matching the mobility of the analyte with that of the co-ion in the BGE. Later, Foret et al. illustrated experimentally the development of EMD for mono- and oligoprotic weak electrolyte analytes [6]. In 1996, Beckers studied the change of pH in the sample zone and the development of EMD in BGEs that contained two-coins [7]. The author distinguished between eight cases depending on the character of the analyte (strong or weak electrolyte) and its co-ion and counter-ion. He also derived rules of thumb for the electrophoretic behavior of weak bases in such systems. In the same year, Xu et al. found that both the pH and conductivity (composition) of the BGE influenced the extent of EMD [8]. They showed that in special cases the pH- and conductivity-dependent parts of EMD can act in opposite direction, cancel each other and lead to sharp and symmetrical peaks. The authors also established a so called EMD constant whose value determines the direction and degree of peak triangulation.

The tendency of an analyte to undergo EMD was later characterized by Gebauer et al. [9,10] by its velocity slope, S'_X. Velocity slope is defined as the change in the velocity of the analyte with its mole fraction at infinitely low analyte concentration. The authors also showed that for $S'_X < 0$ the zones are fronting, for $S'_X > 0$ they are tailing. Consequently, the magnitude of the velocity slope serves as a measure of EMD. Using computer simulations together with the peak shape diagrams that show the combinations of the pK_a

* Corresponding author at: Charles University in Prague, Faculty of Science, Albertov 2030, CZ-128 40 Prague 2, Czech Republic. Tel.: +420 221951399; fax: +420 224919752.
E-mail address: svobod.j@seznam.cz (J. Svobodová).

0021-9673/$ – see front matter © 2012 Elsevier B.V. All rights reserved.
http://dx.doi.org/10.1016/j.chroma.2012.06.053

value of the buffering species in a BGE and the ionic mobility of the charged form of that species that lead to an $S'_X = 0$ for a particular analyte, the authors predicted the asymmetry of the analyte peak. In 2005, Horka and Slais [11] introduced the relative velocity slope parameter, S_X, defined as

$$S_X = \lim_{c_X \to 0} \frac{\kappa}{v_X} \frac{dv_X}{dc_X} \quad (1)$$

where κ is the conductivity of the BGE, v_X is the velocity of the analyte, c_X is the concentration of the analyte. Since the value of S_X depends on the physical properties of the analyte, the nature, and pH of the BGE, S_X can be used as the quantity that characterizes the asymmetry and broadening of the analyte peak in a given BGE. Similarly to Gebauer and Bocek, they use the modified peak shape diagrams to predict the development of EMD in a BGE of selected pH and conductivity.

In 2002, our group developed the theoretical linearized model of electromigration [12–14]. The model allows the calculation of the relative velocity slope and provides a picture of the migration of the analytes and their EMD. We also focused on the interrelationship of EMD and the slope of a signal in a conductivity detector. We determined that in the case of strong electrolytes the relative velocity slope is equal to the molar conductivity response, while for weak electrolytes it contains not only the conductivity term, but also a pH-dependent term that can lead to a sufficiently high conductivity signal accompanied by low EMD. This fully proves the results of Xu et al., who predicted that EMD is caused by both conductivity and pH effects [8]. The mathematical model was later implemented in our software, PeakMaster (current version 5.3) [15]. It is able to predict the positions of system zones, calculate the characteristics of the BGE (pH, conductivity, buffer capacity, ionic strength, *etc.*) and the electrophoretic parameters of the analytes (effective mobility, transfer ratio, molar conductivity slope, detection responses and, especially, relative velocity slope). Thus, a complete picture of the electrophoretic separation can be obtained and the separation conditions can be optimized in order to maximize the detection response and minimize EMD [16,17].

Recently, we extended the theoretical model of electromigration by a nonlinear term in a way that can be solved in the matrix form enabling the calculation of the shape of the system zones as well. The nonlinear model is implemented in the new version of PeakMaster, Ver. 5.3. [18,19]. The measure of EMD is characterized by the term nonlinear migration mobility, u_{EMD}, which experimentally corresponds to the difference in the mobility at the apex of the analyte peak and at its center at infinite dilution, as long as the concentrations of all constituents at the peak apex remain close to the initial concentrations, *i.e.*, until it becomes dispersed.

Although as discussed above the electrophoretic separation is very well described theoretically, all these results were derived only for the case of systems that did not contain complexing agents. Recently, we presented the complete theoretical model of electromigration for separation systems that involved complexation [20]. This model was implemented in the simulation program Simul 5 Complex and is applicable for any number of multivalent constituents and one multivalent ligand. The model considered 1:1 complexation stoichiometry, which is common for enantiomer separations. The mathematical model, together with the Simul 5 Complex program were verified experimentally using three different systems [21]. The analyte peaks in these systems often revealed significant EMD, which could not result either from conductivity or pH effects. Consequently, we proposed that EMD in such systems is a direct consequence of complexation.

The aim of this paper is to present the complete linearized model of EMD in systems that contain neutral ligands and strong electrolyte (or at least fully charged) analytes. The mathematical model that was described in Part III: Theory [22] has been implemented in the newest version of our program, PeakMaster 5.3 Complex, which can be used to calculate the relative velocity slope and predict its dependence on the concentration of the ligand. We prove that complexation can play a major role in the development of EMD. This model is especially useful for the study of enantiomer separations where a neutral cyclodextrin is used as the complexing agent. It can be advantageously used for the optimization of the separation conditions that lead to minimum EMD and sharp, symmetrical peaks.

2. Materials and methods

2.1. Chemicals

All chemicals were of analytical grade purity. Buffer constituents tris(hydroxymethyl)aminomethane (Tris) and *N*-[tris(hydroxymethyl)methyl]glycine (Tricine), the EOF marker dimethyl sulfoxide (DMSO), the analyte (R)-(−)-2-fluoro-α-methyl-4-biphenylacetic acid (R-flurbiprofen) and chiral selectors heptakis(2,6-di-*O*-methyl)-β-cyclodextrin (DM-β-CD), heptakis(2,3,6-tri-*O*-methyl)-β-cyclodextrin (TM-β-CD) and β-cyclodextrin (β-CD) were obtained from Sigma Aldrich (Prague, Czech Republic). Water used for preparation of all solutions was purified by a Milli-Q water purification system (Millipore, Bedford, USA).

2.2. Instrumentation

All experiments were performed using the Agilent ^{3D}CE electrophoretic system operated by ChemStation software (Agilent Technologies, Waldbronn, Germany). The instrument was equipped with a built-in diode-array detector (DAD). Fused silica capillary 50 μm id, 375 μm od was purchased from Polymicro Technologies (Phoenix, AZ, USA). The total length of the capillary and its length to the DAD were 52.0 cm and 43.5 cm, respectively. A PHM 220 pH meter (Radiometer, Denmark) was used to measure the pH of the BGEs. The computer program PeakMaster 5.3 [15] was used to optimize the composition of the BGEs and to calculate the characteristics of the BGEs and the analytes. The programs Origin 8.1 (OriginLab Corporation, Northampton, MA, USA) and Microsoft Office Excel 2003 were used for data evaluation.

2.3. Experimental conditions

The running buffer (BGE) in all examples was composed of 50 mM Tris and 50 mM Tricine having an experimental pH of 8.13 and an ionic strength of 25.76 mM. The neutral chiral selectors were different in the three examples – Example 1: β-CD, Example 2: DM-β-CD, Example 3: TM-β-CD, concentration range 0–10 mM, and were dissolved directly in the running buffer. Detection was performed with the DAD at a detection wavelength of 214 nm. The operating temperature was set at 25 °C. The samples contained 0.3 mM R-flurbiprofen as the analyte and 0.02% (v/v) DMSO as the marker of EOF, dissolved directly in the running buffer. Samples were injected hydrodynamically at 10 mbar pressure for 3 s. The running voltage was 20 kV (cathode at the detector side). All solutions used in the experiments were filtered with syringe filters (Whatman, Clifton, NJ, USA), pore size 0.45 μm and degassed in an ultrasonic bath for 5 min.

For conditioning of the inner wall of the capillary, a new capillary was rinsed with 0.1 M NaOH for 30 min and three times with water for 3 min each, followed by application of a voltage of 20 kV for 20 min on the capillary filled with the running BGE to stabilize the EOF. Prior to each run, the capillary was flushed with the running

buffer for 3 min. Every measurement was performed at least three times.

2.4. Simulation conditions

The experimental conditions used in the simulations performed by Simul 5 Complex were set the same as in the measurements. In order to minimize simulation time, the EOF movement was imitated by the movement of the detector, which was initially situated outside the simulated section of the capillary, thus, only the part of the capillary, which the analyte passed through by its own effective mobility, was simulated. During simulation, the electric field strength was kept at the same value as in the experiment. This simplification did not principally influence the outcome of the simulations.

The length of simulated capillary was in the 140–345 mm range. The electric field strength was 38.46 kV m^{-1}, the current was 9.319 μA. The width of the injection zone was 0.4 mm and the peak edge width was set at 0.2 mm. The number of nodes in the *x*-axis was always 50 000. The simulations were performed by a computer that had an Intel® Core™ i7-960 Processor 3.40 GHz. The simulation time was in the range of hours.

3. Results and discussion

The quantities $S_{EMD,A}$ (nonlinear electromigration mobility slope of the analyte zone) and S_X (relative velocity slope) were chosen as the most suitable parameters to compare the extent of electromigration dispersion in systems that contained a complexing agent. $S_{EMD,A}$ can be calculated from the experimental or simulated data as

$$S_{EMD,A} = \frac{u_{MAX,A} - u_{eff,A}}{c_A}, \quad (2)$$

where $u_{MAX,A}$ is the mobility of an analyte determined from the peak maximum, $u_{eff,A}$ is the effective mobility of the analyte determined from the peak center at infinitely low analyte concentration (determined by fitting the peak with the HVL function [23,24]) and c_A is the actual analyte concentration in sample zone. Since the analyte concentration in the sample zone is influenced by both diffusion and electromigration dispersion, its value is changing during each experimental and simulated run. That is why we roughly approximate this concentration by the analyte concentration at the apex of the analyte peak. This approximation does not interfere with our conclusions we want to show in this work.

S_X can be calculated from $S_{EMD,A}$:

$$S_X = \frac{1}{2}\frac{S_{EMD,A}\kappa_0}{u_{eff,A}}, \quad (3)$$

where κ_0 is the conductivity of the BGE.

The mathematical model of electromigration dispersion in electrophoretic systems that contain a neutral complexing agent and a strong electrolyte analyte (described in Part III: Theory [22]) was implemented in the last version of PeakMaster 5.3 Complex. PeakMaster 5.3 Complex yields the values for both $S_{EMD,A}$ and S_X of the analyte. The necessary input data are the experimental conditions, the constituent parameters (dissociation constant, limiting mobility) and the complexation parameters (complexation constant and mobility of the complex). The new version of PeakMaster 5.3 Complex is also able to plot the dependence of $S_{EMD,A}$ and S_X on the cyclodextrin concentration, which can be advantageously used to choose the best separation conditions that maintain electromigration dispersion low and yield sharp, narrow analyte peaks while using the minimum concentration of the complexing agent.

The established theory as well as the new version of PeakMaster 5.3 Complex were verified experimentally and by simulations using the simulation program Simul 5 Complex [20,21]. The experimental separation systems used for the verification process differed in the choice of the neutral complexing agent, while the same analyte R-flurbiprofen (fully charged at the actual pH of the BGE and at the actual ionic strength of the BGE having an effective mobility in the non-complexing environment equal to -19.81×10^{-9} m^2 V^{-1} s^{-1}) was used. The neutral complexing agent were selected to provide different complexation constants with the R-flurbiprofen analyte. The complexation constants and the mobilities of the complexes were determined by affinity capillary electrophoresis (ACE) experiments [25–29]. In the ACE experiments the cyclodextrin was added directly to the BGE and the cyclodextrin concentration was varied in the range 0–10 mM for the systems that contained β-CD or DM-β-CD, and in the 0–50 mM range for the systems with TM-β-CD. The resulting complexation parameters are summarized in Table 1.

Table 1
Complexation constants and mobilities of the complexes. Analyte: R-flurbiprofen (mobility of the free analyte at the actual ionic strength $u_A^0 = 19.81 \times 10^{-9}$ m^2 V^{-1} s^{-1}, limiting mobility 24.5×10^{-9} m^2 V^{-1} s^{-1}). Complexing agent – Example 1: β-cyclodextrin, Example 2: heptakis(2,6-di-*O*-methyl)-β-cyclodextrin, Example 3: heptakis(2,3,6-tri-*O*-methyl)-β-cyclodextrin.

	Example 1	Example 2	Example 3
K (mol dm^{-3})$^{-1}$	4037	4800	552
u_X (10^{-9} m^2 V^{-1} s^{-1})	8.82	7.54	6.50

The complexation constants and the complex mobilities were used as the input data for the simulations of the experimental runs. Additionally, a high cyclodextrin concentration (100 mM) system was also simulated to show the behavior of the system with the "fully" complexed analyte. The system with the cyclodextrin concentration of 100 mM cannot be performed experimentally, because such high concentration exceeds the solubility limits of the cyclodextrins used. Finally, the $S_{EMD,A}$ and S_X values of the analyte were calculated for each experimental and simulated run according to Eqs. (2) and (3) and compared with those calculated by PeakMaster 5.3 Complex.

3.1. Comparison of EMD predicted by PeakMaster with the simulated and the experimentally obtained data

The experimental analyte peaks and those simulated by Simul 5 Complex are shown in Fig. 1. They are in almost perfect agreement as regards position, peak shape and amplitude. Values of $S_{EMD,A}$ and S_X were calculated using PeakMaster 5.3 Complex with the implemented complexation mode as well as from the experimental and the simulated detector traces. The resulting values are summarized in Table 2. The $S_{EMD,A}$ and S_X values obtained by PeakMaster 5.3 Complex agree very well with those calculated from the simulated electropherograms for all three chiral selector systems. Only at very low complexing agent concentration (0.1 mM, Examples 1 and 2) is there a difference of about 15% between values calculated by PeakMaster and those obtained from the simulated detector traces. At this low complexing agent concentration the analyte peaks are strongly distorted by EMD indicating that the approximate linearized model used in PeakMaster 5.3 Complex is not able to perfectly describe the nonlinear behavior of the system. In order to eliminate the significantly nonlinear effects and achieve better agreement between the calculated and simulated values it would be necessary to inject the analyte at lower concentration.

Though the values determined from the experimental electropherograms slightly differ from the values obtained by either PeakMaster 5.3 or the simulations, they follow the same trends. The differences between the experimental and the simulated/calculated data can be explained by realizing that the exact concentration of the analyte in the analyte zone is not known in

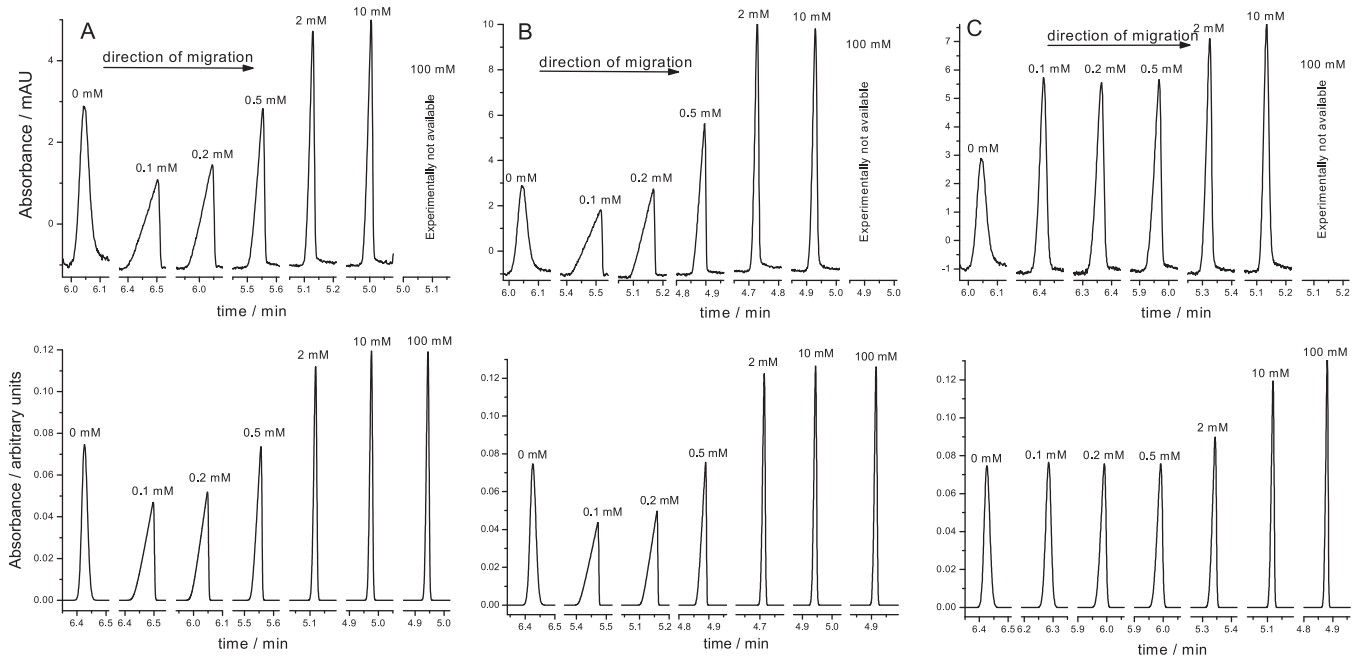

Fig. 1. Comparison of the experimental (upper panels) and simulated (lower panels) electropherograms for R-flurbiprofen as the analyte and (A) β-CD, (B) DM-β-CD, (C) TM-β-CD as the complexing agent for different cyclodextrin concentrations. The BGE concentration of the cyclodextrin used is shown next to the peaks.

Table 2
Values of $S_{EMD,A}$ and S_X calculated using PeakMaster 5.3 with the newly implemented complexation module and determined from simulated and experimental runs for different cyclodextrin concentrations in the BGE for systems containing R-flurbiprofen as the analyte and three different cyclodextrins as the chiral selector. Mark X indicates that data for a cyclodextrin concentration of 100 mM are experimentally not available.

	c_L (mM)	$S_{EMD,A}$ (10^{-9} m^5 V^{-1} s^{-1} mol^{-1})			S_X (10^{-3} m^2 S mol^{-1})		
		PeakMaster 5.3 Complex	Simul 5 Complex	Experiment	PeakMaster 5.3 Complex	Simul 5 Complex	Experiment
	0	0.11	0.11	0.23	−0.33	−0.35	−0.72
	0.1	−6.17	−5.55	−8.71	22.85	20.70	32.37
	0.2	−5.11	−4.85	−7.17	21.17	20.20	29.94
	0.5	−2.17	−2.11	−2.71	10.72	10.50	13.50
1. Example	1	−0.87	−0.87	−1.09	4.88	4.90	6.06
R-flurbiprofen + β-CD	2	−0.46	−0.48	−0.75	2.83	2.93	4.60
	5	−0.38	−0.38	−0.59	2.48	2.53	3.90
	8	−0.37	−0.37	−0.70	2.52	2.51	4.72
	10	−0.37	−0.37	−0.84	2.54	2.51	5.76
	100	−0.38	−0.38	X	2.64	2.64	X
	0	0.11	0.11	0.23	−0.33	−0.35	−0.72
	0.1	−9.25	−8.21	−12.5	36.06	32.67	49.38
	0.2	−7.02	−6.54	−9.72	31.40	29.78	44.63
	0.5	−2.64	−2.55	−2.98	14.60	14.31	16.74
2. Example	1	−0.99	−0.98	−0.95	6.34	6.34	6.07
R-flurbiprofen + DM-β-CD	2	−0.51	−0.53	−0.47	3.62	3.75	3.30
	5	−0.41	−0.42	−0.47	3.16	3.24	3.55
	8	−0.41	−0.41	−0.33	3.20	3.21	3.56
	10	−0.41	−0.40	−0.43	3.23	3.20	3.43
	100	−0.41	−0.41	X	3.35	3.34	X
	0	0.11	0.11	0.23	−0.33	−0.35	−0.72
	0.1	−0.39	−0.32	−0.28	1.26	1.04	0.90
	0.2	−0.74	−0.63	−1.08	2.47	2.11	3.61
	0.5	−1.26	−1.13	−1.49	4.60	4.12	5.51
3. Example	1	−1.38	−1.28	−1.40	5.67	5.27	5.85
R-flurbiprofen + TM-β-CD	2	−1.11	−1.06	−0.85	5.32	5.11	4.14
	5	−0.61	−0.62	−0.22	3.77	3.81	1.33
	8	−0.49	−0.50	−0.11	3.36	3.47	0.75
	10	−0.46	−0.47	−0.07	3.30	3.42	0.52
	100	−0.43	−0.43	X	3.93	3.96	X

the experiments and it can be only roughly approximated from the simulations as described above.

3.2. Influence of complexation on EMD

In the Example 1, native β-CD was chosen as the complexing agent. The complexation constant and the mobility of the complex determined by ACE are summarized in Table 1. The corresponding experimental and simulated analyte peak shapes are shown in Fig. 1A. Obviously, the peak shape changes significantly with the cyclodextrin concentration. In the cyclodextrin-free BGE, the analyte peak has an almost Gaussian profile: the calculated value of $S_{EMD,A}$ is 0.11×10^{-9} m^5 V^{-1} s^{-1} mol^{-1} and that of S_X is -0.33×10^{-3} m^2 S mol^{-1} (values calculated by PeakMaster 5.3 Complex). These values are exactly the same as those calculated by the basic version of PeakMaster 5.3 (without complexation mode), as expected. Clearly, the analyte peak is slightly fronting but the effect is too small to be observable by the naked eye. However, at a chiral selector concentration of 0.1 mM, the analyte peak is suddenly significantly influenced by electromigration dispersion ($S_{EMD,A} = -0.62 \times 10^{-9}$ m^5 V^{-1} s^{-1} mol^{-1}, $S_X = 22.9 \times 10^{-3}$ m^2 S mol^{-1}; values calculated by PeakMaster 5.3 Complex). Thus, the resulting analyte peak is small and strongly tailing. Interestingly, by increasing the concentration of the cyclodextrin in the BGE the value of $S_{EMD,A}$ decreases: at a cyclodextrin concentration of 2 mM and higher, the analyte peaks become almost Gaussian again.

Generally, electromigration dispersion can be observed if the velocity of the analyte depends on its concentration in the sample zone. Mostly this is due to the fact that the presence of the analyte significantly influences the conductivity and/or pH of the BGE. However, in our case the addition of a small amount of neutral cyclodextrin to the running buffer does not change either the conductivity or the pH of the BGE. Thus, the electromigration dispersion observed at low cyclodextrin concentration must be related to the complexation of analyte by the cyclodextrin.

As discussed in detail in Part III: Theory of this series of papers [22], electromigration dispersion observed in separation systems that contain a neutral complexing agent and a strong electrolyte (or fully charged) analyte has three main contributors: (1) impact of analyte in the sample zone on the conductivity of the BGE, (2) complexation, and (3) impact of the analyte–ligand complex on the conductivity of the BGE.

Fig. 2A shows the dependence of $S_{EMD,A}$ on the neutral complexing agent concentration. At the initial point of this dependence (cyclodextrin-free BGE, $c_L = 0$ mM) complexation is not involved in the separation. Consequently, the analyte peak has to be distorted only by the first contribution, as in the usual non-complexing systems. At the virtually infinite cyclodextrin concentration the analyte is fully complexed and is present only as the complex. This situation is equivalent to the system where the analyte migrates in a cyclodextrin-free BGE with an effective mobility that is equal to the mobility of the complex. The characteristics of electromigration dispersion calculated for such a non-complexing system are $S_{EMD,A} = -0.38 \times 10^{-9}$ m^5 V^{-1} s^{-1} mol^{-1} and $S_X = 2.66 \times 10^{-3}$ m^2 S mol^{-1}. As shown in Fig. 2A (insert), dependence of $S_{EMD,A}$ on cyclodextrin concentration limits exactly to this value. Thus, at high cyclodextrin concentration the third contribution to electromigration dispersion prevails. In this particular system (high complexation constant), the analyte is almost fully complexed already at a cyclodextrin concentration as low as 2 mM and $S_{EMD,A}$ almost reaches its limiting value (Fig. 2A). Between these two extreme cyclodextrin concentrations (0 mM and 2 mM), $S_{EMD,A}$ passes through a sharp minimum as the cyclodextrin concentration is increased (Fig. 2A). EMD in this region is caused by the combination of all three contributions. The $S_{EMD,A}$ at the two

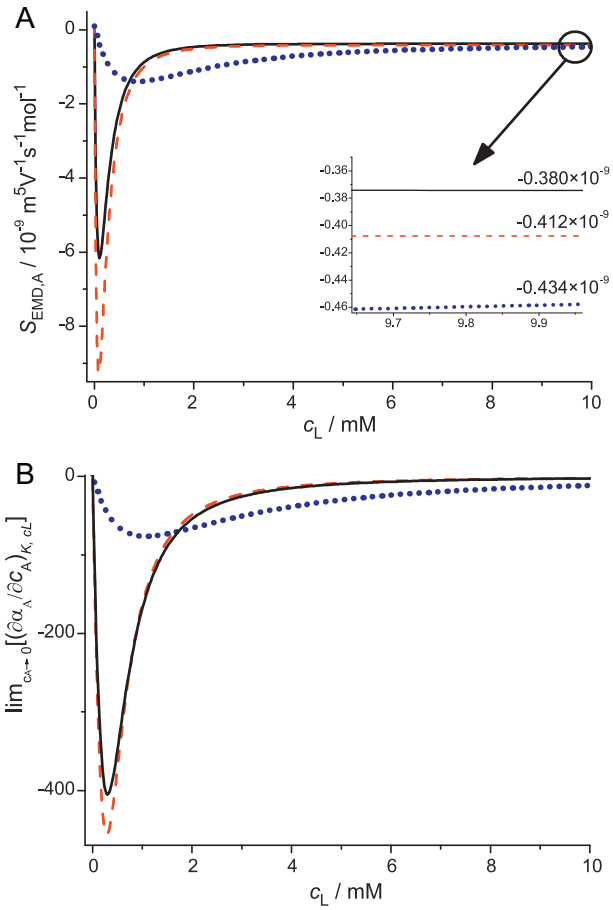

Fig. 2. $S_{EMD,A}$, predicted by PeakMaster 5.3 Complex, (Panel A) and $\lim_{c_A \to 0}(\partial\alpha_{A,X}/\partial c_A)_{c_L,K}$ (Panel B) as a function of the analytical cyclodextrin concentration in the BGE. Complexing agent: β-CD (solid line), DM-β-CD (dashed line), TM-β-CD (dotted line). Insert (A) zoomed part of depicted curves in the vicinity of a complexing agent concentration of 10 mM.

extremes correspond directly to the 1st and the 3rd EMD contributions, respectively. These values are relatively low and they do not cause observable EMD. Thus, complexation of the analyte with the cyclodextrin, as the second contribution, has to play the major role in the development of EMD in the low cyclodextrin region.

In BGEs that contain a complexing agent, the effective mobility of an analyte, $u_{eff,A}$, depends on the mole fraction of the complexed analyte, α_X, according to the following equation:

$$u_{eff,A} = \alpha_X u_X + (1 - \alpha_X) u_A^0, \quad (4)$$

where u_X is the mobility of the analyte–cyclodextrin complex and u_A^0 is the mobility of the free analyte. Electromigration dispersion occurs when the velocity of the analyte depends on its concentration and the composition of the BGE in the sample zone. The mobilities of the free and complexed forms of the analyte are constant for each particular system and only the mole fraction of the complexed analyte depends on the analytical concentration of both the cyclodextrin (c_L) and the analyte (c_A) as follows

$$\alpha_X = \frac{2Kc_L}{K(c_A + c_L) + 1 + \sqrt{[K(c_A + c_L) + 1]^2 - 4K^2 c_A c_L}}, \quad (5)$$

where K is the stability constant of the analyte–cyclodextrin complex.

Further, dependence of α_X on the concentration of the analyte in the sample zone can be expressed as the partial derivative of α_X with respect to c_A in BGE where $c_A \to 0$:

$$\lim_{c_A \to 0} \left(\frac{\partial \alpha_X}{\partial c_A} \right)_{c_L,K} = \frac{-2K^2 c_L}{(Kc_L + 1)^3}. \quad (6)$$

The dependence of this parameter on the concentration of the cyclodextrin for our particular system is shown in Fig. 2B. The similarity to the dependence of $S_{EMD,A}$ on the cyclodextrin concentration is obvious. At low cyclodextrin concentration, the amount of cyclodextrin present is not sufficient to "saturate" the complexation of the analyte with the cyclodextrin. The mole fraction of the complexed analyte strongly depends on the analyte concentration in the sample zone, the observed limit is high and electromigration dispersion occurs. With increasing cyclodextrin concentration the limiting form of the partial derivative approaches zero. A value sufficiently close to zero is reached at a cyclodextrin concentration of about 2 mM. At – and above – this cyclodextrin concentration the degree of complexation depends only slightly on the concentration of analyte and electromigration dispersion is avoided. This agrees very well with the result deduced previously that complexation is the main cause of EMD in the low cyclodextrin concentration region in this separation system. A detailed description of the individual contributions to the development of EMD can be found in our paper, the Part III: Theory [22].

In Example 2 DM-β-CD is used as a complexation agent. The complexation constant is about 20% higher, while the complex mobility is approximately 15% lower than in Example 1 (see Table 1). The peak shape changes significantly with the cyclodextrin concentration and follows the same trends as in the Example 1 (see Fig. 1B). At zero cyclodextrin concentration the analyte peak has an almost Gaussian profile. With the addition of a small amount of cyclodextrin to BGE, the analyte peak is strongly influenced by EMD. This effect is observable up to a cyclodextrin concentration of 2 mM. At this – and higher – concentrations the analyte peaks have an almost Gaussian profile again.

The dependence of $S_{EMD,A}$ and $\lim_{c_A \to 0} (\partial \alpha_{A,X} / \partial c_A)_{c_L,K}$ on the cyclodextrin concentration for this particular system are shown in Fig. 2A and B, respectively. The initial value of $S_{EMD,A}$ is the same as in the previous example, because without cyclodextrin the analyte and the separation systems are identical. Thus, EMD is caused only by the influence of the analyte on the conductivity of the BGE. The limiting value of $S_{EMD,A}$ is $-0.41 \times 10^{-9}\ m^5\ V^{-1}\ s^{-1}\ mol^{-1}$ (calculated for the infinitely high cyclodextrin concentration as described in Example 1). The value is slightly lower (higher in the absolute value) than in previous example because the mobility of the analyte–cyclodextrin complex is lower. Between these two extremes there is a sharper and deeper minimum than in Example 1. This difference is caused by both the higher value of the complexation constant and the lower value of the mobility of the complex. The influence of complexation constant can be explained by the dependence of $\lim_{c_A \to 0} (\partial \alpha_{A,X} / \partial c_A)_{c_L,K}$ on the cyclodextrin concentration. As shown in Fig. 2B, this dependence has a steeper decrease and reaches a deeper minimum than in Example 1 with the lower complexation constant. It means that the mobility depends more significantly on the cyclodextrin concentration, and therefore, EMD is more pronounced. Simultaneously, because of the higher mobility difference between the complexed and the free analyte, the effective mobility of analyte in the sample zone changes more significantly with the mole fraction than in Example 1, see Eq. (3). These two effects act together and result in higher absolute values of $S_{EMD,A}$ in the cyclodextrin concentration range of 0.1–2 mM. At a cyclodextrin concentration of 2 mM and higher, the degree of complexation depends only slightly on the analyte concentration, thus EMD is not observed, similarly to what was found in Example 1.

In the third example, Example 3, TM-β-CD was used as the neutral complexing agent. The complexation constant is about seven-times lower than in Example 1 (see Table 1).

As shown in Fig. 1C, the analyte peaks have almost Gaussian profiles, independently of the cyclodextrin concentration. The same behavior is observed for the dependence of $S_{EMD,A}$ on the complexing agent concentration, see Fig. 2A. The initial point of the dependence (in the absence of the complexing agent) is common for all three systems. At this point the analyte peak is only slightly distorted by EMD, which is caused by the first conductivity contribution. At infinitely high complexing agent concentrations the limiting value of $S_{EMD,A}$ is $-0.43 \times 10^{-9}\ m^5\ V^{-1}\ s^{-1}\ mol^{-1}$ due to the third conductivity contribution. This value is low, that is why EMD is not observable and the peak has an almost Gaussian profile. Contrary to the previous examples, the dependence of $S_{EMD,A}$ on the cyclodextrin concentration does not show a sharp and deep minimum between these two extreme complexing agent concentrations, but a very shallow one in the concentration range of 0.5–1 mM. At the same time, the absolute values of $S_{EMD,A}$ are insignificant over the whole cyclodextrin concentration range. Again, the approximate contribution of complexation to EMD can be found using $\lim_{c_A \to 0} (\partial \alpha_{A,X} / \partial c_A)_{c_L,K}$. Because of the low complexation constant, the mole fraction of the complexed analyte depends only slightly on the analyte concentration in a sample zone and causes significantly lower EMD than in previous two Examples, see Fig. 2B. The other result arising from the lower complexation constant value is that full complexation is achieved at a much higher cyclodextrin concentration, thus, the complexation contribution plays role over a wider cyclodextrin concentration range.

3.3. Influence of the complexation constant and the mobility of the complex on EMD

The $S_{EMD,A}$ values are plotted in Fig. 3A as a function of the concentration of the neutral complexing agent using the same complexation constant and free analyte mobility values as in Example 1 ($K = 4037\ (mol\ dm^{-3})^{-1}$, $u_A^0 = 19.81 \times 10^{-9}\ m^2\ V^{-1}\ s^{-1}$), but five different mobilities of the complexed forms ranging from a high mobility of $u_X = 19.81 \times 10^{-9}\ m^2\ V^{-1}\ s^{-1}$ to a low mobility of $u_X = 1 \times 10^{-9}\ m^2\ V^{-1}\ s^{-1}$. For each set of parameter combinations, the $S_{EMD,A}$ values go through a minimum as the cyclodextrin concentration is increased. The minima become sharper, their depth increases and the limiting $S_{EMD,A}$ values (observed at very high cyclodextrin concentrations) remain farther away from zero as the difference between u_A^0 and u_X increases from 0 to $18.81 \times 10^{-9}\ m^2\ V^{-1}\ s^{-1}$, leading to increased EMD and worsened peak shape across the entire cyclodextrin concentration range. However, the minima occur at the same cyclodextrin concentration irrespectively of the magnitude of the difference between u_A^0 and u_X.

The $S_{EMD,A}$ values are plotted in Fig. 3B as a function of the cyclodextrin concentration using the same complex mobility and free analyte mobility values as in Example 1 ($u_X = 8.82 \times 10^{-9}\ m^2\ V^{-1}\ s^{-1}$, $u_A^0 = 19.81 \times 10^{-9}\ m^2\ V^{-1}\ s^{-1}$), but five different complexation constants ranging from a low $K = 100\ (mol\ dm^{-3})^{-1}$ to a high $K = 8000\ (mol\ dm^{-3})^{-1}$. Again, for each set of parameter combinations, the $S_{EMD,A}$ values go through a minimum as the cyclodextrin concentration is increased. As the K values increase from 100 to $8000\ (mol\ dm^{-3})^{-1}$ the minima occur at lower cyclodextrin concentrations, become sharper, their depth increases, and approach their limiting $S_{EMD,A}$ values sooner (at lower cyclodextrin concentrations). This means that though EMD is increased and peak shape is worsened as K becomes larger, the

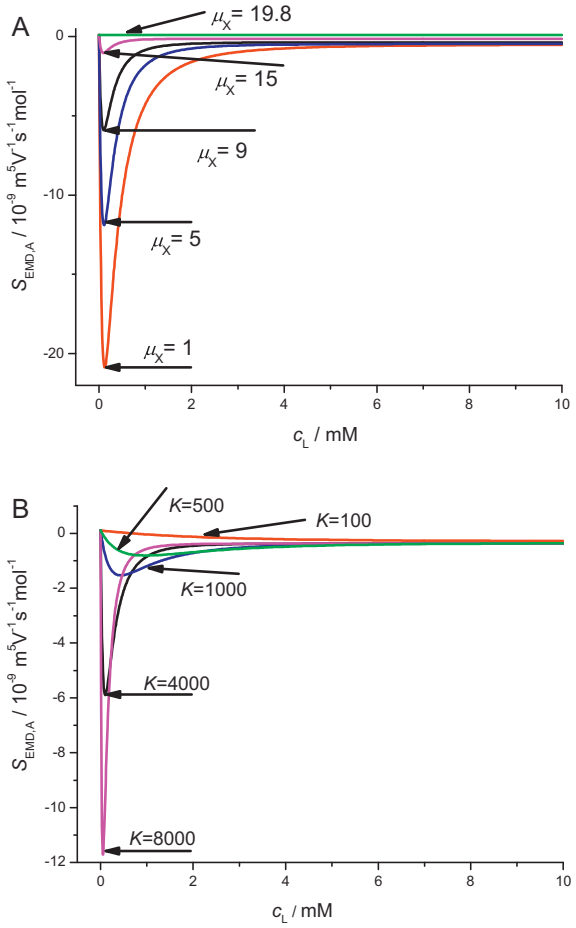

Fig. 3. $S_{EMD,A}$ as a function of the cyclodextrin concentration in the BGE for R-flurbiprofen as the analyte and different theoretical complexing agents. (A) Complexation parameters: $u_X = 1$, 5, 9, 15, and 19.8×10^{-9} m^2 V^{-1} s^{-1}, $K = 4000$ (mol dm^{-3})$^{-1}$. The curves are marked by the mobility of the complex. (B) Complexation parameters: $u_X = 9 \times 10^{-9}$ m^2 V^{-1} s^{-1}, $K = 100$, 500, 1000, 4000, and 8000 (mol dm^{-3})$^{-1}$. The curves are marked by the value of complexation constant.

complexation induced distortion persists over a narrower cyclodextrin concentration range.

4. Conclusions

The theoretical model of EMD in systems that contain a neutral complexing agent and a fully charged analyte, described in Part III: Theory [22], was implemented in the simulation program PeakMaster 5.3 Complex. The new module of PeakMaster 5.3 Complex can be used to predict the impact of EMD on the shape of the analyte peak by calculating both the relative velocity slope (S_X) and the nonlinear electromigration mobility slope of the analyte zone ($S_{EMD,A}$). The newly established theoretical model was verified by simulations (using Simul 5 Complex) and experiments using three systems with different complexing agents. The calculated values of S_X and $S_{EMD,A}$ were compared with those obtained from simulations and experimental data. The good agreement allowed us to discuss and explain the influence of complexation on EMD development. The new version of PeakMaster 5.3 Complex extended with the complexation module is a powerful tool for eliminating EMD to obtain symmetrical and sharp peaks, and thus, can be used for optimization of the conditions of enantiomer separations.

Acknowledgments

The support of the Grant Agency of the Czech Republic, Grant No. 203/08/1428, Grant Agency of Charles University, Grant No. 323611, Grant No. 669412 and the long-term research plan of the Ministry of Education of the Czech Republic (MSM 0021620857), are gratefully acknowledged.

References

[1] B. Gas, E. Kenndler, Electrophoresis 23 (2002) 3817.
[2] B. Gas, E. Kenndler, Electrophoresis 21 (2000) 3888.
[3] S. Hjerten, Electrophoresis 11 (1990) 665.
[4] F.E.P. Mikkers, F.M. Everaertst, P.E.M. Verheggen, J. Chromatogr. 169 (1979) 11.
[5] F.E.P. Mikkers, F.M. Everaertst, P.E.M. Verheggen, J. Chromatogr. 169 (1979) 1.
[6] F. Foret, S. Fanali, L. Ossucinip, P. Bocek, J. Chromatogr. 470 (1989) 299.
[7] J.L. Beckers, J. Chromatogr. A 741 (1996) 265.
[8] X. Xu, W.T. Kok, H. Poppe, J. Chromatogr. A 742 (1996) 211.
[9] P. Gebauer, P. Bocek, Anal. Chem. 69 (1997) 1557.
[10] P. Gebauer, P. Borecka, P. Bocek, Anal. Chem. 70 (1998) 3397.
[11] M. Horka, K. Slais, Electrophoresis 21 (2000) 2814.
[12] M. Stedry, M. Jaros, B. Gas, J. Chromatogr. A 960 (2002) 187.
[13] M. Stedry, M. Jaros, K. Vcelakova, B. Gas, Electrophoresis 24 (2003) 536.
[14] M. Stedry, M. Jaros, V. Hruska, B. Gas, Electrophoresis 25 (2004) 3071.
[15] M. Jaros, V. Hruska, M. Stedry, I. Zuskova, B. Gas, Electrophoresis 25 (2004) 3080.
[16] M. Jaros, K. Vcelakova, I. Zuskova, B. Gas, Electrophoresis 23 (2002) 2667.
[17] M. Jaros, T. Soga, T. van de Goor, B. Gas, Electrophoresis 26 (2005) 1948.
[18] V. Hruska, M. Riesova, B. Gas, Electrophoresis 33 (2012) 923.
[19] M. Riesova, V. Hruska, B. Gas, Electrophoresis 33 (2012) 931.
[20] V. Hruška, M. Beneš, J. Svobodová, I. Zusková, B. Gaš, Electrophoresis 33 (2012) 938.
[21] J. Svobodova, M. Benes, V. Hruska, K. Uselova, B. Gas, Electrophoresis 33 (2012) 948.
[22] V. Hruska, J. Svobodova, M. Benes, B. Gas, J. Chromatogr. A 1267 (2012) 102.
[23] P.C. Haarhoff, H.J. van der Linde, Anal. Chem. 38 (1966) 573.
[24] G.L. Erny, E.T. Bergstrom, D.M. Goodall, Anal. Chem. 73 (2001) 4862.
[25] K.L. Rundlett, D.W. Armstrong, Electrophoresis 22 (2001) 1419.
[26] M.H.A. Busch, L.B. Carels, H.F.M. Boelens, J.C. Kraak, H. Poppe, J. Chromatogr. A 777 (1997) 311.
[27] Y. Tanaka, S. Terabe, J. Chromatogr. B 768 (2002) 81.
[28] K. Uselova-Vcelakova, I. Zuskova, B. Gas, Electrophoresis 28 (2007) 2145.
[29] C.X. Jiang, D.W. Armstrong, Electrophoresis 31 (2010) 17.

V.

Complexation of Buffer Constituents with Neutral Complexation Agents: Part I. Impact on Common Buffer Properties

M. Riesová, J. Svobodová, Z. Tošner, M. Beneš, E. Tesařová, B. Gaš
Analytical Chemistry, 2013, 85, 8518-8525

analytical chemistry

Article

pubs.acs.org/ac

Complexation of Buffer Constituents with Neutral Complexation Agents: Part I. Impact on Common Buffer Properties

Martina Riesová,[†] Jana Svobodová,*[,†] Zdeněk Tošner,[‡] Martin Beneš,[†] Eva Tesařová,[†] and Bohuslav Gaš[†]

[†]Charles University in Prague, Faculty of Science, Department of Physical and Macromolecular Chemistry, Prague, Czech Republic
[‡]Charles University in Prague, Faculty of Science, Department of Chemistry, Prague, Czech Republic

Supporting Information

ABSTRACT: The complexation of buffer constituents with the complexation agent present in the solution can very significantly influence the buffer properties, such as pH, ionic strength, or conductivity. These parameters are often crucial for selection of the separation conditions in capillary electrophoresis or high-pressure liquid chromatography (HPLC) and can significantly affect results of separation, particularly for capillary electrophoresis as shown in Part II of this paper series (Beneš, M.; Riesová, M.; Svobodová, J.; Tesařová, E.; Dubský, P.; Gaš, B. *Anal. Chem.* **2013**, DOI: 10.1021/ac401381d). In this paper, the impact of complexation of buffer constituents with a neutral complexation agent is demonstrated theoretically as well as experimentally for the model buffer system composed of benzoic acid/LiOH or common buffers (e.g., CHES/LiOH, TAPS/LiOH, Tricine/LiOH, MOPS/LiOH, MES/LiOH, and acetic acid/LiOH). Cyclodextrins as common chiral selectors were used as model complexation agents. We were not only able to demonstrate substantial changes of pH but also to predict the general complexation characteristics of selected compounds. Because of the zwitterion character of the common buffer constituents, their charged forms complex stronger with cyclodextrins than the neutral ones do. This was fully proven by NMR measurements. Additionally complexation constants of both forms of selected compounds were determined by NMR and affinity capillary electrophoresis with a very good agreement of obtained values. These data were advantageously used for the theoretical descriptions of variations in pH, depending on the composition and concentration of the buffer. Theoretical predictions were shown to be a useful tool for deriving some general rules and laws for complexing systems.

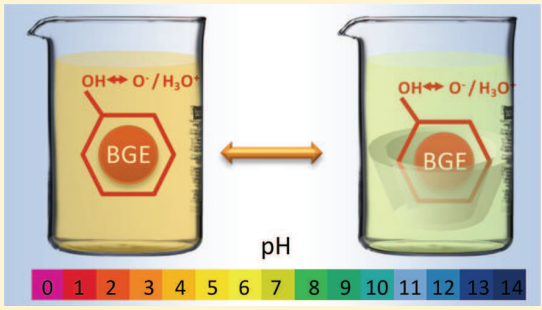

Guest–host interactions have a significant impact in many biological processes, and they are also substantial for a number of separation techniques. The additional interaction of an analyte can improve results of separation or enable separation of chiral compounds if a chiral selector is used as a complexation agent. Simultaneously, this kind of interaction was shown to influence the physicochemical properties of the complexed compounds, particularly acid–base behavior, which can result in shifts of its pK_A. The pK_A shifts for various compounds complexing with cyclodextrins (CDs),[1−3] cucurbiturils,[4,5] or even micelles or compartmentalized lipids[6] were observed by different techniques particularly fluorescence,[1,5] potentiometry,[6−8] induced circular dichroism,[9] electrophoresis,[2,10−12] and NMR.[3] Such pK_A shifts can have a crucial impact on the selection of optimum separation conditions, as was shown for chiral separation in capillary electrophoresis (CE) by Rizzi et al.[12] and Hammitzsch-Wiedmann et al.[11]

The extent of the pK_A shift of an analyte depends on the ratio of the complexation constants of both dissociated and nondissociated forms of the analyte with a complexation agent. Thus, a pH potentiometric titration of the desired compound was used to determine the complexation constants by Gelb et al.[8,13] Nowadays this method has been replaced by more accurate techniques, such as NMR and electrophoretic techniques. In NMR, the concentration of the complexation agent is varied, while chemical shift, relaxation rates, or diffusion coefficients are most frequently measured as a response.[14,15] An advantage of NMR is that it can be used to estimate the stoichiometry of the resulting complex or to obtain the additional information on the structure of the complex. In electrophoresis, affinity capillary electrophoresis (ACE) is the most common setup,[16−20] in which mobility of an analyte is determined against the concentration of a complexation agent added into the background electrolyte (BGE). ACE-like separation is also frequently used for practical purposes in analytical chemistry. Despite the fact that electrophoretic separation is a complicated nonlinear process, it is very well described theoretically and it generally results in being the common physicochemical property of the buffer (i.e., BGE) that determines the separation efficiency in CE. Some computer programs exist that enable to predict the parameters of the used BGE and/or simulate the separation process. Out of

Received: May 7, 2013
Accepted: July 27, 2013
Published: July 27, 2013

these, Simul[21−24] and PeakMaster[25−27] have been developed in our laboratory, and their latest versions were designed to account for complexation in CE.

Clearly, the complexation of the analyte and complexation agent is widely studied. On the other hand, other consequences, such as the impact of the complexation of buffer constituents on the properties of the buffer, are discussed only rarely and in special cases.[28,29] In the present study, we show, both theoretically and experimentally, that an addition of any (even neutral) complexation agent into a BGE might significantly influence buffer properties, e.g., pH, ionic strength, or conductivity. We simultaneously demonstrate that changes in pH can reveal some fundamental characteristics of complexation. For example it follows that complexation of common buffer constituents such as CHES, MES, and MOPS with common neutral CDs is much stronger if they are present in the charged form than in the neutral one. These findings are in direct consequence with the zwitterion character of these compounds and are additionally proved by independent NMR measurements. The obtained complexation characteristics were used as input data for Simul 5 Complex software to calculate and demonstrate the fundamental buffer properties in the dependence on the concentration of the neutral complexation agent (β-cyclodextrin) complexing with present buffer constituents. Practical impacts of this study, such as a shift of complexation constant, system peak occurrences, or even deterioration of separation, are consequently discussed in Part II of this series of papers.[30]

THEORY

If a weak electrolyte forms the complex with a neutral complexation agent, simultaneous dissociation and complexation equilibria have to be considered, as shown, e.g., for weak acid HA in Scheme 1.

Scheme 1. Reaction Scheme for Simultaneous Dissociation and Complexation of a Complexation Agent and a Weak Electrolyte Compound[a]

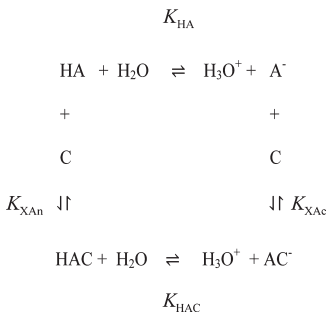

[a]C and HA represent the complexation agent and the weak electrolyte, respectively.

Each equilibrium is characterized by its individual complexation constant (K_{XAn}, K_{XAc} for the neutral or the charged form of the analyte, respectively) or dissociation constant (K_{HA}, K_{HAC})

$$K_{XAn} = \frac{[HAC]}{[HA][C]} \quad (1)$$

$$K_{XAc} = \frac{[AC^-]}{[A^-][C]} \quad (2)$$

$$K_{HA} = \frac{[H_3O^+][A^-]}{[HA]} \quad (3)$$

$$K_{HAC} = \frac{[H_3O^+][AC^-]}{[HAC]} = K_{HA}\frac{K_{XAc}}{K_{XAn}} \quad (4)$$

where [ ] stands for the equilibrium concentration of individual compounds. We use concentrations rather than activities and thus apparent rather than true thermodynamic equilibrium constants for simplicity without a loss of validity of the theory. However, the resulting values of apparent complexation constants can be corrected for actual ionic strength, as shown in our previous publication.[31]

Simultaneously, total (analytical) concentrations of the analyte and the complexation agent correspond to the sum of equilibrium concentrations of individual forms

$$c_{HA} = [HA] + [A^-] + [AC^-] + [HAC] \quad (5)$$

$$c_C = [C] + [AC^-] + [HAC] \quad (6)$$

The complete set of these equations together with the electroneutrality condition, conductivity equation and the expression for ionic product of water (K_w) can be solved numerically using our simulation tool Simul 5 Complex[22−24] with the implemented complexation mode. Simul 5 also enables to apply ionic strength correction based on the Debye−Hückel equation with the linear term. Thus, the precise values of the pH, ionic strength, and conductivity can be obtained by the software.

The pH is a fundamental property of the separation buffer solution. For this reason, we also derived simplified analytical expressions for the pH of the interacting buffer. However, these equations are limited to buffers consisting of a weak acid or conjugate weak acid and a strong base at an acidic (eq 7) or alkaline (eq 8) pH region, respectively, where concentrations of hydroxide or hydroxonium ions can be neglected. Further, a sufficient excess of the amount of complexation agent is required, so the equilibrium concentration of the complexation agent can be approximated by its analytical (total) concentration.

$$[H_3O^+] = \frac{-(K_{HA}Z_A + [B^+])}{2} + \frac{\sqrt{(K_{HA}Z_A - [B^+])^2 + 4K_{HA}c_{HA}Z_A}}{2} \quad (7)$$

$$[H_3O^+] = \frac{-(K_{HA}([B^+] - c_{HA})Z_A - K_w)}{2[B^+]} + \frac{\sqrt{(K_{HA}([B^+] - c_{HA})Z_A - K_w)^2 + 4K_{HA}K_w[B^+]Z_A}}{2[B^+]} \quad (8)$$

where

$$Z_A = \frac{1 + K_{XAc}c_C}{1 + K_{XAn}c_C} \quad (9)$$

and $[B^+]$ is the analytical concentration of the strong base utilized for buffer preparation. Analogous equations can be

dx.doi.org/10.1021/ac4013804 | Anal. Chem. 2013, 85, 8518−8525

derived also for other buffer types, see the Supporting Information S1. These equations (eqs 7 and 8) are simple enough to make some general conclusions about behavior of such systems. The illustrative dependence of pH on the concentration of cyclodextrin and the buffer concentration plotted according to the eq 7 is shown in the Supporting Information in Figure S1-1.

By comparison of these equations with those valid for systems without complexation, one can see that the complexation introduces the complexation induced pK_A shift of the weak acid by the factor of Z_A as shown already by Yoshida et al.[3] Thus the system behaves as if a weak acid with its apparent dissociation constant equal to $K_{HA}^{app} = K_{HA}Z_A$ was present and the complexation induced pK_A shift can be expressed as $\Delta pK_{HA} = pK_{HA}^{app} - pK_{HA} = pZ_A$. Whether the complexation induced pK_A shift is negative or positive depends only on the ratio of complexation constants as a resulted of eq 9. We especially emphasize that the dissociation constant of the weak acid in its complexed form (K_{HAC}) is not needed to calculate the pZ_A value, which is a consequence of eq 4. In our particular case of a buffer composed of a weak acid or conjugate weak acid and a strong base, the acid becomes weaker ($pZ_A > 0$) as the complexation of the neutral form of the acid is preferred over the complexation of its charged form ($K_{XAn} > K_{XAc}$). This indeed results in a shift in pH of the buffer, which increases as the neutral form of the weak acid complexes stronger with the complexation agent than the charged one does and vice versa.

Notice that the complexation induced pK_A shift is changing gradually with increasing complexation agent concentration. At a sufficiently high agent concentration (so that min $\{K_{XAc}c_c; K_{XAn}c_c\} \gg 1$), it effectively reaches its limit when $K_{HA}^{app} = K_{HAC}$ (see eq 4).

Therefore, at a high concentration of the complexation agent, the pH converges to a certain value, which is the function of only the dissociation and complexation constants of weak acid and the initial concentration of buffer constituents. In other words a different buffer composed of a fully complexed weak electrolyte constituent with the shifted value of its dissociation constant (see eq 4) is formed. This indicates that one might estimate some fundamental complexation characteristics even from the very simple pH measurements.

MATERIALS AND METHODS

Chemicals. All chemicals were of analytical grade purity. Lithium hydroxide monohydrate, benzoic acid, [Tris(hydroxymethyl)methyl]glycine (Tricine), and acetic acid were purchased from Fluka (Steinheim, Germany). Formic acid was the product of Lachema (Brno, Czech Republic). 2-(*N*-morpholino)ethanesulfonic acid (MES), 3-morpholinopropane-1-sulfonic acid (MOPS), *N*-cyclohexyl-2-aminoethanesulfonic acid (CHES), 3-[[1,3-dihydroxy-2-(hydroxymethyl)-propan-2-yl]amino]propane-1-sulfonic acid (TAPS), ethanolamine, sodium hydrogenphosphate, and sodium dihydrogenphosphate were obtained from Sigma Aldrich (Steinheim, Germany). Neutral cyclodextrins (2-hydroxypropyl)-β-cyclodextrin (HP-β-CD) of 0.8 M substitution and average M_r = 1460, heptakis(2,6-di-*O*-methyl)-β-cyclodextrin (DM-β-CD), β-cyclodextrin (β-CD), and native α-CD all from Sigma Aldrich (Steinheim, Germany) were used as complexation agents. Water for solution preparation was deionized by the Watrex Ultrapur system (Prague, Czech Republic). Deuterated water (99.8% D) was obtained from Chemotrade, Leipzig, Germany.

Instrumentation. CE experiments were carried out by using the Agilent HP^{3D}CE capillary electrophoresis instrument operated by ChemStation software from Agilent Technologies (Waldbronn, Germany). Detection was performed with the built-in diode array detector (DAD) and the contactless conductivity detector (CCD) of our construction.[32] Uncoated fused silica capillaries with i.d. of 50 μm and o.d. of 375 μm (Polymicro Technologies, Phoenix, AZ) were utilized for all electrophoretic experiments. CE measurements were performed at temperature 25 °C, samples were injected hydrodynamically at 30 mbar × 3 s. A new capillary was flushed with deionized water for 20 min and conditioned with actual running buffer prior to each run. All running buffers were filtered with Minisart syringe filters (Sartorius Stedim Biotech, Goettingen, Germany), pore size 0.45 μm.

All the ^{1}H NMR data were recorded on a Bruker Avance III 600 MHz spectrometer at 25 °C (temperature controlled by the manufacturer system) equipped with the cryogenically cooled TCI probe. A chemical shift was referenced according to the residual water signal set to the value of 4.700 ppm. The accuracy of the shift values was estimated to ±0.001 ppm from repeated experiments. Measurements of translational diffusion coefficients were performed with the double stimulated echo experiment with bipolar pulse field gradients described by Jerschow et al.[33] This pulse sequence is optimized to suppress flow and convection artifacts as well as eddy current effects. The use of bipolar gradients removes the possible modulation of the intensity decay curves by a chemical exchange occurring between the sites with different chemical shifts.[34] The gradients were 1 ms long with 16 different linearly spaced amplitudes spanning the range 1−59 G cm^{-1}, the diffusion time was 0.8 s, and 16 scans were acquired to complete the phase cycle. The calibration was done using a standard sample of 1% H_2O in D_2O (doped with $GdCl_3$) for which the value of the HDO diffusion coefficient at 25 °C is 1.9 × 10^{-9} m^2 s^{-1}.[35] All data processing and fitting of the diffusion coefficients has been done using the spectrometer software (Topspin 2.1, Bruker) with the precision of the results estimated to 2%.

The PHM240 pH/ion meter (Radiometer, Copenhagen, Denmark) calibrated with standard IUPAC buffers, pH 1.679, pH 7.000, pH 10.012, and pH 12.450 (Radiometer Analytical, Lyon, France) was used for pH measurements.

CE Measurements. A model buffer system was composed of benzoic acid (24 mM) as a weak electrolyte and lithium hydroxide (9.9 mM) as a corresponding strong base, pH 4.01. The complexation parameters of benzoic acid with β-CD were determined using the ACE method. The complexation constant of the dissociated (charged) form, K_{XAc}, of benzoic acid was determined at pH where it is fully dissociated, i.e., Tricine/LiOH buffer (19.41 mM/10 mM), pH = 8.13. The complexation constant of the nondissociated (neutral) form of benzoic acid, K_{XAn}, was determined in acetic acid/LiOH buffer (61 mM/9.9 mM), pH = 3.98. Ionic strength (IS) was always 10 mM. β-CD was dissolved directly in the running buffer, concentration range 0−10 mM. The corresponding sets of ACE measurements were performed also for CHES and Tricine compounds complexing with β-CD. The complexation constants of the charged form of CHES and Tricine were determined at pH where these compounds have deprotonized their amino groups and fully dissociated acidic groups, in Tricine/LiOH buffer (4.0 mM/8.0 mM), pH = 11.57, IS = 7.96 mM, and acetic/LiOH buffer (4.0 mM/8.0 mM), pH = 11.42, IS = 7.96 mM, respectively. The complexation constant of the

dx.doi.org/10.1021/ac4013804 | Anal. Chem. 2013, 85, 8518−8525

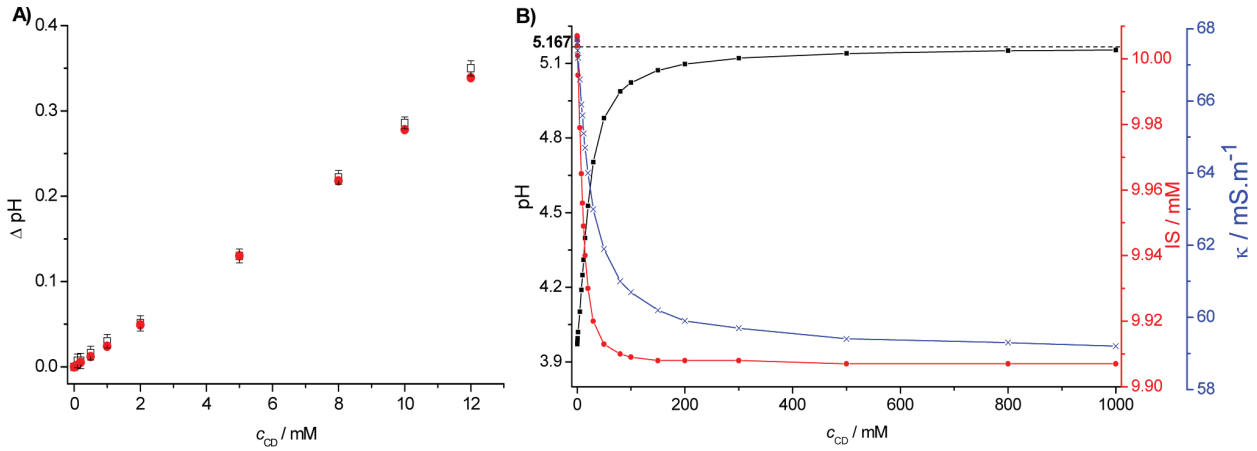

Figure 1. (A) Comparison of dependences of Δ pH of 24 mM benzoic acid/9.9 mM LiOH buffer on β-CD concentration (C_{CD}) obtained from experiments (□) and calculated by Simul 5 Complex (red ●). (B) Dependence of pH (left axis, ■), ionic strength (right axis, red ●) and conductivity (second right axis, blue ×) of 24 mM benzoic acid/9.9 mM LiOH buffer on β-CD concentration calculated by Simul 5 Complex. The dashed line and highlighted value represent the limiting values of pH calculated by eq 7.

neutral (zwitterionic) forms, K_{XAn}, were obtained in ethanolamine/Tricine buffer (22 mM/8.1 mM), pH = 9.86, IS = 7.99 mM and phosphate/LiOH buffer (8 mM/14.5 mM), pH = 7.68, IS = 7.67 mM for CHES and Tricine, respectively. An additional set of measurements for the determination of the complexation constant of the fully charged form of CHES was performed in Tricine/LiOH buffer (35 mM/11 mM) pH = 12.17, IS = 34.0 mM. β-CD was dissolved directly in the running buffer, its concentration varied in the range of 0−10 mM.

NMR Measurements. For NMR measurements, the studied compounds (CHES, Tricine, MES, MOPS) were dissolved in deuterated water (99.8% D, Chemotrade, Leipzig) at the concentration of 2 mM. At these conditions, these compounds are neutral. To achieve a neutral form of benzoic acid, 8 mM HCl was added to its 2 mM solution. The samples of the charged forms were prepared by addition of NaOH. The pH was selected by means of PeakMaster 5.3 to achieve fully charged forms of all compounds. pH* measured by a classical glass pH electrode was 12.06. The host β-CD molecule was dissolved at various concentrations ranging from 0 to 10 mM in the final solutions of CHES and Tricine. The complexation constants were calculated from the dependence of the analyte diffusion coefficient on β-CD concentration. In the case of benzoic acid, MES, and MOPS, the diffusion coefficients were measured in cyclodextrin free solution and at 10 mM concentration of the host β-CD molecule.

Measurements of pH. All pH measurements were carried out using a combined pH electrode at ambient temperature (24−25 °C). The pH measurements of buffers with and without complexation agents were conducted in short time intervals to eliminate changes of temperature or other external effects. CDs were always dissolved directly in the measured buffer and, if necessary, further diluted with the same buffer solution. The concentrations of β-CD in the model system (24 mM benzoic acid/9.9 mM LiOH buffer) were 0, 0.1, 0.2, 0.5, 1, 2, 5, 8, 10, and 12 mM. All tested buffers were composed of 10.0 mM weak acid (acetic acid, formic acid, Tricine, TAPS, MOPS, MES, or CHES), 5.0 mM LiOH, and 10.0 ± 0.5 mM neutral CDs (α-CD, β-CD, DM-β-CD, or HP-β-CD). The pH of the CHES buffer was measured in dependence on its concentration, concentration range 0.01 mM to 80 mM. β-CD was always dissolved directly in the buffer at concentration 10 mM. All measurements were performed in triplicates.

Software. Our simulation program Simul 5 Complex[22−24] with the implemented complete mathematical model of electromigration for separation systems with complexation agents was utilized to calculate buffer properties. The computer program PeakMaster 5.3[25,26] was used to optimize the composition of buffers for ACE and NMR measurements. The Simul 5 and PeakMaster software are available as freeware on our Web site.[36] The program Origin 8.1 (OriginLab Corporation, Northampton, MA) and Microsoft Office Excel 2010 were used for data evaluation.

RESULTS AND DISCUSSION

The theoretical predictions were demonstrated experimentally on the model system: benzoic acid/LiOH (24 mM/9.9 mM) buffer (pH = 4.01, IS = 10 mM) and a neutral β-CD. The pH of this buffer was measured at various concentrations of β-CD. The resulting dependence of the pH shift on the concentration of cyclodextrin (c_{CD}) is shown in Figure 1A. Clearly, pH increases significantly with the increasing concentration of the complexation agent. At 10 mM concentration of β-CD, the pH shift was about 0.3 pH units. The increase of pH in this separation system should result from the higher complexation constant of the neutral (nondissociated) form of benzoic acid in comparison to the charged (dissociated) form as discussed in the section Theory.

To confirm this assumption, the complexation constants of the charged (dissociated) and neutral (nondissociated) forms of benzoic acid were determined by ACE, where the dependence of the mobility of benzoic acid on the concentration of the complexation agent was measured at high pH (benzoic acid is fully charged) and low pH (where benzoic acid is only partially dissociated) regions. Obtained dependences were fitted by appropriate theoretical functions, see the Supporting Information S2, eqs S2-1 and S2-2, respectively. The dissociation constant of the resulting complex was calculated by eq 4. The determined complexation parameters of benzoic acid−β-CD complex for the actual ionic strength of 10 mM are K_{XAn} = 460 ± 20 M^{-1}, K_{XAc} = 29 ±

dx.doi.org/10.1021/ac4013804 | Anal. Chem. 2013, 85, 8518−8525

1 M^{-1} (the error is presented as standard error of nonlinear fitting), and K_{HAC} = 4.780 × 10^{-6} M. The value of the dissociation constant of benzoic acid at this ionic strength is K_{HA} = 7.638 × 10^{-5} M. Clearly, the complexation constant of the neutral (nondissociated) form is indeed more than 10 times higher than that of the charged (dissociated) one, which matches well with the significant positive pH shift.

Determined complexation parameters can be easily used as input data for simulations by Simul 5 Complex and calculations by means of eq 7 to propose the general behavior of this separation system even at those conditions, which are not obtainable experimentally due to the low solubility of β-CD. At first, the pH predicted by Simul 5 Complex was compared with the experimental data to confirm the correctness of the established model, see Figure 1A. Here a very good agreement of theoretical and experimental values was observed. Thus, the values of the pH, conductivity, and ionic strength were calculated by Simul 5 for theoretical cyclodextrin concentration range of 0−1000 mM, see Figure 1B. All the calculated properties change significantly with increasing concentration of β-CD, and pH clearly limits to the value of 5.17 as predicted by the theory (eq 7). This value corresponds to the pH of the buffer composed of the resulting benzoic acid−β-CD complex, with dissociation constant K_{HAC} = 4.780 × 10^{-6} M, calculated by eq 4.

Next, the pH shifts when adding the complexation agent were observed in commonly used buffers composed of weak acids (10 mM Tricine (pK_A = 8.15); 10 mM MES (pK_A = 6.09); 10 mM MOPS (pK_A = 7.20); 10 mM TAPS (pK_A = 8.30), 10 mM CHES (pK_A = 9.55); 10 mM acetic acid (pK_A = 4.76); 10 mM formic acid (pK_A = 3.75)) and a strong base 5 mM LiOH. pH was measured in the pure buffer and at a 10 mM concentration of several neutral CDs. The resulting pH shifts are shown in Figure 2. Clearly, the biggest pH changes among common buffers tested were observed in the case of the CHES buffer for all cyclodextrins studied. Significant shifts were also found out for MOPS, for MES buffers, and for the acetic buffer after the addition of α-CD. The pH shifts in the other buffers were less pronounced.

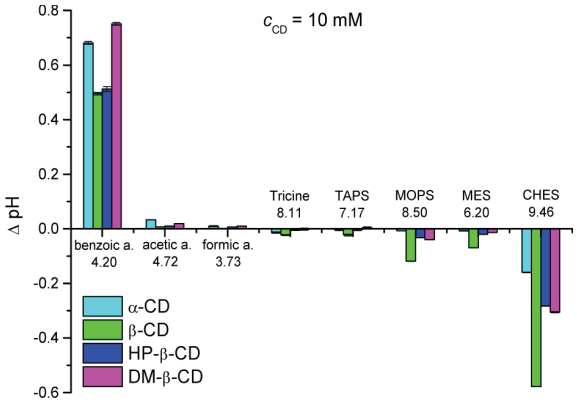

Figure 2. Shifts in pH (ΔpH) after addition of 10 ± 0.5 mM α-CD (cyan), β-CD (green), HP-β-CD (blue), or DM-β-CD (magenta) in seven commonly used buffers and the model system (benzoate buffer). Groups of columns are marked by the name of the buffering compound and pH value of the original buffer (without addition of CD). Error bars represent standard deviation of the measured value.

The pH shifts, shown in Figure 2, point to an interesting consequence. While in the model system consisting of benzoic acid and LiOH, pH significantly increased with the concentration of β-CD, in the case of common buffer constituents CHES, MES, MOPS, TAPS, and Tricine, pH decreased when adding CDs. The increase of the pH of the benzoic acid buffer stems from the higher complexation constant of the neutral (nondissociated) form than the charged (dissociated) one, as discussed above. To the contrary, the decrease of the pH of common buffers in Figure 2 has to result from a higher value of the complexation constant of the charged form of the buffering constituent in comparison to the neutral one. This is the direct consequence of the zwitterionic character of these buffering compounds. CHES, MES, MOPS, and TAPS are amino alkanesulfonic acids, and Tricine is an amino alkanecarboxylic acid, so their buffering properties are based on the amonnium/amine dissociation equilibrium. It means that the molecule behaves as "neutral" at a low pH, where amino groups are protonated and sulfo (carboxyl) groups are dissociated. Consequently, protonation of the amino group hinders the inclusion of the molecule into the cavity and results in weaker complexation. In the "charged" state of these compounds, only the sulfo (carboxyl) group is dissociated, which enables deeper inclusion and stronger complexation of the compound.

To confirm these findings we employed NMR measurements of translational diffusion coefficients of the buffer constituents. In the first run we compared those properties for the free analytes and in solutions with excess of β-CD, both in conditions with different pH: (i) in the alkaline solution of 8 mM NaOH where the buffering compounds are charged and (ii) in water where the electrolytes were virtually in the neutral form, in the case of benzoic acid in 8 mM HCl solution. The buffering compounds benzoic acid, CHES, MES, MOPS, and Tricine were always in 2 mM concentration and the complexation agent was at 10 mM concentration. The resulting NMR derived absolute values of translational diffusion coefficients, as summarized in Table 1, fully confirmed our hypothesis. The observed diffusion characteristics of the β-CD remained constant in all samples (D = 2.4 ± 0.1 × 10^{-10} m^2 s^{-1}, which compares well with 2.9 × 10^{-10} m^2 s^{-1} determined in H_2O[37]), and it seems quite safe to assume that the complex behaves in the same way. It then becomes possible to estimate a fraction of the analyte bound in the complex, as the apparent diffusion constant is a weighted average of the free and the bound form. The charged forms of (CHES, MOPS, MES, and Tricine) always showed a higher degree of complexation after adding the β-CD compared to the neutral ones in contrast to benzoic acid, where the results were exactly opposite. The most profound effects of the cyclodextrin complexation of buffer constituents in common buffers were observed for CHES and benzoic acid, where also the pH shifts were the most significant, as the phenyl and cyclohexyl moieties include in the cyclodextrin cavity. The translational diffusion coefficient of the charged CHES molecule was very close to the value of β-CD, suggesting a tight complex. The same holds for the neutral form of benzoic acid. That is why we studied also the spatial proximity of the hydrogens of the two analytes to β-CD by means of the nuclear Overhauser effect in rotating frame (ROE) combined with selective excitation (excitation sculpting experiment[38]). Clear contacts were observed between the cyclohexyl and phenyl moieties and the 3 and 5 hydrogens from

dx.doi.org/10.1021/ac4013804 | Anal. Chem. 2013, 85, 8518−8525

Table 1. Diffusion Coefficients of Charged (C^-) and Neutral (N) Forms of Buffer Constituents in Cyclodextrin Free Solution (D_A) and at a 10 mM Concentration of β-CD (D_C)[a]

	benzoic acid		CHES		MOPS		MES		Tricine	
	N	C^-	N	C^-	N	C^-	N	C^-	N	C^-
$D_A/10^{-10}$ m^2 s^{-1}	7.20	6.57	5.21	4.83	5.42	5.17	6.13	5.45	5.26	5.14
$D_C/10^{-10}$ m^2 s^{-1}	3.23	5.77	4.74	2.76	5.42	4.48	6.08	4.67	5.09	4.81
$((D_A - D_C)/(D_A - D_{ACD})) \times 100$	83%	19%	17%	85%	0%	25%	1%	26%	6%	12%

[a]Ratio $((D_A - D_C)/(D_A - D_{ACD})) \times 100$ corresponds to the fraction of the complexed analyte, where D_{ACD} is the diffusion coefficient of the complex, which was approximated by the diffusion coefficient of free CD $D_{ACD} = 2.4 \times 10^{-10}$ m^2 s^{-1}.

the inside of the β-CD cavity confirming their deep inclusion (for further details see the Supporting Information S3).

The complexation is much weaker in the case of the MES and MOPS compounds. This is in agreement with the worse inclusion of the morpholine moiety into the cyclodextrin cavity due to the presence of the oxygen atom, which makes the morholine moiety less hydrophobic in comparison with cyclohexyl or phenyl groups.[39] Very weak complexation was observed also for Tricine whose polar character does not allow deep inclusion into the cavity.

Determination of the Complexation Constants of CHES with β-CD Both by NMR and ACE Techniques. For a mutual comparison with benzoic acid we observed the complexation constants of CHES and Tricine, the most and least complexing buffer constituents, respectively, with β-CD both by NMR and ACE techniques. Both the diffusion coefficients derived from the NMR measurements and the effective mobilities of CHES resulting from ACE were measured as a function of cyclodextrin concentration.

The ACE measurements were performed at pH 11.57 and 9.86 in order to determine the complexation constant of the charged and neutral form of CHES, respectively. Unfortunately the dissociation of β-CD at a high pH (the pK_A of cyclodextrin is about 12.20) brings additional complexity to the system. At the high pH, a part of cyclodextrin becomes negatively charged. Complexation of the charged form of cyclodextrin with CHES is assumed to be negligible due to electrostatic repulsion; therefore, the concentration of β-CD must be corrected to obtain the concentration of the neutral form of β-CD in the buffer. This correction was done by PeakMaster 5.3 software, which allows the calculation of the concentrations of the individual dissociation forms of each buffer constituent. Such corrected concentrations of the nondissociated (neutral) form of cyclodextrin were used for data evaluation in the ACE measurements. The plausibility of corrections was proved by ACE measurements at a higher pH of 12.17, where β-CD is dissociated to a different extent. The appropriate fitting functions for data evaluation are described in the Supporting Information S2. The measurements at different pH values provided the same values of the complexation constant in the range of experimental error.

In the NMR study, the diffusion coefficients of CHES were measured for dependence on the concentration of cyclodextrin. The complexation constant of the charged form of CHES was measured in the 2 mM solution of CHES with 8 mM NaOH added and that of the neutral form was measured in a 2 mM deutered water solution of CHES. Analogous corrections due to the dissociation of β-CD were performed as in the ACE measurements. However, pK_A of β-CD in D_2O is much higher, 13.66, so this correction was much smaller.[40]

Both NMR and ACE techniques provided similar values of complexation constants. The complexation constant of the charged form of CHES with β-CD determined by ACE and NMR were 440 ± 30 M^{-1} and 360 ± 30 M^{-1} (the error is presented as the standard error of nonlinear fitting), respectively. Unfortunately, the complexation constant of the neutral form of CHES could not be determined with a sufficient precision by any method, as its value is certainly very small. For the purpose of simulations, the complexation constant of the neutral form was estimated as 30 M^{-1}. For more details regarding the determination of the complexation constants by ACE and NMR see the Supporting Information S2. Clearly, the complexation constants are in the same range as those of benzoic acid but opposite in regards to the complexation of the charged and neutral form. This fully agrees with the similar value of the pH shift of these two compounds only in the opposite direction (ΔpH (CHES) = −0.58, ΔpH (benzoic acid) = 0.50), see Figure 2.

The same sets of NMR and ACE measurements were performed for the Tricine compound. However, both techniques showed that the complexation of Tricine and β-CD is negligible, and the values of complexation constants cannot be evaluated. This result is in agreement with the very small pH deviations observed for the Tricine buffer (ΔpH (Tricine) = −0.02).

Impact of Buffer Concentration on pH Shifts. Determined values of complexation constants can be again used as input parameters for calculations in the Simul 5 Complex to predict the general properties of the buffer systems. This was already shown for the dependence of pH, IS, and conductivity on the concentration of the complexation agent in the model benzoic acid buffer, see Figure 1B. The complexation constants determined for interaction of CHES with β-CD were used to calculate how the pH is influenced when the 10 mM solution of β-CD is added to the CHES/LiOH buffer (ratio of CHES and LiOH concentration was kept constant 2:1) of different concentrations. For comparison, we also calculated the pH of the cyclodextrin free CHES/LiOH buffer at gradually increasing concentration. Both dependences are shown in Figure 3. In the same figure we also show experimentally measured values of pH. A very good agreement of the experimental and calculated values is clear. (Such measurements are not obtainable in a benzoic acid buffer due to its low solubility, for this reason a CHES buffer was used for this demonstration.)

It is worth noting that at a high concentration of the buffer, the pH difference between the pure buffer and the buffer containing 10 mM β-CD diminishes and limits to zero, while at a low concentration the pH difference was almost 1 pH unit. This is expected because at a high concentration of the buffer the concentration of CD is insufficient to complex a significant part of CHES and pH cannot be significantly influenced.

In summary, the complexation of buffer constituents with the complexation agent added to the buffer can significantly

dx.doi.org/10.1021/ac4013804 | Anal. Chem. 2013, 85, 8518−8525

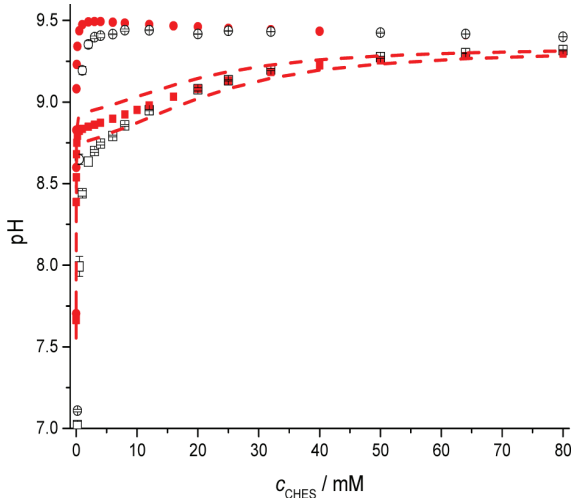

Figure 3. Dependence of pH on concentration of CHES buffer, the ratio of CHES and LiOH was kept at 2:1. Circle and square symbols represent data for the cyclodextrin free solution and at a 10 mM concentration of β-CD, respectively. Solid red symbols are simulated data (K_{XAc} = 440 M^{-1}, K_{XAn} = 30 M^{-1}), and transparent black symbols are experimental data. Red dashed lines represent the confidence interval taking into account the error of estimate of the determination of complexation constants: the upper curve (K_{XAc} = 410 M^{-1}, K_{XAn} = 70 M^{-1}) and the lower curve (K_{XAc} = 470 M^{-1}, K_{XAn} = 1 × 10^{-3} M^{-1}).

influence its pH and other important properties such as IS or conductivity. The pH of the complexing buffer depends not only on the concentration of complexation agent but also on the type of buffer and concentration of buffer constituents.

CONCLUDING REMARKS

Complexation of buffer constituents with a complexation agent present in the buffer, even if the complexation agent is neutral, can severely influence the buffer properties. This results to a shift in pH, ionic strength, and conductivity, which can significantly affect the CE or HPLC separations when such buffers are used as background electrolytes or present in mobile phases. This is demonstrated for CE in Part II of this series of papers.[30] Herein, we propose a theory of this phenomenon and show that is in good agreement with experimental results.

We revealed that some common chemicals used for preparation of buffers, such as CHES, MES, and MOPS form complexes with β-cyclodextrin. The complexation is much stronger with the charged forms of the buffer constituents when compared to their neutral forms due to their characteristic zwitterion behavior. This fact was further proved by NMR measurements. We determined the complexation constants of β-cyclodextrin with both the charged and neutral form of benzoic acid and CHES, which were consequently used as input data for simulations. Simulation program Simul 5 Complex was shown to be a precise tool for the prediction of behavior of complexing buffer systems. Clearly, but against the contemporary usual practice, the pH of the buffer should always be controlled after the addition of the complexation agent (even a neutral chiral selector) to reveal a possible complexation with the constituents of the buffer.

ASSOCIATED CONTENT

Supporting Information

Additional information as noted in text. This material is available free of charge via the Internet at http://pubs.acs.org.

AUTHOR INFORMATION

Corresponding Author

*E-mail: svobod.j@natur.cuni.cz. Phone: +420-2-2195-1399. Fax: +420-2-2491-9752.

Notes

The authors declare no competing financial interest.

ACKNOWLEDGMENTS

The support of the Grant Agency of the Czech Republic, Grant No.13-01440S, Grant Agency of Charles University, Grant No. 323611 and Grant No. 570213, and the long-term research plan of the Ministry of Education of the Czech Republic, Grant MSM0021620857, is gratefully acknowledged.

REFERENCES

(1) Singh, M. K.; Pal, H.; Ainavarapu, R. K.; Sapre, A. V. *J. Phys. Chem. A* **2004**, *108*, 1465−1474.
(2) Lelievre, F.; Gareil, P.; Jardy, A. *Anal. Chem.* **1997**, *69*, 385−392.
(3) Yoshida, N.; Seiyama, A.; Fujimoto, M. *J. Phys. Chem.* **1990**, *94*, 4254−4259.
(4) Marquez, C.; Nau, W. M. *Angew. Chem., Int. Ed.* **2001**, *40*, 3155−3160.
(5) Mohanty, J.; Bhasikuttan, A. C.; Nau, W. M.; Pal, H. *J. Phys. Chem. B* **2006**, *110*, 5132−5138.
(6) Eftink, M. R.; Andy, M. L.; Bystrom, K.; Perlmutter, H. D.; Kristol, D. S. *J. Am. Chem. Soc.* **1989**, *111*, 6765−6772.
(7) Gelb, R. I.; Schwartz, L. M.; Cardelino, B.; Fuhrman, H. S.; Johnson, R. F.; Laufer, D. A. *J. Am. Chem. Soc.* **1981**, *103*, 1750−1757.
(8) Gelb, R. I.; Schwartz, L. M.; Johnson, R. F.; Laufer, D. A. *J. Am. Chem. Soc.* **1979**, *101*, 1869−1874.
(9) Zhang, X. Y.; Gramlich, G.; Wang, X. J.; Nau, W. M. *J. Am. Chem. Soc.* **2002**, *124*, 254−263.
(10) Righetti, P. G.; Ettori, C.; Chafey, P.; Wahrmann, J. P. *Electrophoresis* **1990**, *11*, 1−4.
(11) Hammitzsch-Wiedemann, M.; Scriba, G. K. E. *Electrophoresis* **2007**, *28*, 2619−2628.
(12) Rizzi, A. M.; Kremser, L. *Electrophoresis* **1999**, *20*, 2715−2722.
(13) Schwartz, L. M.; Gelb, R. I. *Anal. Chem.* **1978**, *50*, 1571−1576.
(14) Fielding, L. *Prog. Nucl. Magn. Reson. Spectrosc.* **2007**, *51*, 219−242.
(15) Fielding, L. *Tetrahedron* **2000**, *56*, 6151−6170.
(16) Dvorak, M.; Svobodova, J.; Benes, M.; Gas, B. *Electrophoresis* **2013**, *34*, 761−767.
(17) Uselova-Vcelakova, K.; Zuskova, I.; Gas, B. *Electrophoresis* **2007**, *28*, 2145−2152.
(18) Rundlett, K. L.; Armstrong, D. W. *Electrophoresis* **2001**, *22*, 1419−1427.
(19) Jiang, C. X.; Armstrong, D. W. *Electrophoresis* **2010**, *31*, 17−27.
(20) Busch, M. H. A.; Carels, L. B.; Boelens, H.F. M.; Kraak, J. C.; Poppe, H. *J. Chromatogr., A* **1997**, *777*, 311−328.
(21) Hruska, V.; Jaros, M.; Gas, B. *Electrophoresis* **2006**, *27*, 984−991.
(22) Svobodova, J.; Benes, M.; Dubsky, P.; Vigh, G.; Gas, B. *Electrophoresis* **2012**, *33*, 3012−3020.
(23) Svobodova, J.; Benes, M.; Hruska, V.; Uselova, K.; Gas, B. *Electrophoresis* **2012**, *33*, 948−957.
(24) Hruska, V.; Benes, M.; Svobodova, J.; Zuskova, I.; Gas, B. *Electrophoresis* **2012**, *33*, 938−947.
(25) Hruska, V.; Svobodova, J.; Benes, M.; Gas, B. *J. Chromatogr., A* **2012**, *1267*, 102−108.
(26) Benes, M.; Svobodova, J.; Hruska, V.; Dvorak, M.; Zuskova, I.; Gas, B. *J. Chromatogr., A* **2012**, *1267*, 109−115.

(27) Gas, B.; Jaros, M.; Hruska, V.; Zuskova, I.; Stedry, M. *LC−GC Eur.* **2005**, *18*, 282.
(28) Fang, L.; Yin, X. B.; Wang, E. *Anal. Lett.* **2007**, *40*, 3457−3471.
(29) Chen, Y. R.; Ju, D. D.; Her, G. R. *J. High Resolut. Chromatogr.* **2000**, *23*, 409−412.
(30) Benes, M.; Riesova, M.; Svobodova, J.; Tesarova, E.; Dubsky, P.; Gas, B. *Anal. Chem.* **2013**, DOI: 10.1021/ac401381d.
(31) Benes, M.; Zuskova, I.; Svobodova, J.; Gas, B. *Electrophoresis* **2012**, *33*, 1032−1039.
(32) Gas, B.; Zuska, J.; Coufal, P.; van de Goor, T. *Electrophoresis* **2002**, *23*, 3520−3527.
(33) Jerschow, A.; Muller, N. *J. Magn. Reson.* **1997**, *125*, 372−375.
(34) Johnson, C. S. *Prog. Nucl. Magn. Reson. Spectrosc.* **1999**, *34*, 203−256.
(35) Longsworth, L. G. *J. Phys. Chem.* **1960**, *64*, 1914−1917.
(36) The group of Electrophoretic and Chromatographic Separation Methods, echmet.natur.cuni.cz.
(37) Pavlov, G. M.; Korneeva, E. V.; Smolina, N. A.; Schubert, U. S. *Eur. Biophys. J.* **2010**, *39*, 371−379.
(38) Stonehouse, J.; Adell, P.; Keeler, J.; Shaka, A. J. *J. Am. Chem. Soc.* **1994**, *116*, 6037.
(39) Meo, P. I.; ĎAnna, F.; Riela, S.; Gryttaduria, M.; Noto, M. *Org. Biomol. Chem.* **2003**, *1*, 1584−1590.
(40) Maeztu, R.; Tardajos, G.; Gonzalez-Gaitano, G. *J. Inclusion Phenom. Macrocyclic Chem.* **2011**, *69*, 361−367.

VI.

Complexation of Buffer Constituents with Neutral Complexation Agents: Part II. Practical Impact in Capillary Zone Electrophoresis

M. Beneš, M. Riesová, J. Svobodová, E. Tesařová, P. Dubský, B Gaš
Analytical Chemistry, 2013, 85, 8526-8534

analytical chemistry

Article

pubs.acs.org/ac

Complexation of Buffer Constituents with Neutral Complexation Agents: Part II. Practical Impact in Capillary Zone Electrophoresis

Martin Beneš, Martina Riesová, Jana Svobodová,* Eva Tesařová, Pavel Dubský, and Bohuslav Gaš

Charles University in Prague, Faculty of Science, Department of Physical and Macromolecular Chemistry, Prague, Czech Republic

Supporting Information

ABSTRACT: This article elucidates the practical impact of the complexation of buffer constituents with complexation agents on electrophoretic results, namely, complexation constant determination, system peak development, and proper separation of analytes. Several common buffers, which were selected based on the pH study in Part I of this paper series (Riesová, M.; Svobodová, J.; Tošner, Z.; Beneš, M.; Tesařová, E.; Gaš, B. *Anal. Chem.*, **2013**, DOI: 10.1021/ac4013804); e.g., CHES, MES, MOPS, Tricine were used to demonstrate behavior of such complex separation systems. We show that the value of a complexation constant determined in the interacting buffers environment depends not only on the analyte and complexation agent but it is also substantially affected by the type and concentration of buffer constituents. As a result, the complexation parameters determined in the interacting buffers cannot be regarded as thermodynamic ones and may provide misleading information about the strength of complexation of the compound of interest. We also demonstrate that the development of system peaks in interacting buffer systems significantly differs from the behavior known for noncomplexing systems, as the mobility of system peaks depends on the concentration and type of neutral complexation agent. Finally, we show that the use of interacting buffers can totally ruin the results of electrophoretic separation because the buffer properties change as the consequence of the buffer constituents' complexation. As a general conclusion, the interaction of buffer constituents with the complexation agent should always be considered in any method development procedures.

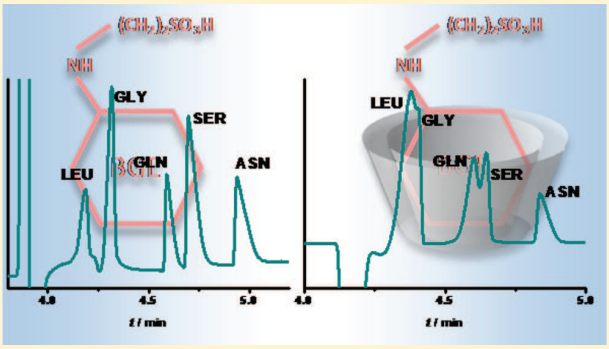

Capillary electrophoresis (CE) is a widely employed separation technique. It offers many useful modifications that make use of the presence of complexation agents in background electrolyte (BGE). This so-called pseudostationary phase brings beneficial interaction possibilities, which are traditionally utilized to increase separation efficiency, to achieve enantioseparation, or to change the migration order of analytes. Additionally, the fact that interactions between analytes and complexation agents are reflected in changes of electrophoretic behavior of the respective compounds can be advantageously used to determine complexation constants or for other studies of noncovalent binding in chemistry or biology.

Utilization of complexation agents, most frequently chiral selectors, has widely expanded within the last 2 decades.[1] For this reason, several attempts were made to describe electrophoretic separation with complexation agents theoretically, and based on the theory, propose optimization approaches, which would help to save separation time and costs. In 1992 Wren and Rowe[2] presented a theoretical model of the separation of fully charged analytes with neutral chiral selectors. This model was later extended by Rawjee and Vigh[3,4] for weak electrolyte analytes. On the basis of these theoretical models, several objective functions (e.g., selectivity, difference in mobilities or resolution) were used for optimizing the separation conditions. However, the authors admitted that for a correct and complete description of such complex separation systems a numerical simulation would be necessary.[5−11] In 2012, Hruska et al.[12] and Breadmore et al.[13] presented a complete theoretical model of electromigration for separation systems with complexation agents. These models were successfully implemented into new versions of simulation programs Simul 5 Complex[14] and GENTRANS, respectively. Simul 5 Complex was shown to provide deep insight into electrophoretic separation in systems with complexation agents and can be used to explain different unexpected phenomena. We used Simul 5 Complex to explain the development of electromigration dispersion (EMD),[15,16] which is responsible for the deterioration of the analyte peaks' shape. The results showed that EMD can be directly related to complexation. An alternative to numerical simulation is the linearized theory of electromigration, which was introduced by Poppe[17] and was extensively developed in our group[18] and implemented in the PeakMaster software.[19] The most important outcome of this theory is the fundamental understanding of the development of so-called system peaks. The system peaks appear as perturbations in the BGE

Received: May 7, 2013
Accepted: July 27, 2013
Published: July 27, 2013

Table 1. Composition, Concentrations of the Constituents (c), pH, and Ionic Strength (IS) of the Running Buffers for Determining the Complexation Constants of *R*-FLU[a]

buffer constituents	CHES/LiOH	D: CHES/LiOH	MOPS/LiOH	D: MOPS/LiOH	MES/LiOH	D: MES/LiOH
c/mM	50/25.76	10/5.15	50/25.76	10/5.15	50/25.76	10/5.15
IS/mM	25.76	5.15	25.76	5.15	25.76	5.15
pH	9.51	9.54	7.16	7.19	6.06	6.09
buffer constituents	Tricine/LiOH	D: Tricine/LiOH	phosphoric acid/NaOH	maleic acid/LiOH	NH_3/HCl	ethanolamine/HCl
c/mM	50/25.76	10/5.15	11/18	12/19	36/25.76	50/25.76
IS/mM	25.76	5.15	25.0	26.0	25.76	25.76
pH	8.11	8.14	7.27	6.18	8.91	9.53

[a]D: diluted buffer.

concentration profile traveling through the system independently of the very presence of any analyte. Currently the PeakMaster software was extended for complexing systems with neutral complexation agents complexing with one fully charged analyte.[20] Both software programs are freeware and can be downloaded from our Webpage.[14]

The complexation of analyte(s) with complexation agent(s) is described in detail in the literature nowadays. However, possible changes of the BGE properties due to the complexation of buffer constituents with the complexation agent are mentioned rarely. Rawjee et al.[21] utilized the complexation of buffer constituent with complexation agents to affect the electrophoretic mobility of the co-ion in order to minimize electromigration dispersion of the analyte. Chen et al.[22] observed system peaks originating from the interaction of neutral α-, β-, and γ-cyclodextrins with *N*-cyclohexyl-2-aminoethanesulfonic acid (CHES) buffer during the cyclodextrin (CD) assisted separation of underivatized gangliosides. Fang et al.[23] noticed the induction of an additional peak registered by electrochemiluminescence detection when sulfated β-cyclodextrin and acetonitrile were simultaneously present in BGE. They attributed the presence of the induced peak to the physical interaction between CD and acetonitrile. Potential changes of the basic buffer properties, such as pH or ionic strength that can appear after the addition of a neutral complexation agent are considered rarely. Just a few authors proposed to control the pH of the buffer after the addition of a ligand.[24] The theoretical description of the interaction of buffer constituents with a complexation agent as regards to the fundamental properties of the buffer was proposed in Part I[25] of this series of papers.

Complexation constants and the mobilities of complexes of various compounds as determined by CE can be further used as input data for prediction models or simulation programs. The overview of existing methods and their limitations can be found in several review papers.[26−28] The most commonly used technique is affinity capillary electrophoresis (ACE), where the effective mobility of the injected analyte is determined depending on the concentration of the complexation agent dissolved directly in the running buffer. Complexation parameters are evaluated by the fitting of the obtained dependence with an appropriate fitting function. This method relies on constant and precise experimental conditions, and suitable corrections for ionic strength (IS), viscosity, or temperature have to be applied to obtain thermodynamic complexation constants as shown in our previous paper.[29]

The aim of this work is to demonstrate, by means of simulations and experiments, the practical impact of the interaction of buffer constituents with the complexation agent on the electrophoretic separation and determination of complexation constants by CE. Several interacting buffers were selected based on the results shown in Part I[25] of this series of papers. The influence of the interaction is demonstrated to determine the complexation constants of fully charged as well as neutral analytes by ACE. The dependence of the resulting value of the complexation constant on the type and concentration of the running buffer is revealed. We also demonstrate the effect of the interaction of BGE constituents on the development of system peaks, which clearly differs from their behavior as explained by the linearized theory of electromigration[18] for noncomplexing systems. Finally, the influence of the complexation on the results of electrophoretic separation is discussed.

MATERIALS AND METHODS

Chemicals. All chemicals were of analytical grade purity. Lithium hydroxide monohydrate, benzoic acid, [Tris(hydroxymethyl)methyl]glycine (Tricine), and acetic acid were purchased from Fluka (Steinheim, Germany). Hydrochloric acid and maleic acid were products of Lachema (Brno, Czech Republic). 2-(*N*-morpholino)ethanesulfonic acid (MES), 3-morpholinopropane-1-sulfonic acid (MOPS), *N*-cyclohexyl-2-aminoethanesulfonic acid (CHES), 3-[[1,3-dihydroxy-2-(hydroxymethyl)propan-2-yl]amino]propane-1-sulfonic acid (TAPS), Tri(hydroxymethyl)aminomethane (Tris), ethanolamine, sodium hydrogenphosphate, sodium dihydrogenphosphate, ammonium hydroxide solution, (*R*)-(−)-2-fluoro-α-methyl-4-biphenylacetic acid (*R*-flurbiprofen, *R*-FLU), dimethylsulfoxide (DMSO), glycine, L-leucine, L-glutamine, L-serin, and L-asparagine were obtained from Sigma Aldrich (Steinheim, Germany). Neutral cyclodextrins (2-hydroxypropyl)-β-cyclodextrin (HP-β-CD) of 0.8 M substitution and average M_r = 1460, heptakis(2,6-di-*O*-methyl)-β-cyclodextrin (DM-β-CD), β-cyclodextrin (β-CD), and native α-cyclodextrin all from Sigma Aldrich (Steinheim, Germany) were used as complexation agents. Water for solution preparation was deionized by the WatrexUltrapur system (Prague, Czech Republic).

Instrumentation. All experiments were performed using Agilent 3D^{CE} capillary electrophoresis equipment operated under ChemStation software (Agilent Technologies, Waldbronn, Germany) control. Fused silica capillaries (50 μm i.d., 375 μm o.d.) were provided by Polymicro Technologies (Phoenix, AZ). The experiments were performed in a bare fused silica capillary with a total length and effective length to the detector (diode array detector (DAD)/contactless conductivity detector (CCD)) of approximately 50.0 cm and 41.5/34.5 cm, respectively. The PHM 220 instrument (Radiometer, Copenhagen, Denmark) calibrated with standard IUPAC

dx.doi.org/10.1021/ac401381d | Anal. Chem. 2013, 85, 8526−8534

buffers, pH 1.679, pH 7.000, pH 10.012, and pH 12.450 (Lyon, France) was used for pH measurements.

Experimental Conditions. Running voltage and parameters of the capillaries were chosen to keep the electric current low (the current was always lower than 33 μA) and thus to avoid the effects of excessive Joule heating. New capillaries were flushed with deionized water for 20 min and 3 min with actual BGE before each experiment. The operating temperature was always 25 °C. All running buffers were filtrated with Minisart syringe filters (Sartorius Stedim Biotech, Goettingen, Germany), pore size 0.45 μm. Every measurement was repeated four times. All analyte or system peaks were fitted by the Haarhoff-van der Linde (HVL) function[30,31] to eliminate the effect of electromigration dispersion on migration time.

Determining Complexation Constants in Interacting Buffers by ACE. The composition and parameters of the running BGE used for ACE measurements of the fully charged form of *R*-FLU are summarized in Table 1. The complexation constant of the neutral form of *R*-FLU was determined in 61.0 mM acetic acid/9.9 mM LiOH and 24.9 mM benzoic acid/9.9 mM LiOH buffer, both pH 3.98 and IS = 10 mM. The chiral selector β-CD, concentration range 0−10 mM, was dissolved directly in the running buffers. The injected sample was 0.3 mM *R*-FLU and 0.15% DMSO, which served as the electroosmotic flow (EOF) marker, and both were dissolved directly in the running buffer. For determination of the mobility of β-CD interacting with buffer constituents, β-CD was injected as the sample at concentration 0.3 mM, 0.15% DMSO again as an EOF marker. Detection was performed with the DAD at the wavelength of 214 nm. The samples were injected hydrodynamically for 100 mbar s. The total capillary length (L_{tot}) and the length to DAD (L_{DAD}) were 49.75 and 41.25 cm, respectively. The applied voltage was 20 kV (cathode at the detector side).

Impact of Buffer Complexation on Development of System Peaks. The BGE of the model system contained 5.0 mM benzoic acid, 2.5 mM LiOH, IS 2.57 mM; pH 4.20. HP-β-CD was dissolved directly in the running buffer in a concentration range of 0−40 mM. Samples contained neither analyte nor an EOF marker; only disturbed BGE was injected to generate system peaks. Compositions of the disturbances at the particular HP-β-CD concentration are summarized in Table 2. Composition of the sample injected into the buffer without HP-β-CD was designed by PeakMaster 5.3 in order to obtain convenient shapes, polarities, and amplitudes of system peaks. As the complexation model is not included in PeakMaster 5.3, disturbances of BGEs containing HP-β-CD were optimized experimentally to keep similar shapes and polarity of system peaks. The driving voltage was 20 kV (cathode at the detector site). The L_{tot} and the L_{DAD} were 48.7 and 40.2 cm, respectively. Indirect UV detection of system zones was performed by DAD at the wavelength 200 nm. System peak investigation was performed in the same common buffers (10 mM weak acid, MES, MOPS, CHES, Tricine, acetate, and 5 mM LiOH) as in the pH measurements in Part I[25] of this series of papers. The concentration of various neutral cyclodextrins in BGEs used for electrophoretic measurements was approximately 5 mM. All samples were composed of 11.0 mM weak acid (i.e., + 10% of buffering compound against the BGE composition) and 5.0 mM LiOH. This sample composition was designed by PeakMaster 5.3 software to induce system zones with suitable shapes and amplitudes. The samples were injected hydrodynamically for 90 mbar s. Conductivity detection was performed because of the absence of UV absorbing chromophore in the majority of the tested buffers. The L_{tot} of the capillaries and the length to CCD (L_{CCD}) were always 49.8 and 35.0 cm, respectively. Driving voltages were 25 kV for the acetate buffer, 20 kV for the Tricine buffer, and 10 kV for the MOPS, MES, and CHES buffers, always with the cathode at the detector side.

Influence of Interaction of Buffer Constituents on Result of Electrophoretic Separation. A set of amino acids was separated in 10 mM ethanolamine/5 mM HCl and 10 mM CHES/5 mM LiOH buffers, both pH 9.41 and IS 5 mM. The experiments were performed either in a pure buffer or at a 10 mM concentration of β-CD, which was dissolved directly in the buffer. The sample was composed of a mixture of 5 amino acids (1 mM Leu, 1 mM Gly, 1 mM Gln, 1 mM Asn, 1 mM Ser). The samples were injected hydrodynamically for 90 mbar s. The L_{tot} of the capillary and L_{CCD} were always 49.3 and 34.5 cm, respectively. Applied voltage was 8 kV, with the cathode at the detector side.

Software. Our simulation program Simul 5 Complex[16] with an implemented complete mathematical model of electromigration for the separation systems with complexation agents was utilized for simulations of experimental electropherograms and for determining background electrolyte properties. The computer program PeakMaster[19] was used to optimize the composition of BGEs. The new version of this software, PeakMaster 5.3,[32,33] which is able to predict shapes and amplitudes of system peaks, was employed to design suitable disturbance in order to induce system peaks with convenient polarity and amplitude. The Simul 5 Complex and PeakMaster 5.3 software are available as freeware at our Web site.[14] The program Origin 8.1 (OriginLab Corporation, Northampton, MA) and Microsoft Office Excel 2003 were used for data evaluation.

Table 2. Composition of the Samples/Disturbances Used for Determination of System Peaks in Model System[a]

BGE	sample/disturbance composition		
$c_{HP\text{-}\beta\text{-}CD}$/mM	$c_{benzoic\ acid}$/mM	c_{LiOH}/mM	$c_{HP\text{-}\beta\text{-}CD}$/mM
0.0	4.0	0.0	0.0
5.0	2.5	0.0	6.0
10	0.0	0.0	11
20	0.0	0.0	21
30	0.0	0.0	31
40	0.0	0.0	41

[a]Model system composition: 5.0 mM benzoic acid, 2.5 mM LiOH, and 0−40 mM HP-β-CD.

RESULTS AND DISCUSSION

As shown in Part I[25] of this series of papers, an interaction of buffer constituents with the complexation agent seriously influences buffer properties. However, the complexation of buffer constituents might have other practical consequences, e.g., they might play a role in the determination of physical-chemical parameters of compounds, if incorrectly considered, or have a significant impact on electrophoretic separations in general. In this paper we will focus on three major points: (1) determination of complexation constants in interacting buffers by ACE, (2) impact of buffer complexation on the development of system peaks, and (3) influence of the interaction of buffer constituents on the results of electrophoretic separation.

dx.doi.org/10.1021/ac401381d | Anal. Chem. 2013, 85, 8526−8534

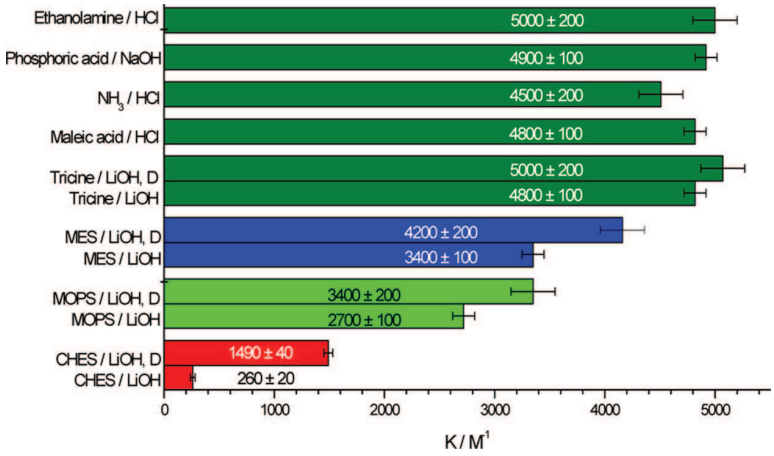

Figure 1. Complexation constants of *R*-FLU with β-CD determined in various buffers. Errors are expressed as standard deviations. Exact compositions and experimental conditions of used buffers are summarized in Table 1. D: diluted buffer.

Table 3. Effective Mobilities of Neutral β-CD Corrected for Ionic Strength and Determined in Various Buffers[a]

buffer	CHES	D: CHES	MOPS	D: MOPS	MES	D: MES
$u_{CD}^{eff}/10^{-9}$ m^2 V^{-1} s^{-1}	−13.4 ± 0.1	−10.4 ± 0.2	−9.1 ± 0.1	−4.1 ± 0.1	−7.5 ± 0.1	−1.8 ± 0.2

[a]Composition of buffers: 50 mM CHES, MOPS, MES, and 25.76 mM LiOH; ionic strength 25.76 mM. D: diluted buffers, 10 mM CHES, MOPS, MES and 5.15 mM LiOH; ionic strength 5.15 mM.

On the basis of the pH and NMR study presented in Part I[25] of this series, we selected suitable buffers to demonstrate the influence of the interaction of buffer constituents with the complexation agent. The MES/LiOH, MOPS/LiOH, and CHES/LiOH buffers were used as the interacting buffer systems, while Tricine/LiOH was suggested as a noninteracting one.

Determination of Complexation Constants in Interacting Buffers. *System of Fully Charged Analyte and Neutral Complexation Agent.* At first we focused on the determination of the complexation constants of a fully charged analyte and a neutral complexation agent. The typical setup for determining the complexation constants by ACE is that the complexation agent is dissolved directly in the BGE and the analyte is injected as the sample. The effective mobility of an analyte is measured depending on the concentration of the complexation agent and the resulting data are fitted by the following function

$$u_A^{eff} = \frac{u_A + u_{AC}K_{XAc}[C]}{1 + K_{XAc}[C]} \quad (1)$$

where K_{XAc} is the complexation constant of the charged analyte, and u_A and u_{AC} are the mobilities of the free analyte and the complex, respectively. [C] is the equilibrium concentration of the complexation agent. The equilibrium concentration can be substituted by an analytical one, if the exact position that the analyte peak would have at virtually infinite dilution is known. This position can be determined by fitting the analyte peak with the HVL function.[30,31] However, if a buffer constituent interacts with the complexation agent, part of the complexation agent's concentration is "consumed" by this interaction, and its equilibrium concentration definitely differs from the analytical one even at the infinite dilution of the analyte. The situation is even more complicated because the buffering constituent is present in both dissociated and nondissociated forms, which interact with the complexation agent to different extents.[34] Thus, not only is the effective concentration of complexation agent influenced by the presence of the interacting buffer, but the pH, ionic strength, and conductivity of the buffer are mutually affected by the presence of the complexation agent, particularly so depending on its actual concentration as shown in the first part of this series.[25]

The complexation constant of *R*-FLU with β-CD determined in different buffers, MES/LiOH, MOPS/LiOH, CHES/LiOH, Tricine/LiOH, maleic acid/LiOH, phosphoric acid/NaOH, ammonium/HCl, and ethanolamine/HCl, demonstrates the influence of the interaction of buffer constituents with the complexation agent. The exact composition and parameters of the buffers are summarized in Table 1, and the pH of the buffers was chosen to ensure the complete dissociation of *R*-FLU (pK_A = 4.16). The obtained values of the complexation constants were corrected for ionic strength as proposed in our previous paper[29] and are depicted in Figure 1. Clearly, the complexation constants obtained in ethanolamine, ammonium, maleic, phosphoric, and Tricine buffers are the same, about 4800 M^{-1} in the range of experimental error. This result confirms that the interaction of these buffers with β-CD is either the same or most likely negligible. However, complexation constants determined in MES (3500 M^{-1}), MOPS (2800 M^{-1}), and CHES (270 M^{-1}) buffers are significantly lower. Thus, these complexation constants can be regarded as apparent only and valid for this particular separation system including the same concentration of the buffer. These apparent complexation constants are always lower than the true thermodynamic values as an analytical instead of a free concentration of the complexation agent is used for fitting.

To demonstrate the strength of the interaction of the buffering compounds, we injected the β-CD as a sample to the pure buffer. The stronger the interaction the higher the effective mobility of β-CD was expected. Effective mobilities of β-CD in CHES, MOPS, and MES buffers corrected for ionic strength are summarized in Table 3. The mobility of β-CD in the

dx.doi.org/10.1021/ac401381d | Anal. Chem. 2013, 85, 8526−8534

Tricine buffer was close to zero. It is clear that the highest mobility of β-CD and consequently the strongest interaction was observed in the CHES buffer followed by the MOPS and MES buffers. This finding fully agrees with the differences in values of complexation constants and the results of the NMR study, see Part I.[25]

As the next step we repeated the ACE measurements in five times diluted MES, MOPS, CHES, and Tricine separation buffers. It is obvious from Figure 1 that the complexation constant of Tricine did not change with the concentration of the buffer, while in the case of MES, MOPS, and CHES buffers the complexation constants increased significantly with buffer dilution. Simultaneously, we observed a decrease of mobilities of β-CD, see Table 3. It means that the complexation constants determined in the interacting buffers do not depend only on the type of analyte and complexation agent but also on the type and concentration of the buffer used.

In order to confirm our finding that the interaction of buffer constituents is the major reason of the discrepancy of the complexation constants values we mimicked the ACE measurements in the CHES buffer by using our simulation program Simul 5 Complex. The complexation constant and mobility of the complex of *R*-FLU with β-CD determined in the Tricine buffer and the complexation parameters of CHES with β-CD determined by ACE in Part I[25] of this series of papers were used as the necessary input parameters. The comparison of experimental and simulated data for CHES and Tricine buffers is shown in Figure 2. Very good agreement of the experimental and simulated curves was obtained that proves that interaction of the buffer with the complexation agent is the only reason for the deviation of the data.

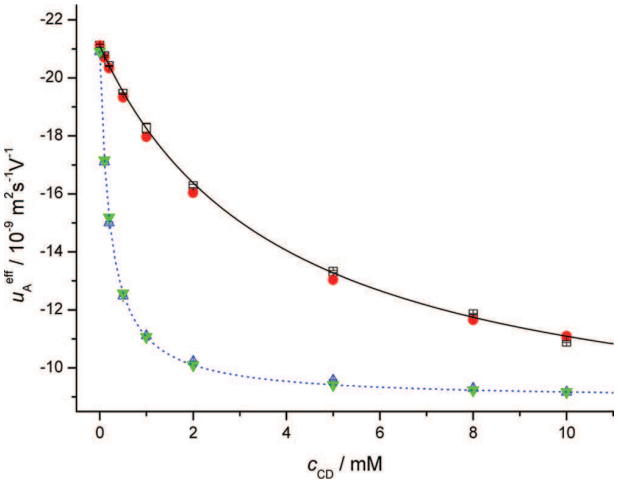

Figure 2. Dependence of effective mobility of *R*-FLU on concentration of β-CD. Red ● and □ are experimental and simulated data in 50 mM CHES/25.76 mM LiOH buffer, respectively. Blue △ and green ▼ are experimental and simulated data for 50 mM Tricine/25.76 mM LiOH buffer, respectively. Black solid and blue dotted lines are the fitted curves by eq 1. Errors are expressed as standard deviations.

Weak Electrolyte Analyte and Neutral Complexation Agent. An even more complicated situation arises in the case of determining the complexation constants of weak electrolyte analytes, where both complexation constants of a neutral and charged form of the analyte are desired. The complexation constant of the neutral form is observed at pH, where the analyte is only partially dissociated. The resulting dependence of the effective mobility of the weak electrolyte analyte on the concentration of the complexation agent can be fitted by the following equation to obtain complexation parameters

$$u_A^{eff} = u_A \frac{1 + \frac{u_{AC}}{u_A} K_{XAc}[C]}{1 + K_{XAc}[C] + \frac{[H_3O^+]}{K_{HA}}(1 + K_{XAn}[C])} \quad (2)$$

where K_{XAn} is the complexation constant of the neutral form of analyte, and K_{HA} is the dissociation constant of the analyte. It is important to note that this method relies on the constant separation conditions, especially on a constant pH value. However, as shown in Part I[25] of this series of papers, the pH of the interacting buffer changes significantly with the concentration of the complexation agent. It means that the method for determining complexation constants may completely malfunction in interacting buffers. To confirm this statement we performed two sets of ACE experiments with *R*-FLU complexing with β-CD in an acetic acid/LiOH buffer and in a benzoic acid/LiOH buffer, both pH 3.98 and IS 10 mM. At the given pH, *R*-FLU is only partially dissociated (pK_A = 4.16). As shown in Part I[25] of this series of papers, while the acetic acid buffer does not interact substantially with β-CD, benzoic acid complexes quite strongly. (The pH changes are depicted in Figure 2 of Part I[25] of this series of papers). Obtained dependencies of the effective mobility of *R*-FLU on the concentration of β-CD fitted by eq 2 are shown in Figure 3. The mobility of the free analyte, complex and complexation constant of the fully charged form of *R*-FLU were obtained by separate measurement in the Tricine/LiOH buffer of the same ionic strength and were used as fixed input parameters. In the acetic buffer, the quality of the fit was good (reduced χ^2 = 44; R^2 = 0.9936) and the resulting complexation constant was 11 100 ± 200 M^{-1}; however, in the benzoic buffer the data did not follow the expected hyperbolic trend and could not be fitted by eq 2 with sufficient precision (reduced χ^2 = 490, R^2 = 0.9574), see Figure 3.

Both complexation constants of dissociated and nondissociated forms of benzoic acid, which were determined in Part I[25] of this series of papers, were used as input data for Simul 5 Complex now. The comparison of the simulated and experimental dependencies is shown in Figure 3. Clearly, the data agree well. Both experimental and theoretical dependencies obtained in the benzoic acid buffer show interesting trends at a concentration of β-CD higher than 8 mM, and the mobility of *R*-FLU increases with the increasing concentration of β-CD. This is highly surprising because the increase of the concentration of the neutral complexation agent should always suppress the mobility of analytes. However, in this particular case the increase of mobility of the weak acid (*R*-FLU) is caused by the increase of pH, which is the consequence of the interaction of the buffering constituent with β-CD and that yields to the increase of dissociation of the weak acid *R*-FLU. At a certain concentration where the analyte is almost saturated by CD, as its concentration is small and its complexation constant high, its mobility almost reaches the limiting value (mobility of complex) and does not decrease steeply anymore. However, at this point the pH changes are still significant because the concentration of the buffer is rather high, and a much higher amount of the complexation agent is needed to saturate the buffering compound. Thus, the effect of increasing pH on the

dx.doi.org/10.1021/ac401381d | *Anal. Chem.* 2013, 85, 8526−8534

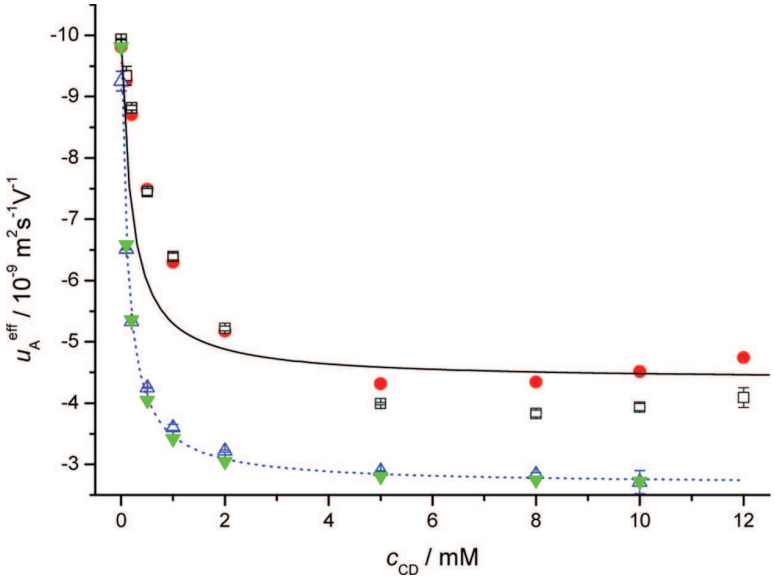

Figure 3. Dependence of effective mobility of *R*-FLU on concentration of β-CD. Red ● and □ are experimental and simulated data, respectively, in a 24 mM benzoic acid/9.9 mM LiOH buffer. Blue △ and green ▼ are experimental and simulated data, respectively, for a 61 mM acetic acid/9.9 mM LiOH buffer, both pH 3.98 and IS 10 mM. Black solid and blue dotted lines are the fitted curves by eq 2. Errors are expressed as standard deviations.

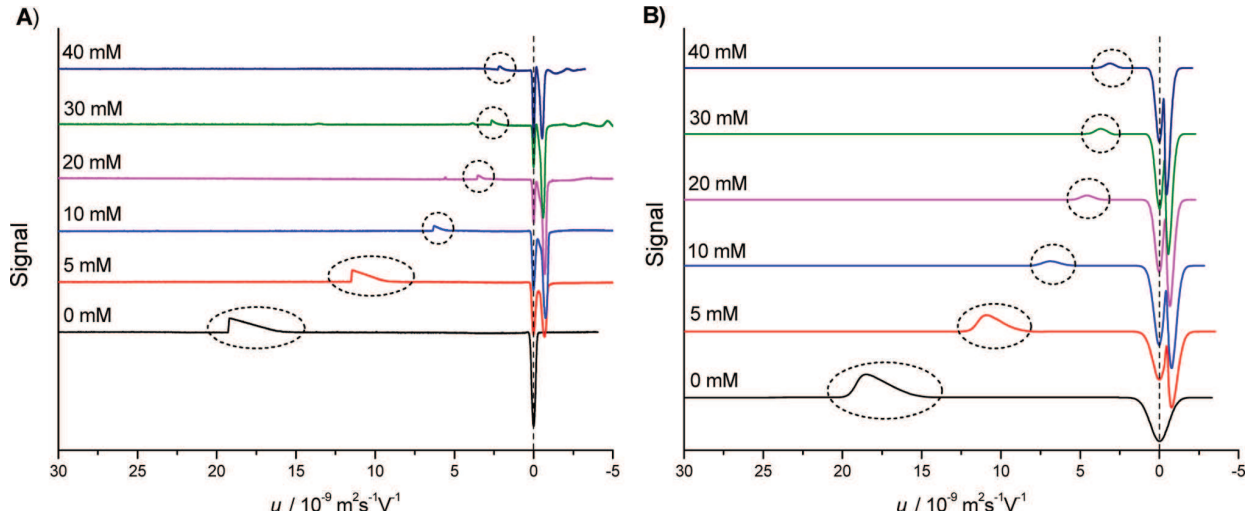

Figure 4. (A) Experimental electropherograms recalculated to mobility scale showing changes in mobility and number of system peaks in BGEs with complex-forming ligand. BGE: 5.0 mM benzoic acid, 2.5 mM LiOH, and various concentrations of HP-β-CD. Samples: disturbed BGE, compositions summarized in Table 2. Indirect UV detection was performed at a detection wavelength of 200 nm. The curves are marked by concentrations of HP-β-CD in BGE. Cationic system peaks are labeled by dashed circles. (B) Simulated electropherograms transformed to mobility scale; conditions for simulations were set according to corresponding real experiments. Curves are marked by concentrations of HP-β-CD in the BGE. Cationic system peaks are labeled by dashed circles.

mobility of the analyte prevails over the effect of the complexation of the analyte itself.

In conclusion, the complexation constants in interacting buffers determined by ACE may be incorrect and provide confusing information about the strength of the interaction of analytes with complexation agents. Moreover, at first sight, unexpected behavior, such as herein demonstrated in an increase in mobility with the increasing concentration of the neutral CD, may appear with analytes that are weak acids or bases. Thus, the potential complexation of the buffer constituents with the complexation agent should be examined independently prior to ACE measurements.

Impact of Buffer Complexation on the Development of System Peaks. The development of system peaks in electrophoretic separation systems is well described by the linear theory of electromigration,[26] and their behavior can be easily predicted using the simulation programs. However, the occurrence of system peaks in the interacting buffer systems has not been sufficiently described by now, although we presented that it might differ from expected trends. Thus, we shall demonstrate here the behavior of system peaks in interacting electrolytes, in a model system of a buffer composed of benzoic acid, which was shown to interact strongly with various cyclodextrins, and also in the common separation buffers. The

dx.doi.org/10.1021/ac401381d | *Anal. Chem.* 2013, 85, 8526−8534

changes of system zones mobilities for the benzoic acid buffer after the addition of complexation agent HP-β-CD were examined both experimentally and by simulations using the Simul 5 Complex program. The HP-β-CD was selected for this demonstration because of its higher solubility in aqueous environments in comparison to β-CD. The necessary input data for simulations were determined by independent ACE measurements, and the resulting complexation constants and mobilities of complexes are K_{XAc} = 22.3 ± 0.5 M^{-1}, K_{XAn} = 330 ± 30 M^{-1}, u_{AC} = −9.9 ± 0.5 × 10^{-9} m^2 s^{-1} V^{-1}. Experimental and simulated electropherograms for a 5.0 mM benzoic acid/2.5 mM LiOH buffer with 0−40 mM HP-β-CD are shown in parts A and B of Figure 4, respectively. All detector records were recalculated for the mobility scale (x-axis) to illustrate changes in system peaks' mobility in a more transparent way. The buffering system without any complexation agent forms two system peaks as results from the linear theory of electromigration. According to calculations in PeakMaster, one of those system peaks has zero mobility and the second one is a cationic system peak with mobility u = 17.3 × 10^{-9} m^2 s^{-1} V^{-1}. The experimental results were in a perfect agreement with the simulated ones in regard to positions, amplitudes, and shapes of the system zones, see Figure 4 (curve marked as 0 mM). The other electropherograms in Figure 4 show behavior of system peaks at the indicated complexation agent concentration. The addition of HP-β-CD (5 mM) into the 5.0 mM benzoic acid/2.5 mM LiOH buffer caused substantial slowdown of the cationic system peak and gave rise to a new slow anionic system peak. The third system peak kept nearly zero mobility.

Dependence of the mobility of experimental and simulated cationic system peaks on HP-β-CD concentration is depicted in Figure 5. Both dependencies agree very well. Such development

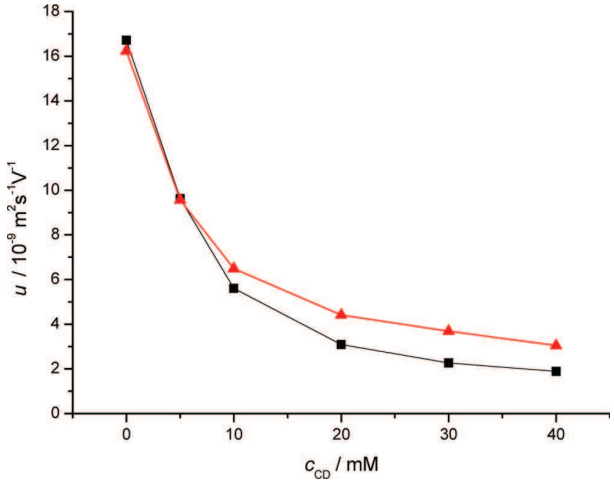

Figure 5. Dependences of the mobilities of cationic system peaks on concentration of HP-β-CD in BGE composed of 5.0 mM benzoic acid and 2.5 mM LiOH calculated from experimental (■) and simulated (red ▲) electropherograms.

of system peaks is not predictable using the classical linear theory of electromigration for noncomplexing systems. The addition of a neutral noninteracting compound into BGE should definitely result in the formation of a system peak with zero mobility and should not influence the mobility of other system peaks. Complete linear theory of electromigration for complexing systems was not presented so far. Thus, simulations can be used as the only tool for prediction and explanation of system peaks in such systems.

The development of system peaks was examined also in commonly used buffer systems that were selected based on the results of the pH study. Considering these results (see Figure 2 of Part I[25] of this series of papers), the most significant changes of the system peaks' behavior were expected in the CHES/LiOH buffer because the addition of all the tested CDs caused a considerable shift of pH in this buffer. Figure 6 shows

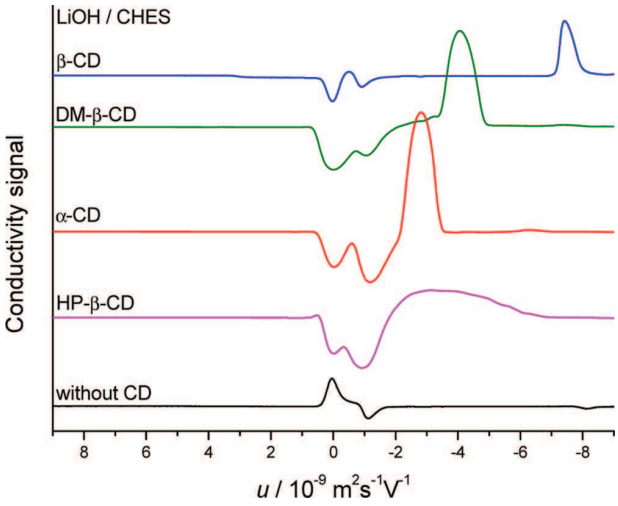

Figure 6. Experimental electropherograms for CHES/LiOH buffer with various CDs. Concentrations of α-CD, β-CD, DM-β-CD, and HP-β-CD in 10.0 mM CHES/5.0 mM LiOH buffer were 5.20, 4.54, 4.56, and 4.68 mM, respectively. Sample: 11 mM CHES, 5.0 mM LiOH.

experimental electrophoregrams obtained after the addition of the neutral CDs to this buffer. Clearly, the addition of all CDs induced an additional system peak. HP-β-CD gave rise to a system peak, which was broadened, and therefore it was difficult to determine its mobility. The presence of α-CD and DM-β-CD in BGEs led to an anionic system peak with a mobility about −3 × 10^{-9} m^2 s^{-1} V^{-1} and −4 × 10^{-9} m^2 s^{-1} V^{-1}, respectively. The strongest effect was observed again with β-CD. The addition of β-CD in BGE resulted in the development of an anionic system peak with rather high mobility, about −8 × 10^{-9} m^2 s^{-1} V^{-1}. As the result, the CHES buffer could not be recommended for electrophoretic experiments if a neutral CD is employed because the originating system peak can migrate in the same region as analytes, interact with them, and distort them. In addition the pH changes observed are so significant that they can seriously affect the separation results. The development of additional system peaks and changes in system peaks mobility was observed also in other common buffers. The detailed results can be found in the Supporting Information.

Influence of the Interaction of Buffer Constituents on the Result of Electrophoretic Separation. It is well-known that the result of electrophoretic separation is extremely sensitive to the selection of a buffer and its pH or ionic strength. Thus, the change of BGE properties connected with the complexation of buffer constituents with the complexation agent present in BGE might have significant impact on the results of electrophoretic separation. To demonstrate this behavior, we performed separations of a mixture of amino acids

dx.doi.org/10.1021/ac401381d | Anal. Chem. 2013, 85, 8526−8534

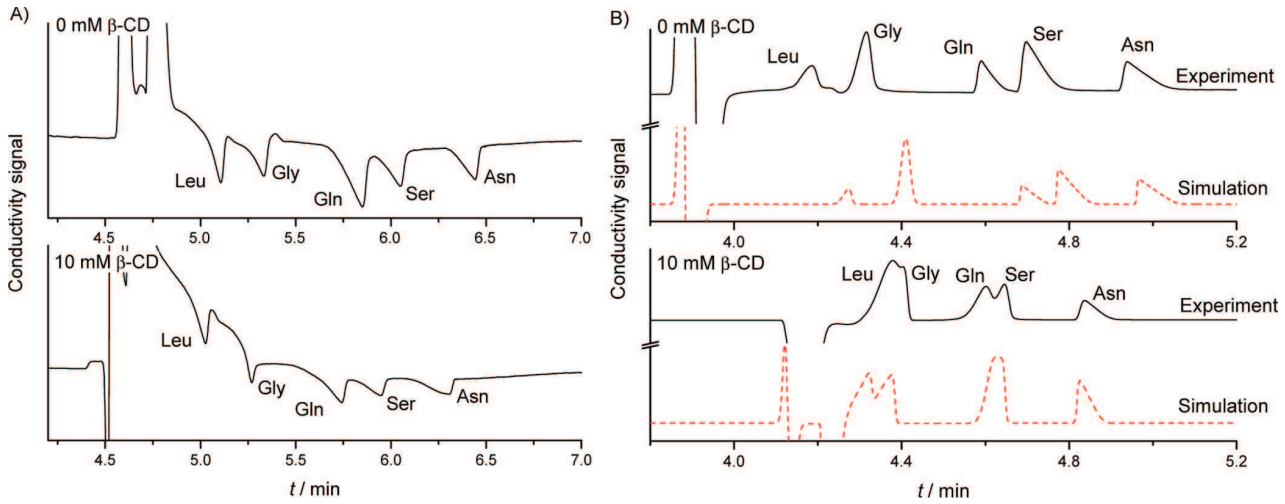

Figure 7. Comparison of the separation of a set of amino acids (Leu, Gly, Gln, Ser, Asn) in (A) 10 mM ethanolamine/5 mM HCl buffer and (B) 10 mM CHES/5 mM LiOH buffer, both pH 9.41 and IS 5 mM. Upper picture, pure buffer marked as 0 mM β-CD. Lower picture: 10 mM concentration of β-CD. Black solid curves, experiment; red dashed curve, simulations obtained by PeakMaster and Simul 5 Complex for cyclodextrin free BGE and BGE at a 10 mM concentration of β-CD, respectively. Individual amino acids are labeled by their respective abbreviation.

(namely, Leu, Gly, Gln, Ser, Asn) in 10 mM ethanolamine/5 mM Tricine and 10 mM CHES/5 mM LiOH buffers, both pH 9.41 and IS 5 mM. The separations were performed both in cyclodextrin free buffer and after addition of 10 mM β-CD. The pH of ethanolamine/Tricine buffer did not change substantially after the addition of β-CD, while the pH of the CHES buffer decreased to the value of 8.86. It confirms that the ethanolamine/Tricine buffer does not interact with β-CD remarkably, while the CHES buffer complexes strongly. The comparison of the obtained electropherograms is shown in parts A and B of Figure 7, respectively. While the electropherograms obtained in ethanolamine/Tricine buffer before and after the addition of β-CD are almost the same, in the case of the CHES buffer not only position but also the shape of the separated peaks changed significantly after the addition of β-CD. The resolution deteriorated substantially in the latter system. The explanation could be either the complexation of analytes with β-CD or the changes in BGE properties connected with the complexation of buffer constituents. The former possibility is not probable because no similar effect was observed in the noninteracting ethanolamine/Tricine buffer. It means that it is the complexation of buffer constituents that should be the major reason for the presented changes.

To prove these assumptions, we mimicked the experiments in the CHES buffer using our simulation software Simul 5 Complex. Complexation constants of CHES determined in Part I[25] of this series of papers were corrected for actual ionic strength and used as input data for simulations, the complexation of amino acids with β-CD was neglected. The comparison of simulated and experimental profiles is shown in Figure 7B. A very good agreement between the theoretical predictions and measured electropherograms was obtained. It was confirmed that the interaction of the CHES buffer with the complexation agent had a fatal impact on the separation and that ethanolamine/Tricine buffer should be the buffer of choice for this separation.

We proved that the complexation of buffer constituents with the complexation agent present in BGE might significantly influence the result of separation as it affects the BGE properties, e.g., pH and IS changes. The possible interaction of BGE constituents with the selected complexation agent must always be considered.

CONCLUSION

In this Part II of this series of papers we illustrate the practical impact of the complexation of buffer constituents with the complexation agents present in BGE. Three highly relevant aspects of electrophoresis were inspected. First, it was shown that the complexation constants of analytes interacting with the complexation agent resulting from ACE measurements can be completely incorrect if the buffer constituents concurrently interact with the agent. The stronger the concurrent interaction, the bigger the effect on the complexation constant value. Moreover, the final effect depends on both the type of the buffer and its concentration and it can lead to virtually abnormal behavior of weak acidic or alkaline analytes. Among the buffers tested, the highest impact was attributed to the CHES buffer if β-CD was used as the complexation agent. Second, the influence of the complexation of buffer constituents with the complexation agent on the development of system peaks and their behavior was demonstrated depending on the complexation agent concentration by experiment and further confirmed by simulation using our simulation software Simul 5 Complex. Perfect agreement of the simulation and experimental data was achieved, showing that system peaks can substantially change their mobilities and that an additional system peak of nonzero mobility can develop in the system even if a neutral agent is added into the interacting buffer. Last but not least, the substantial effect of the complexation of BGE constituents on the result of CE separation was demonstrated on a mixture of 5 amino acids. It was clearly shown that changes of the BGE properties, that could moreover be different for different buffers, must be considered in method development procedures. This importantly applies to all analytes in a sample, even those not supposed to interact with the agent themselves.

dx.doi.org/10.1021/ac401381d | Anal. Chem. 2013, 85, 8526−8534

■ ASSOCIATED CONTENT

Supporting Information

System peaks in common buffers interacting with various cyclodextrins. This material is available free of charge via the Internet at http://pubs.acs.org.

■ AUTHOR INFORMATION

Corresponding Author

*E-mail: svobod.j@natur.cuni.cz. Phone: +420-2-2195-1399. Fax: +420-2-2491-9752.

Notes

The authors declare no competing financial interest.

■ ACKNOWLEDGMENTS

The support of the Grant Agency of the Czech Republic, Grant No. P206/12/P630, Grant Agency of Charles University, Grant No. 323611, the project Kontakt LH11018, and the long-term research plan of the Ministry of Education of the Czech Republic (Grant MSM0021620857), is gratefully acknowledged.

■ REFERENCES

(1) Kalikova, K.; Riesova, M.; Tesarova, E. *Cent. Eur. J. Chem.* **2012**, *10*, 450−471.
(2) Wren, S. A. C.; Rowe, R. C. *J. Chromatogr.* **1992**, *603*, 235−241.
(3) Rawjee, Y. Y.; Staerk, D. U.; Vigh, G. *J. Chromatogr.* **1993**, *635*, 291−306.
(4) Rawjee, Y. Y.; Williams, R. L.; Vigh, G. *J. Chromatogr., A* **1993**, *652*, 233−245.
(5) Breadmore, M. C.; Quirino, J. P.; Thormann, W. *Electrophoresis* **2009**, *30*, 570−578.
(6) Dubrovcakova, E.; Gas, B.; Vacik, J.; Smolkova-Keulemansova, E. *J. Chromatogr.* **1992**, *623*, 337−344.
(7) Dubsky, P.; Tesarova, E.; Gas, B. *Electrophoresis* **2004**, *25*, 733−742.
(8) Dubsky, P.; Svobodova, J.; Gas, B. *J. Chromatogr., B: Anal. Technol. Biomed. Life Sci.* **2008**, *875*, 30−34.
(9) Dubsky, P.; Svobodova, J.; Tesarova, E.; Gas, B. *J. Chromatogr., B: Anal. Technol. Biomed. Life Sci.* **2008**, *875*, 35−41.
(10) Svobodova, J.; Dubsky, P.; Tesarova, E.; Gas, B. *Electrophoresis* **2011**, *32*, 595−603.
(11) Tesarova, E.; Sevcik, J.; Gas, B.; Armstrong, D. W. *Electrophoresis* **2004**, *25*, 2693−2700.
(12) Hruska, V.; Benes, M.; Svobodova, J.; Zuskova, I.; Gas, B. *Electrophoresis* **2012**, *33*, 938−947.
(13) Breadmore, M. C.; Kwan, H. Y.; Caslavska, J.; Thormann, W. *Electrophoresis* **2012**, *33*, 958−969.
(14) The group of Electrophoretic and Chromatographic Separation Methods. echmet.natur.cuni.cz.
(15) Svobodova, J.; Benes, M.; Hruska, V.; Uselova, K.; Gas, B. *Electrophoresis* **2012**, *33*, 948−957.
(16) Svobodova, J.; Benes, M.; Dubsky, P.; Vigh, G.; Gas, B. *Electrophoresis* **2012**, *33*, 3012−3020.
(17) Poppe, H. *Anal. Chem.* **1992**, *64*, 1908−1919.
(18) Stedry, M.; Jaros, M.; Hruska, V.; Gas, B. *Electrophoresis* **2004**, *25*, 3071−3079.
(19) Jaros, M.; Hruska, V.; Stedry, M.; Zuskova, I.; Gas, B. *Electrophoresis* **2004**, *25*, 3080−3085.
(20) Hruska, V.; Svobodova, J.; Benes, M.; Gas, B. *J. Chromatogr., A* **2012**, *1267*, 102−108.
(21) Rawjee, Y. Y.; Williams, R. L.; Vigh, G. *Anal. Chem.* **1994**, *66*, 3777−3781.
(22) Chen, Y. R.; Ju, D. D.; Her, G. R. *J. High Resolut. Chromatogr.* **2000**, *23*, 409−412.
(23) Fang, L.; Yin, X. B.; Wang, E. *Anal. Lett.* **2007**, *40*, 3457−3471.
(24) Evans, C. E.; Stalcup, A. M. *Chirality* **2003**, *15*, 709−723.
(25) Riesova, M.; Svobodova, J.; Tosner, Z.; Benes, M.; Tesarova, E.; Gas, B. *Anal. Chem.* **2013**, DOI: 10.1021/ac4013804.
(26) Tanaka, Y.; Terabe, S. *J. Chromatogr., B: Anal. Technol. Biomed. Life Sci.* **2002**, *768*, 81−92.
(27) Uselova-Vcelakova, K.; Zuskova, I.; Gas, B. *Electrophoresis* **2007**, *28*, 2145−2152.
(28) Jiang, C. X.; Armstrong, D. W. *Electrophoresis* **2010**, *31*, 17−27.
(29) Benes, M.; Zuskova, I.; Svobodova, J.; Gas, B. *Electrophoresis* **2012**, *33*, 1032−1039.
(30) Haarhoff, P. C.; Van der Linde, H. J. *Anal. Chem.* **1966**, *38*, 573−582.
(31) Erny, G. L.; Bergstrom, E. T.; Goodall, D. M. *J. Chromatogr., A* **2002**, *959*, 229−239.
(32) Hruska, V.; Riesova, M.; Gas, B. *Electrophoresis* **2012**, *33*, 923−930.
(33) Riesova, M.; Hruska, V.; Gas, B. *Electrophoresis* **2012**, *33*, 931−937.
(34) Gelb, R. I.; Schwartz, L. M.; Johnson, R. F.; Laufer, D. A. *J. Am. Chem. Soc.* **1979**, *101*, 1869−1874.